DYNAMICS OF ROBOTIC MANIPULATORS WITH FLEXIBLE LINKS AND KINEMATIC LOOPS

Abbas Fattah

B.Sc. (Shiraz University), 1978

M.Sc. (Isfahan University of Technology), 1989

Department of Mechnical Engineering

McGill University

Montreal, Quebec, Canada

A thesis submitted to the Faculty of Graduate Studies and Research

in partial fulfillment of the requirements for the degree of

Doctor of Philosophy

May 1995

ISBN 0-612-05702-X

Abstract

The necessity of modelling multibody systems with flexible links in high-speed operations and space structures has become apparent. In this thesis, a general formulation for the simulation of multibody systems with multiple kinematic loops and flexible links of arbitrary shapes is developed. Parallel manipulators, space structures, multi-armed manipulators, and cooperating serial manipulators are examples of these systems.

Finite element method is used for discretization of the flexible links, while the Lagrange formulation is used to derive the equations of motion of the uncoupled links. The kinematic constraint equations are generated next by using the *natural orthogonal complement* (NOC) of the twist-constraint matrix. Here, the formulation of the problem is obtained both in joint and in Cartesian spaces. Using the NOC, the constraint forces are eliminated from the equations of motion to obtain the governing equations of the system in minimum coordinates. Moreover, the formulation incorporates geometric nonlinearities in the elastic displacements, which can be very crucial in large rigid-body motions.

A simulation environment is developed to perform the procedures underlying the above formulations for different types of robotic manipulators with kinematic loops and flexible links. To highlight the link flexibility effect, the governing equations of motion are used in the simulation of the aforementioned systems to compare the results obtained with the rigid and the flexible-link models.

Résumé

La modélisation de la flexibilité des membres est nécessaire pour les systèmes mécaniques opérant à hautes vitesses ou pour les structures spatiales. L'auteur de cette thèse présente une formulation générale de la dynamique des systèmes mécaniques à multiples boucles cinématiques et membres flexibles à géométries arbitraires. Les manipulateurs parallèles, les structures spatiales, les manipulateurs à plusieurs bras, ainsi que les manipulateurs sériels en opérations coordonnées, sont des exemples de tels systèmes.

La méthode des éléments finis est utilisée pour discrétiser les membres flexibles, alors que la formulation de Lagrange est utilisée pour obtenir les équations du mouvement des membres non couplés. Les contraintes cinématiques sont déterminées au moyen du *complément orthogonal naturel* de la matrice de contraintes de vitesses. La formulation du problème est obtenue à la fois dans l'espace articulaire et cartésien. En utilisant ledit complément, les forces de contraintes sont éliminées des équations du mouvement, obtenant ainsi, un système d'équations en coordonnées minimales. En outre, la formulation inclut la géométrie non-linéaire des déplacements élastiques, qui peuvent être cruciaux lors de grands mouvements.

Un logiciel de simulation a été développé afin d'étudier différents types de manipulateurs robotiques à multiples boucles cinématiques et membres flexibles. L'effet de la flexibilité des membres est démontré en comparant les résultats de simulations utilisant un modèle rigide et flexible.

Acknowledgements

I would like to express my deep gratitude and sincere thanks to my supervisors, Prof. Jorge Angeles and Prof. Arun K. Misra, for their guidance, assistance and encouragement, without which this thesis could not have been completed. I am indebted to their dedication and their efforts to help me understand and solve the problems that arose during the course of this thesis.

I am very thankful to the Isfahan University of Technology and the Ministry of Culture and Higher Education of Iran for their support under a graduate scholarship that made possible this research work. This was complemented by NSERC (Natural Sciences and Engineering Research Council of Canada) as well as IRIS (Institute for Robotics and Intelligent Systems, a network of Canadian centers of excellence).

I am very grateful to the faculty of the Department of Mechanical Engineering of Isfahan University of Technology from whom I have been encouraged to continue with doctoral studies.

I wish to express many thanks to all my fellow students in my group at the Centre for Intelligent Machines with whom I had fruitful discussions and a great time. Special thanks to Robert Lucyshyn for the invaluable discussions and proofreading of the introduction of my thesis; to John Darcovich for technical assistance; and to Luc Baron and Glen Bilodeau for translating my abstract into French. The excellent computer facilities and pleasant research environment provided by both the Centre for Intelligent Machines and the Department of

Mechanical Engineering of McGill University are gratefully acknowledged.

Last, but not least, wholehearted thanks are also extended to my wife, Sabiheh; my children, Hadi, Shadi and Sara for their great patience, support and understanding throughout my research work. Their tolerances and sacrifices in allowing me to concentrate on my research are gratefully acknowledged.

Claim of Originality

The major contribution in the course of this thesis is the development of a general formulation for the modelling and simulation of multibody systems with flexible links of arbitrary shapes and multiple kinematic loops.

Additional contributions are also made as a result of the thesis, namely,

- Development of a methodology to generate kinematic constraint equations that is applicable to general multiple kinematic loops using the natural orthogonal complement of the velocity-constraint matrix;
- Modelling and simulation of cooperating serial manipulators as well as planar parallel manipulators with flexible links in both Cartesian and joint spaces;
- Kinematic and dynamic simulations of a spatial parallel manipulator with flexible links.

These contributions have been partly reported in a preliminary form in (Fattah, Angeles, and Misra, 1995–a, 1995–b, 1994–a, 1994–b) and (Fattah, Misra, and Angeles, 1995, 1994).

Dedicated to:

my father and mother;

my brothers;

my wife and children.

Contents

List of Figures

List of Tables

Notation

Mathematical Symbols

Bold-face upper-case letters are used to denote matrices, while bold-face lower-case letters denote vectors. Italic letters denote scalars

$[\cdot]_i$: vector or matrix $(\cdot)$ expressed in frame $\mathcal{F}_i$

$[\cdot]_{ij}$: subscripts i and j in vector or matrix $(\cdot)$ stand for the labels of link i and element j, respectively

$\|\cdot\|$: Euclidean norm of vector $(\cdot)$

Greek Symbols

α_i: angle between joint axes Z_i and Z_{i+3}

γ_i: joint angle associated with the flexibility of link i

γ_{ki}: components of the rotation of the tip of the link i associated with the flexibility of the same link

$\mathbf{\Gamma}_i$: mapping between $\mathbf{v}_i$ and $\dot{\mathbf{q}}_i$

$[\epsilon]_{ij}^{nl}$: nonlinear terms in Green's strain tensor

θ_k: joint angle centred at origin O_k

$\boldsymbol{\theta}$: vector of generalized coordinates

$\boldsymbol{\theta}_D$: vector of dependent generalized coordinates

$\boldsymbol{\theta}_I$: vector of independent generalized coordinates

$\dot{\boldsymbol{\theta}}_I$: vector of independent generalized speeds

ϑ: dimension of vector $\boldsymbol{\theta}$

κ_i: number of elements of link i

$\mathbf{\Lambda}_i$: mapping between $\dot{\mathbf{q}}_i$ and $\mathbf{v}_i$

ν: number of joints of the system

Π^K: power developed by nonworking kinematic constraint forces

ρ_i: mass density of link i

$[\boldsymbol{\sigma}]_{ij}$: state of stress because of the inertia loading of element j of link i

$\boldsymbol{\tau}_i$: vector of the external torques applied at joint i

ϕ_i: angle of orientation (planar system) of frame $\mathcal{F}_i$ with respect to $\mathcal{F}_0$

$\mathbf{\Phi}_{ij}$: connectivity matrix of element j of link i

$\mathbf{\Phi}_{ij}^o$: connectivity matrix of the rigid-body position vector of element j of link i

φ_i: total angle of rotation of the joint centred at O_i

$\boldsymbol{\psi}_i^j$: j^{th} column of $\mathbf{\Psi}_{im}$, an n_i-dimensional eigenvector

$\mathbf{\Psi}_{im}$: modal matrix

$\boldsymbol{\omega}_i$, ω_i: angular velocity of frame $\mathcal{F}_i$ with respect to $\mathcal{F}_0$ in the spatial and planar case, respectively

$\boldsymbol{\omega}_C$: angular velocity of the moving platform of the spatial parallel manipulator

$\mathbf{\Omega}_i$: cross-product matrix of $\boldsymbol{\omega}_i$

$\mathbf{\Omega}_C$: cross-product matrix of $\boldsymbol{\omega}_C$

Latin Symbols

$\mathbf{a}_{ik}$: position vector from O_i, origin of the frame $\mathcal{F}_i$, to O_i^k, origin of frame $\mathcal{F}_k$, expressed in the inertial frame

$\mathbf{a}_i$: position vector from O_i to O_{i+3} on link i expressed in the inertial frame (spatial case)

$\mathbf{A}$: twist-constraint matrix

$\mathbf{b}_i^D$, $\mathbf{b}^D$: dissipative wrench of link i and that of the system, respectively

$\mathbf{b}_i^E$, $\mathbf{b}^E$: external wrench of link i and that of the system, respectively

$\mathbf{b}_i^G$, $\mathbf{b}^G$: gravity forces of link i and that of the system, respectively

$\mathbf{b}_i^K$, $\mathbf{b}^K$: kinematic constraint wrench of link i and that of the system, respectively

$\mathbf{b}_i^S$, $\mathbf{b}^S$: system wrench of link i and that of the system, respectively

$\mathbf{c}$: position vector of the centre of mass of the moving-platform

$\mathbf{C}_{kj}^{i3}$, $\mathbf{C}_{kj}^{i4}$, $\mathbf{C}_{kj}^{i5}$, $\mathbf{C}^{i1}$, $\mathbf{C}^{i2}$: constant matrices for computing the mass matrix of link i

$\mathbf{d}_i$: position vector of any point P_i expressed in the inertial frame

$[\mathbf{d}_{ei}]_{ij}$, $[\mathbf{d}_{ei}]_i$: elastic displacement of point P_i expressed in the $\mathcal{F}_{ij}$ and $\mathcal{F}_i$ frames, respectively

DOF: degree(s) of freedom

$\mathbf{D}_i$: cross-product matrix of vector $\mathbf{d}_i$

$\mathbf{E}$: 2×2 orthogonal matrix that rotates vectors in plane through $90°$ counterclockwise

$\mathbf{f}_i$: vector of generalized forces of link i

$\mathbf{f}_i^A$: algebraic constraint wrench of link i due to the algebraic constraint among the components of the Euler parameters

$\mathbf{f}_i^D$: dissipative wrench of link i

$\mathbf{f}_i^E$: external wrench of link i

$\mathbf{f}_i^G$: gravity forces of link i

$\mathbf{f}_i^K$: kinematic-constraint wrench of link i resulting from the kinematic coupling of the links

$\mathbf{f}_i^S$: system wrench of link i

$\mathbf{F}_i$: rotation matrix associated with the flexibility of link i

$\mathcal{F}_i$: spatial coordinate frame $X_iY_iZ_i$ or planar frame X_iY_i, attached to link i

$\mathcal{F}_0$: spatial inertial coordinate frame $X_0Y_0Z_0$ or planar X_0Y_0

$\mathcal{F}_{ij}$: spatial coordinate frame $X_{ij}Y_{ij}Z_{ij}$ or planar frame $X_{ij}Y_{ij}$, attached to element j of link i

$\mathcal{F}_C$: coordinate frame attached to the centre of mass of the moving-platform of the spatial parallel manipulator

$\mathbf{I}_i$: inertia matrix of link i

$\mathbf{K}_i$: stiffness matrix of link i

$\mathbf{K}_{ij}$: stiffness matrix of element j of link i

$\mathbf{K}_{ij}^e$: conventional stiffness matrix of element j of link i

$\mathbf{K}_{ij}^{gn}$: geometric stiffness matrix of element j of link i

$\mathbf{L}_i(P_{0i})$, $\mathbf{L}_{ij}(P_{0i})$: shape-function matrices of link i and element j of the same link evaluated at point P_{0i} in the undeformed configuration of link i

$\mathbf{L}_i^o(P_{0i})$, $\mathbf{L}_{ij}^o(P_{0i})$: shape-function matrices for the rigid-body position vector evaluated at point P_{0i} of link i and element j of the same link

$\mathbf{L}_i^m(P_{0i})$: shape-function matrix based on the modal coordinates

m_i: dimension of vector $\mathbf{u}_i^o$

m_i': dimension of vector $\mathbf{v}_i$

m': dimension of vector $\mathbf{v}$

$\mathbf{M}$: generalized extended mass matrix of the system

$\mathbf{M}_i$: mass matrix of link i

$\hat{\mathbf{M}}$: generalized inertia of the system

n_i: dimension of vector $\mathbf{u}_i(t)$

n_i': dimension of vector $\mathbf{q}_i$

$\mathbf{N}$: natural orthogonal complement matrix of the twist-constraint matrix $\mathbf{A}$

P_i: a nominal point on element j of link i

$\mathbf{p}_i$: position vector of point P_i in the inertial frame

q: number of degrees of freedom of the system

q_j: prescribed manoeuvre for the actuated joint centred at O_j

$\mathbf{q}_i$: vector of the flexible-pose of link i

$\hat{\mathbf{q}}_i$: vector of Euler parameters representing the orientation of the frame $\mathcal{F}_i$

r: number of all moving links in the system

r_f: number of all flexible links in the system

$\mathbf{r}_i$: position vector of origin O_i in the inertial frame defining the global position

$\mathbf{R}_i$: rotation matrix of frame $\mathcal{F}_i$ with respect to the inertial frame

$\mathbf{R}_C$: rotation matrix of frame $\mathcal{F}_C$ with respect to the inertial frame

t: time

T: simulation time

T_i: kinetic energy of link i

$\mathbf{u}_i(t)$, $\mathbf{u}_{ij}(t)$: vectors of generalized coordinates (nodal elastic displacements of link i and element j of the same link) associated with link flexibility

$\mathbf{u}_i^o$: nodal rigid-body position vector of link i

$\mathbf{u}_i^m(t)$: modal coordinates (modal elastic displacements) of link i

v_i: volume of link i

V_i: elastic strain energy of link i

V_{ij}: elastic strain energy of element j of link i

V_{ij}^e: conventional elastic strain energy of element j of link i

V_{ij}^{gn}: elastic strain energy due to the effect of geometric nonlinearities in the elastic displacements of element j of link i

$\mathbf{v}$: vector of generalized flexible-twist of the system

$\mathbf{v}_i$: vector of flexible-twist of link i

$\mathbf{w}_{ik}$, w_{ik}: spatial and planar angular velocities of frame $\mathcal{F}_k$ with respect to frame $\mathcal{F}_i$ resulting from the elastic displacement of link i

$\mathbf{y}$: state-space vector

$\mathbf{Y}_{ij}$: rotation matrix of frame $\mathcal{F}_{ij}$ with respect to $\mathcal{F}_i$

$\mathbf{z}_k$: unit vector parallel to the joint axis Z_k

Chapter 1

Introduction

1.1 Basic Robotic Manipulator Terminology

A mechanical system can be modelled for dynamical analysis as a kinematic chain of interconnected rigid and flexible links. In turn, a kinematic chain may be simple or complex. It is simple if each link is connected to, at most, two other links. Moreover, a simple kinematic chain is closed if all links are connected to two other links; otherwise, it is open, these two concepts being illustrated in Fig. 1.1. Open kinematic chains appear frequently in serial robotic manipulators, while closed kinematic chains appear in linkages. Complex kinematic chains are composed of more than one simple kinematic chain and contain both open and closed subchains. Complex kinematic chains with open subchains are known as tree structures, while complex kinematic chains comprise closed subchains as kinematic loops, as depicted in Fig. 1.2. Tree structures can appear in multi-armed manipulators such as the Special Purpose Dexterous Manipulator (SPDM), shown in Fig. 1.3, one of the robotic manipulators of the Mobile Servicing System (MSS) of the International Space Station Program. Kinematic loops occur in many applications. Examples are parallel manipulators, space structures, cooperating serial

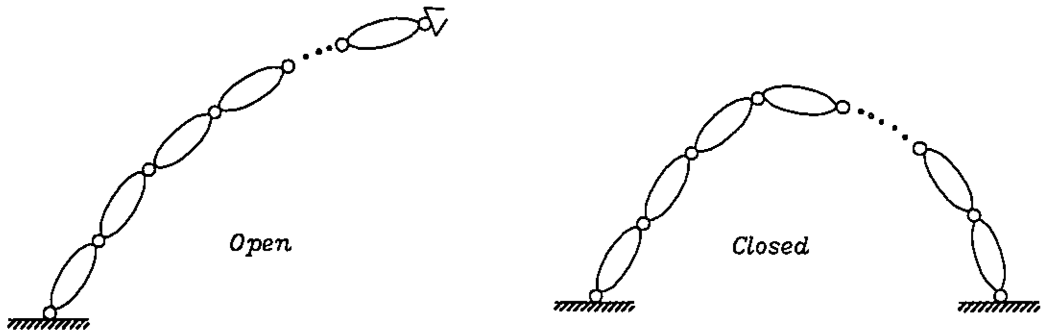

Figure 1.1: Simple kinematic chains

manipulators and multi-armed manipulators in a coordinated activity.

Robotic manipulators, as defined above, can be classified into three basic groups, namely,

a) serial manipulators;

b) multi-armed manipulators;

c) parallel manipulators.

Most industrial robotic manipulators have traditionally been designed as anthropomorphic serial manipulators. Serial manipulators usually have merits such as larger workspace and larger reachability; higher dexterity; simpler modelling requirements. However, they also have drawbacks such as low rigidity because of their cantilever-type configuration, poor dynamic performance during high-speed operations, low accuracy and larger inertia load. To overcome these drawbacks, an alternative type of manipulators, comprising kinematic loops, known as parallel manipulators, has been proposed. The main advantages of parallel manipulators, as compared with their serial counterparts, are greater rigidity, lower inertia load, higher accuracy due to the lack of cantilever structures, and higher load-carrying capacity. Parallel manipulators have potential applications where the demands on workspace and dexterity are low but the dynamic loading is severe, and high-speed operation and precision motion are of primary concern.

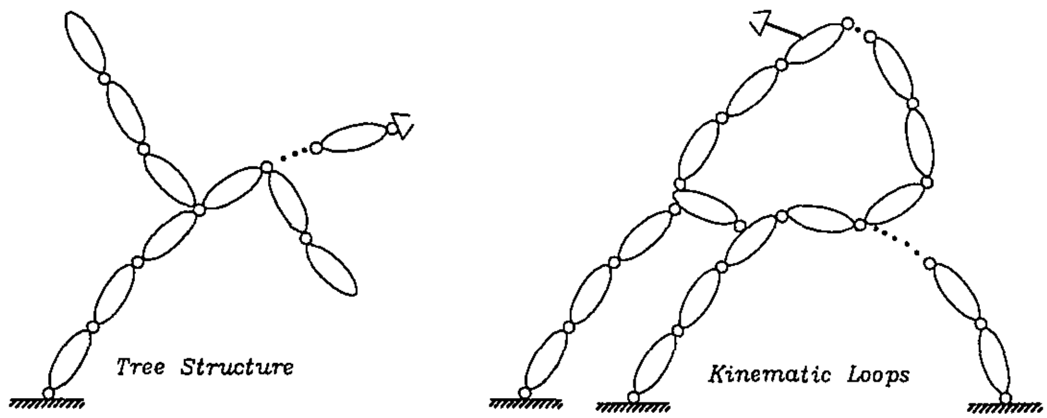

Figure 1.2: Complex kinematic chains

From the kinematic and dynamic modelling points of view, multi-armed and serial manipulators can be considered the same, while multi-armed manipulators in a coordinated activity, cooperating serial manipulators and parallel manipulators can be regarded as robotic manipulators with kinematic loops. Therefore, from now on, the term *robotic manipulators with kinematic loops* shall be used to refer to these manipulators.

Robotic manipulators can be modelled with rigid links in some instances. However, in high-speed operations, the inertia forces become large and the system undergoes substantial elastic displacements. Moreover, space structures usually contain long and light-weight links, and thus, the elasticity of the links becomes important. In these situations, the necessity of modelling robotic manipulators with flexible links becomes apparent. In this thesis, a modelling procedure will be introduced that is applicable to robotic manipulators with kinematic loops and flexible links.

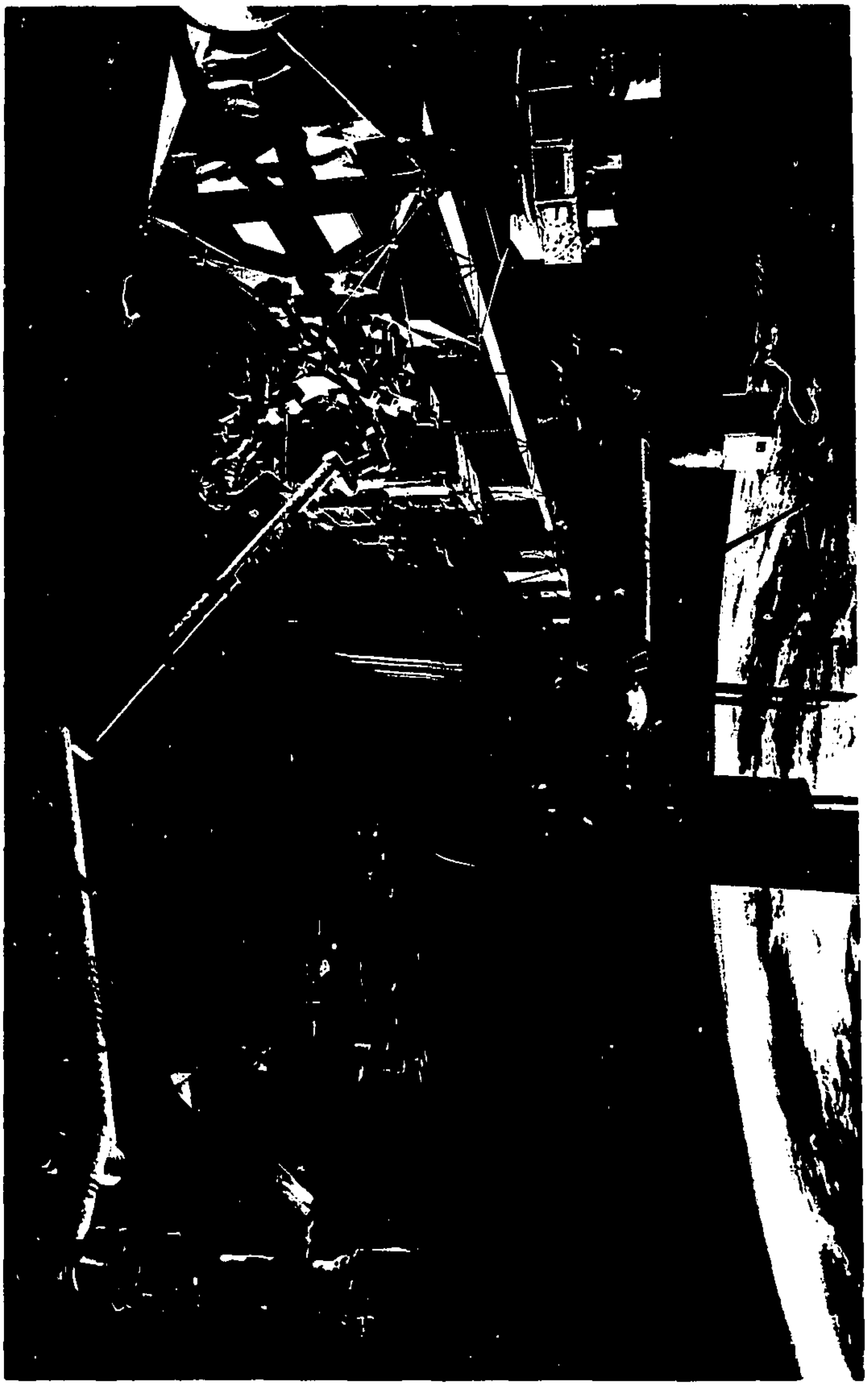

Figure 1.3: A multi-armed manipulator

1.2 General Background and Motivation

Robotic manipulators are modelled for dynamical analysis as multibody mechanical systems, as described in the previous section.

1.2.1 Dynamics of Multibody Mechanical Systems

The modelling of multibody mechanical systems with flexible links is a challenging task. Extensive research in this area, especially for closed kinematic chains, such as linkages and mechanisms, has been reported. The achievements of the seventies have been reviewed by Erdman and Sandor (1972) and Lowen and Jandrasits (1972). A review paper on the subject was published later by Lowen and Chassapis (1986). Recently, some important works in this area are addressed in (Erdman, 1993).

Earlier modelling efforts can be classified into two groups. Some research works were based on a method that considered the elastic body as a continuous system (Jasinski et al., 1971; Chu and Pan, 1975; Badlani and Kleinhenz, 1979; Badlani and Midha, 1982; Tadjbakhsh, 1982; Tadjbakhsh and Younis, 1986). This method assumes infinite degrees of freedom for elastic links, which brings about some difficulties in modelling the system. For this reason, in most cases, researchers considered examples with only one elastic link in the mechanism.

Some other investigators used a method that was based on discretizing the links, so that they have a finite number of elastic degrees of freedom. Earlier work in this group was based on the assumption that elastic displacements have no effect on the rigid-body motion of the system (Winfry, 1972; Erdman et al., 1972; Imam et al., 1973; Imam and Sandor, 1973; Baghat and Willmert, 1976; Ho, 1977; Midha et al., 1979; Cleghorn et al., 1981; Sunada and Dubowsky, 1981; Turcic and Midha, 1984-a; Naganathan and Soni, 1986). This assumption cannot give accurate results when high-speed operations come into play, since it ignores the coupling between the rigid-body motion and the elastic displacements.

Later, Song and Haug (1980), Shabana and Wehage (1983; 1984) and Yoo and Haug (1986) used a method that attempted to consider the coupling between rigid-body motion and elastic displacements. They used the Lagrange equations of motion and either the finite-element method or the assumed-mode method to account for the elastic displacements of the links. Lagrange multipliers were introduced in order to account for the constraint forces. By considering the coupling between the rigid-body motion and the elastic displacements, a system of nonlinear algebraic equations was adjoined to the differential equations of motion. This method thus increases the number of equations and leads to a mixed set of differential and algebraic equations, which brings about additional numerical difficulties. Nagarajan and Turcic (1990-a; 1990-b) used an approach that was similar to the above method but the differential equations of motion were in symbolic form and in terms of minimum variables. In their approach, the dependent rigid-body constraint variables were eliminated and expressed in terms of the rigid-body degrees of freedom. However, constraint forces still should be computed.

An alternative approach can be used to derive the governing equations of motion in terms of a minimum number of equations. Extensive research works using different methods to reduce the generalized coordinates and also to eliminate the constraint forces have been reported, namely, the joint-coordinate method based on a velocity transformation (Jerkovsky, 1978; Kim and Vanderploeg, 1986; Chang and Shabana, 1990; Nikravesh and Gim, 1993), the singular-value-decomposition method (Mani, 1984; Singh and Linkins, 1985); the zero eigenvalue method (Kaman and Huston, 1984); orthogonal complement arrays (Amirouche and Huston, 1988; Ider and Amirouche, 1988); and the pseudo-upper triangular-decomposition method (Amirouche and Jia, 1988). Another method uses Kane's equations (Kane and Levinson, 1985; Singh et al. 1985; Everett, 1989; Amirouche and Xie, 1993). In this method, the constraint forces are eliminated from the equations of motion by introducing partial velocities and partial angular velocities derived from the kinematic constraints. Cyril et al. (1991), Saha and Angeles (1991), Ma (1991) and Darcovich et al. (1992) used the Lagrange or Newton-Euler equations of motion and incorporated the natural orthogonal complement (Angeles and Lee, 1988) to eliminate the constraint forces from the equations of motion to obtain the governing equations in minimum coordinates.

One of the important issues in the area of multibody dynamics is consideration of the effect of geometric nonlinearities in the elastic displacements of the flexible links, also known as geometric stiffening and dynamic stiffening. Although we can, in some instances, obtain acceptable simulation results without considering this effect, we can also obtain incorrect results in simulations involving large rigid-body motions. The effect of geometric nonlinearities has been studied by numerous investigators (Likins et al., 1973; Turcic and Midha, 1984-b; Kane et al., 1987, Modi and Ibrahim, 1988; Ider and Amirouche, 1989-a; Hanguad and Sarkar, 1989; Banerjee and Dickens, 1990; Banerjee and Lemak, 1991; Meirovitch, 1991; Sadigh and Misra, 1993; Banerjee, 1993). Most of these researchers studied the geometric nonlinearities in beam-shaped links, while Banerjee and Dickens (1990), Banerjee and Lemak (1991) and Sadigh and Misra (1993) considered this effect in the dynamics of multibody systems with elastic links of arbitrary shapes.

1.2.2 Dynamics of Robotic Manipulators

The governing equations of motion of a robotic manipulator can be derived in terms of nonlinear differential equations by modelling the manipulator as a multi-body mechanical system. Two basic problems related to the dynamics of robotic manipulators arise, namely, *inverse dynamics* and *direct dynamics.* Inverse dynamics is defined as follows: Given the motion of a robotic manipulator, determine the actuator forces or torques required to produce the desired motion. Direct dynamics, also known as dynamic simulation, is defined as follows: Given the time histories of the actuator forces or torques and the initial state of the system, determine the motion of the robotic manipulator.

Extensive research work on the dynamics of serial manipulators with flexible links has been reported (Hughes, 1979; Kelly and Huston, 1981; Sunada and Dubowsky, 1983; Book, 1984; Usoro et al., 1986; Sharf and D'Eleuterio, 1988; Nagathan and Soni, 1988; Bricout et al., 1990; Bremer and Pfeiffer, 1992; Cyril et al., 1991; De Luca and Siciliano, 1991; Sharf and D'Eleuterio, 1992; Hu and Ulsoy, 1994). A literature survey on the subject was published by Gaultier and Cleghorn (1989). Some works in this research area are explained below.

Hughes (1979) used the recursive Newton-Euler formulation for chains of elastic bodies and carried it out for simulation of the Shuttle Remote Manipulator System. Sunada and Dubowsky (1983) used the finite-element method to consider the dynamical behaviour of robotic manipulators with elastic complex-shape links. However, they did not consider the effect of elastic displacements on the rigid-body motion of the system. One of the earlier important works on the dynamics of elastic serial manipulators was presented by Book (1984). He used 4×4 transformation matrices to represent the joint and deflection motion. The recursive Lagrangian formulation, which has been proven efficient in the rigid-link modelling (Hollerbach, 1980), was used for developing the governing equations of motion for elastic-link manipulators. Moreover, Book considered the coupling between elastic displacements and rigid-body motions. Usoro et al. (1986) used the finite element and the Lagrangian formulation to model a two-link flexible manipulator. Sharf and D'Eleuterio (1988) proposed a general simulation procedure for chains of elastic bodies using the recursive Newton-Euler scheme (Hughes, 1985). They used this method to study the effect of flexibility on the dynamics of robotic manipulators. Sharf and D'Eleuterio (1992) studied parallel simulation dynamics for elastic serial manipulators, which is a new solution method for the simulation of these systems. They used the modelling procedure that was suggested in a series of works (Sincarsin and Hughes, 1989; Hughes and Sincarsin, 1989; D'Eleuterio, 1992) describing the dynamics of an arbitrary multibody system composed of chains of elastic bodies. The advantage of this method is that it concurrently evaluates the solution for constraint forces, using parallel iterative techniques, and the accelerations of the bodies. While the above investigators studied robotic manipulators with open and single closed-chain structures, Bremer and Pfeiffer (1992) treated systems of elastic bodies, such as elastic manipulators, with tree structures.

Nevertheless, the study of the dynamics of robotic manipulators with kinematic loops has been the subject of very few investigations (Lee and Shah, 1988; Sugimoto, 1989; Ma and Angeles, 1989; Reboulet and Berthomieu, 1991; Ma, 1991; Lbert et al., 1993; Gosselin, 1993; Sun et al., 1994; Lilly and Orin, 1994). Most of these works studied the dynamics of rigid-link parallel manipulators, except the last one (Sun et al., 1994), which reported a solution to the inverse dynamics and force optimization of multi-armed manipulators with flexible links. Moreover, Lilly and Orin (1994) presented an algorithm for the dynamic simulation of multiple-chain rigid robotic mechanisms.

Until now, to the best of the author's knowledge, most of the formulations for the modelling of robotic manipulators with flexible links have been confined to open, tree-structure, and single closed-chain systems, while the modelling of robotic manipulators with kinematic loops and flexible links has remained virtually untouched. One of the motivations behind this work is to advance the state-of-the-art of modelling and simulation of robotic manipulators with kinematic loops and flexible links, besides the many applications in space structures

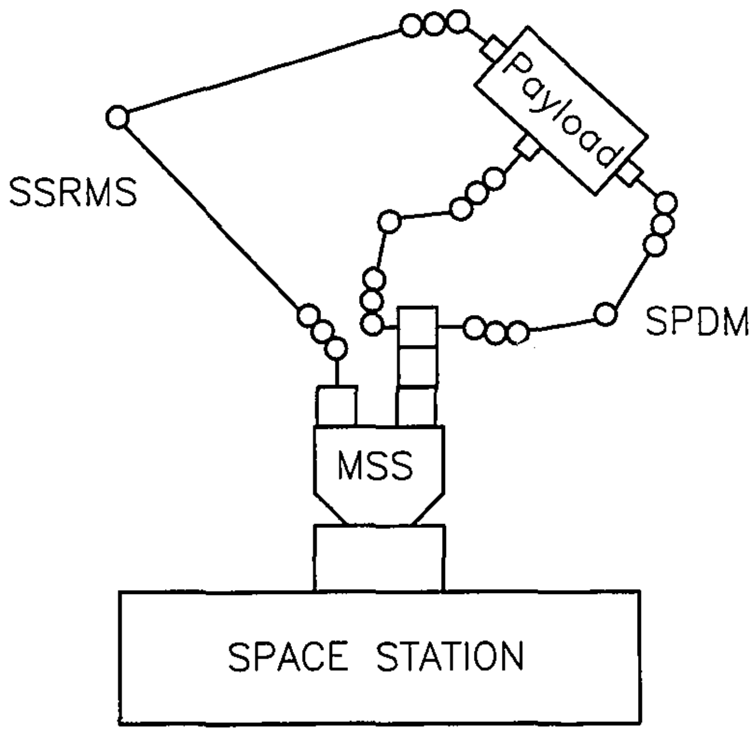

Figure 1.4: Robotic manipulators with kinematic loops

that give rise to robotic manipulators with kinematic loops. Moreover, long and light-weight links, high-speed and accuracy are some important features of space structures whereby consideration of link flexibility in the computation scheme is required. As an example, Carr et al. (1990) consider the SSRMS (Space Station Remote Manipulator System) and the SPDM mounted on the Mobile Servicing System (MSS), and participating in a coordinated activity consisting of the SPDM servicing a payload held by the SSRMS, as shown in Fig. 1.4. These manipulators have long flexible arms and form multiple kinematic loops during their activity.

1.3 Research Objectives and Scope of the Thesis

This research aims at furthering the modelling and simulation techniques meant for robotic manipulators, while extending it to multibody systems containing kinematic loops and flexible links. To achieve this goal, the research work is divided into the following items:

1. Develop a formulation for the simulation of multibody mechanical systems with multiple kinematic loops and flexible links of arbitrary shapes, which can be accomplished through the following steps:

   a) Model each link as a discrete system. To this end, the continuous system is reduced to a discrete system with a finite number of degrees of freedom using a finite-element approximation. Finite-element analyses (FEA) provide a reliable and systematic modelling technique for mechanical systems with flexible links of arbitrary shapes. The Lagrange dynamical equations of motion for the link are then derived under no consideration of kinematic coupling;

   b) Generate kinematic constraint equations. This will be accomplished using the natural orthogonal complement (NOC) of the twist-constraint matrix and will be applicable to multiple kinematic loops. The NOC will eliminate the constraint forces, thereby leading to a minimum number of equations of motion;

   c) Incorporate geometric nonlinearities in the elastic displacements, which can be very important in high-speed operations;

   d) Transform the *nodal coordinates* to *modal coordinates*, so as to reduce the number of the generalized coordinates. In large mechanical systems, using finite elements results in a large number of generalized coordinates, because of the number of nodal coordinates of each link.

2. Develop a simulation environment to implement the procedures underlying the above formulations for different types of robotic manipulators with kinematic loops and flexible links, namely,

   a) parallel manipulators;

   b) multi-armed manipulators in a coordinated activity;

   c) cooperating serial manipulators.

1.4 Thesis Outline

The kinematics of multibody systems with closed-chains and flexible links is discussed in Chapter 2. The first part of this chapter is devoted to deriving the kinematic analysis of a flexible link. Here, a flexible link is discretized by using finite elements. The flexible pose and flexible twist of a link are defined to specify the global position and velocity of the link. The formulation of kinematic constraints is derived by using the methodology of the natural orthogonal complement in the second part of Chapter 2. It is also described here how to formulate the problem in Cartesian space as well as in joint space. Moreover, the procedure to calculate the natural orthogonal complement is explained.

In Chapter 3, the dynamics of multibody systems with kinematic loops and flexible links is discussed. First, the modelling of an individual link is described. Here, using expressions for the kinetic and potential energies of the link, the Lagrange equations of the link are derived. Then, the governing equations of motion of the system are obtained by assembling all the links together via their kinematic constraints, as explained in Chapter 2. The number of the generalized coordinates can be reduced by changing the nodal coordinates to modal coordinates, which is explained in this chapter. Thereafter, the approach to consider the effect of geometric nonlinearities in the elastic displacements is addressed. Finally, a simulation scheme is proposed in this chapter.

The next three chapters are devoted to developing a simulation scheme to carry out the modelling formulations described in Chapters 2 and 3 for different types of robotic manipulators with kinematic loops. The dynamics modelling and simulation of two cooperating flexible-link manipulators are obtained in Chapter 4. The simulation results of the formulation in Cartesian space and joint space are compared in order to obtain insight into the speed of operations for both formulations, as well as to show the accuracy of the simulation results. Moreover, the effect of structural damping on the simulation is studied in this chapter.

Chapter 5 covers another type of robotic manipulators, namely, planar parallel manipulators. The modelling of the manipulator at hand is formulated both in Cartesian and in joint spaces. Some simulation results are presented in this chapter as well.

The first part of Chapter 6 is devoted to the direct kinematics solution of a spatial parallel manipulator. Direct position and direct velocity kinematics solutions are accomplished in this part. The modelling and simulation of this manipulator are carried out later in this chapter.

In Chapter 7, conclusions are drawn based on the achievements of this research work. Some suggestions for further research are also put forward.

Three appendices are included for completeness of this thesis. Euler parameters and several important relations, which are used in Chapters 2 and 3, are presented in Appendix A. Appendices B and C give the detailed description of the derivations of two equations in Chapter 3.

Chapter 2

Kinematics of Multibody Systems with Kinematic Loops and Flexible Links

2.1 Introduction

As mentioned in the previous chapter, robotic manipulators with kinematic loops can be modelled for dynamical analysis as multibody mechanical systems. The pre-requisite to the modelling of a multibody system is the understanding of the underlying kinematics. To this end, the kinematics of multibody systems with kinematic loops and flexible links is studied in this chapter.

First, an arbitrary elastic link, which is a continuous system, is approximated as a discrete system, with the assumption that its dynamics can be described by a finite number of degrees of freedom. Different means for discretizing a flexible link such as the assumed-modes method, the cubic-splines method, the finite-element method, etc. exist. Some of these methods are confined to beam-shaped links. Nevertheless, the finite-element analysis (FEA) provides a reliable and systematic technique for discretizing the flexible links of arbitrary shapes. Therefore, the finite-element approximation is used here in order to reduce the continuous link to a discrete system with a finite number of elastic degrees of freedom. However, there are some drawbacks associated with FEA, such as large CPU time consumption, and the appearance of a large number of elastic degrees of freedom in large mechanical systems. To overcome these drawbacks, FEA is often done off-line, the results being used in on-line simulation in order to reduce the execution time, which is very important for real time control. Moreover, the nodal coordinates can be transformed into modal coordinates in order to reduce the number of elastic degrees of freedom. Both finite-element and assumed-modes methods can be applied to simple flexible links such as beams and plates. However, the main advantage of FEA, as compared with the assumed-modes method, is that the former can be applied to flexible links of complex and general shapes. Using FEA and modal coordinates together with the classical theory of elasticity for the discretization of the elastic displacements lead to a linearization of kinematics and dynamics relationships (Shabana, 1991; Banerjee, 1993). This linearization may lead to errors in large rigid-body motions. How to overcome these errors, which are very crucial in high-speed operations, will be discussed in Chapter 3.

Here, the position and velocity vectors of any point on link i are obtained in order to use them in the next chapter for derivation of the equations of motion.

The kinematic constraints are then formulated using the methodology of the natural orthogonal complement, henceforth abbreviated as NOC. It is also explained here how to define the NOC. Finally, the procedure to evaluate the NOC, which depends on whether the formulation of the problem is in Cartesian space or in joint space, is discussed.

2.2 Some Definitions

For modelling of a flexible link, a general multibody mechanical system with multiple kinematic loops and flexible links of arbitrary shapes is considered first, as shown in Fig. 2.1. Then, an arbitrary link i, which is connected to ν_i links at joints O_i, O_i^2, $\cdots$, O_i^k, $\cdots$ and $O_i^{\nu_i}$, is studied.

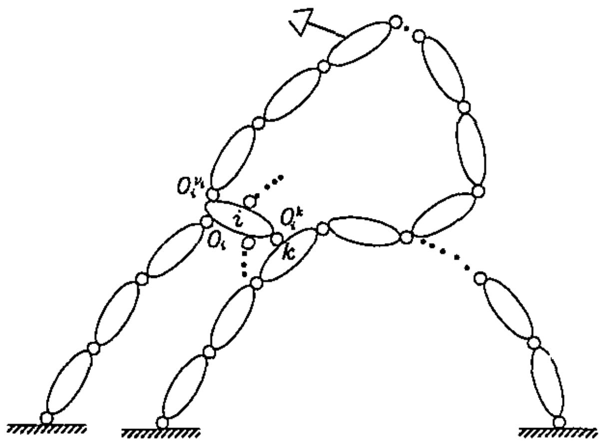

Figure 2.1: A multibody system with kinematic loops

In order to specify the global position and velocity of link i in space, the $n_i'(= 7 + n_i)$-dimensional vector of *flexible-pose* of link i, with n_i determining the number of nodal coordinates of the same link, is defined as

$$\mathbf{q}_i = \begin{bmatrix} \hat{\mathbf{q}}_i^T & \mathbf{r}_i^T & \mathbf{u}_i^T \end{bmatrix}^T \tag{2.1}$$

and the $m_i'(= 6 + n_i)$-dimensional vector of *flexible-twist* of the same link is

$$\mathbf{v}_i = \begin{bmatrix} \boldsymbol{\omega}_i^T & \dot{\mathbf{r}}_i^T & \dot{\mathbf{u}}_i^T \end{bmatrix}^T \tag{2.2}$$

where, with reference to Fig. 2.2,

O_i is the origin of the coordinate frame $X_iY_iZ_i$ ($\mathcal{F}_i$) attached to link i;

$\hat{\mathbf{q}}_i$ is the 4-dimensional vector of Euler parameters representing the orientation of the frame $\mathcal{F}_i$;

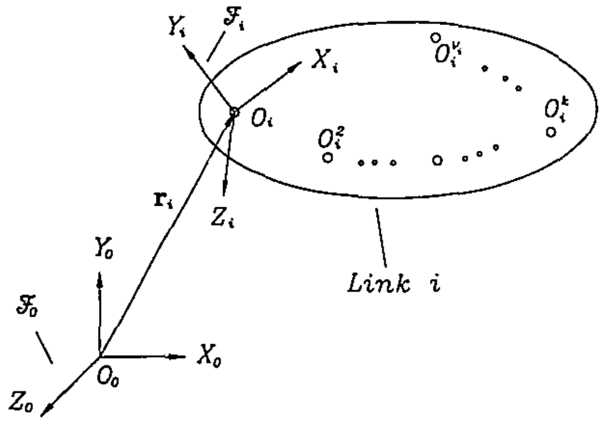

Figure 2.2: An arbitrary link i

$\mathbf{r}_i$ is the position vector of origin O_i in the inertial frame $X_0Y_0Z_0$ ($\mathcal{F}_0$) defining the global position;

$\mathbf{u}_i$ is the n_i-dimensional vector of independent nodal coordinates associated with the link flexibility of link i ($\mathbf{u}_i$ shall be described in more detail later on in this chapter);

$\boldsymbol{\omega}_i$ is the angular velocity of the frame $\mathcal{F}_i$ with respect to $\mathcal{F}_0$.

Moreover, vectors $\mathbf{q}_i$ and $\mathbf{v}_i$, defined in eqs.(2.1) and (2.2), are composed of three parts, the first two are related to the rigid-body motion of link i and the third is related to the generalized coordinates and their time rates of change associated with link flexibility.

Note that the vector of flexible-twist $\mathbf{v}_i$ is not simply the time derivative of the vector of flexible-pose because $\boldsymbol{\omega}_i$ is not a time-derivative of any quantity. One can write instead,

$$\mathbf{v}_i = \mathbf{\Gamma}_i \dot{\mathbf{q}}_i \tag{2.3a}$$

or

$$\dot{\mathbf{q}}_i = \mathbf{\Lambda}_i \mathbf{v}_i \tag{2.3b}$$

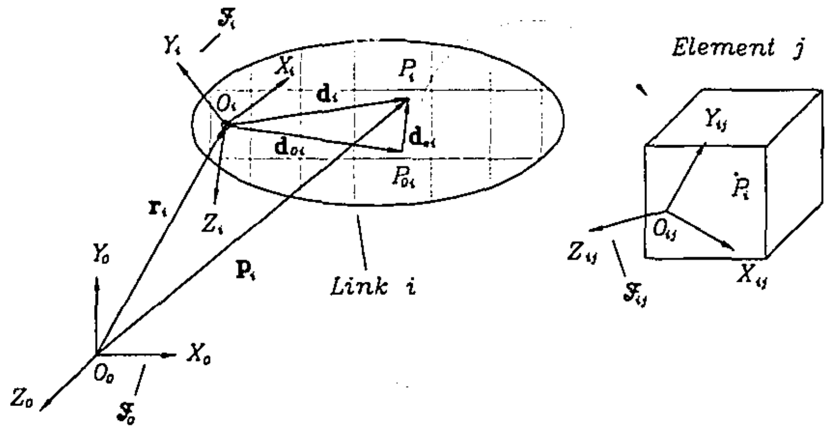

Figure 2.3: Modelling of a flexible link i

where $\mathbf{\Gamma}_i$ is an $m_i' \times n_i'$ matrix, while $\mathbf{\Lambda}_i$ is an $n_i' \times m_i'$ matrix. The forms of $\mathbf{\Gamma}_i$ and $\mathbf{\Lambda}_i$ are found from the relation between ω_i and $\dot{\mathbf{q}}_i$ (Angeles, 1988) and are included in Appendix A.

2.3 Modelling of Flexible Links

From now on, a vector $\mathbf{a}$ or a matrix $\mathbf{A}$ expressed in frame $\mathcal{F}_i$ is represented as $[\mathbf{a}]_i$ or $[\mathbf{A}]_i$, respectively, except for the inertial frame $\mathcal{F}_0$, in which neither brackets nor the subscript 0 are used. Note that the subscripts i and j in all vectors and matrices stand for the labels of link i and element j, respectively.

To model a flexible link, link i is considered as shown in Fig. 2.3. The position vector, in $\mathcal{F}_i$ coordinates, of any point P_i on link i can be written from Fig. 2.3 as

$$[\mathbf{d}_i]_i = [\mathbf{d}_{0i}]_i + [\mathbf{d}_{ei}]_i \tag{2.4}$$

where $[\mathbf{d}_{0i}]_i$ is the position vector of point P_{0i} in the undeformed configuration of link i in frame $\mathcal{F}_i$, while $[\mathbf{d}_{ei}]_i$ is the elastic displacement of point P_i after the deformation of the same link.

To obtain $[\mathbf{d}_{ei}]_i$, an element j, with point P_i being located on it, of link i is considered. The elastic displacement $[\mathbf{d}_{ei}]_{ij}$ of point P_i is first expressed in the $\mathcal{F}_{ij}$ frame, which is attached to the j^{th} element of link i, as shown in Fig. 2.3. The elastic displacement $[\mathbf{d}_{ei}]_{ij}$ can be discretized by the *finite-element method* as follows:

$$[\mathbf{d}_{ei}]_{ij} = \mathbf{L}_{ij}(P_{0i})\mathbf{u}_{ij}(t) \tag{2.5}$$

in which all the quantities have been expressed in the $\mathcal{F}_{ij}$ frame, $\mathbf{L}_{ij}(P_{0i})$ is the $3 \times n_{ij}$ shape-function matrix of element j evaluated at point P_{0i} and $\mathbf{u}_{ij}(t)$ is the n_{ij}-dimensional vector of nodal elastic displacements of that element, with n_{ij} determining the number of nodal elastic displacements of the same element. The form of $\mathbf{L}_{ij}$ depends on the approximation chosen for the problem at hand. The type of the elements used for the flexible links depends on the complexity of the shape of the links (Cook, 1981; Zienkiewicz, 1979). It is assumed that the elastic displacements of link i are small, so that eq.(2.5) can be used. This relation cannot be used for large elastic displacements because the components of matrix $\mathbf{L}_{ij}(P_{0i})$ are only functions of the spatial coordinates.

Furthermore, $\mathbf{u}_{ij}(t)$ can be expressed as a linear transformation of $\mathbf{u}_i(t)$, where $\mathbf{u}_i(t)$ is the vector of independent nodal elastic displacements of the whole link, namely,

$$\mathbf{u}_{ij}(t) = \mathbf{\Phi}_{ij}\mathbf{u}_i(t) \tag{2.6}$$

with $\mathbf{\Phi}_{ij}$ defined as the $n_{ij} \times n_i$ *connectivity matrix* of element j, whose entries are filled with zeros and ones to indicate the locations in $\mathbf{u}_i(t)$ to which elements of $\mathbf{u}_{ij}(t)$ are to be assigned. It may be noted that $\mathbf{u}_i(t)$ is used as generalized coordinates associated with link flexibility, as shown in eq.(2.1).

Moreover, $[\mathbf{d}_{ei}]_i$ and $[\mathbf{d}_{ei}]_{ij}$ can be related by $\mathbf{Y}_{ij}$, the rotation matrix of the

j^{th}-element coordinate system with respect to the frame $\mathcal{F}_i$ as

$$[\mathbf{d}_{ei}]_i = \mathbf{Y}_{ij}[\mathbf{d}_{ei}]_{ij} \tag{2.7}$$

Finally, $[\mathbf{d}_{ei}]_i$ can be expressed using eqs.(2.5)–(2.7) as

$$[\mathbf{d}_{ei}]_i = \mathbf{Y}_{ij}\mathbf{L}_{ij}(P_{0i})\mathbf{\Phi}_{ij}\mathbf{u}_i(t) \tag{2.8}$$

or in a more compact form

$$[\mathbf{d}_{ei}]_i = \mathbf{L}_i(P_{0i})\mathbf{u}_i(t) \tag{2.9}$$

where

$$\mathbf{L}_i(P_{0i}) \equiv \mathbf{Y}_{ij}\mathbf{L}_{ij}(P_{0i})\mathbf{\Phi}_{ij} \tag{2.10}$$

Here, $\mathbf{L}_i(P_{0i})$ is a $3 \times n_i$ matrix. Note that, at any time, one of the $\mathbf{L}_{ij}(P_{0i})$ matrices (the one associated with point P_{0i}) has a nonzero value and the other ones are all zero.

The other component of $[\mathbf{d}_i]_i$ from eq.(2.4), i.e., the position vector $[\mathbf{d}_{0i}]_i$ can now be written as

$$[\mathbf{d}_{0i}]_i = \mathbf{L}^o_{ij}(P_{0i})\mathbf{u}^o_{ij} \tag{2.11}$$

where $\mathbf{u}^o_{ij}$ is the m_{ij}-dimensional nodal rigid-body position vector of element j measured in the frame $\mathcal{F}_i$ and is constant (Nagarajan and Turcic, 1990-a; Zienkiewicz, 1979), while $\mathbf{L}^o_{ij}(P_{0i})$ is the $3 \times m_{ij}$ shape-function matrix for the rigid-body position vector evaluated at point P_{0i} of element j. Moreover, m_{ij} is the dimension of the nodal rigid-body position vector of that element. The m_i-dimensional nodal rigid-body position vector of link i, $\mathbf{u}^o_i$, is related to $\mathbf{u}^o_{ij}$ by

$$\mathbf{u}^o_{ij} = \mathbf{\Phi}^o_{ij}\mathbf{u}^o_i \tag{2.12}$$

where $\mathbf{\Phi}^o_{ij}$ is the $m_{ij} \times m_i$ connectivity matrix of the rigid-body position vector of element j, with m_i determining the dimension of the nodal rigid-body position vector of the link i.

Upon substitution of $\mathbf{u}_{ij}^o$ from eq.(2.12) into eq.(2.11), one obtains

$$[\mathbf{d}_{0i}]_i = \mathbf{L}_i^o(P_{0i})\mathbf{u}_i^o \tag{2.13}$$

in which

$$\mathbf{L}_i^o(P_{0i}) \equiv \mathbf{L}_{ij}^o(P_{0i})\mathbf{\Phi}_{ij}^o \tag{2.14}$$

where $\mathbf{L}_i^o(P_{0i})$ is a $3 \times m_i$ matrix.

Therefore, the position vector $[\mathbf{d}_i]_i$ can be obtained substituting eqs.(2.9) and (2.13) into eq.(2.4) as

$$[\mathbf{d}_i]_i = \mathbf{L}_i^o(P_{0i})\mathbf{u}_i^o + \mathbf{L}_i(P_{0i})\mathbf{u}_i(t) \tag{2.15}$$

2.4 Position Vector and Velocity of a Point on link i

The position vector, in $\mathcal{F}_0$ coordinates, of any point P_i of link i, can be written from Fig. 2.3 as

$$\mathbf{p}_i = \mathbf{r}_i + \mathbf{d}_i = \mathbf{r}_i + \mathbf{R}_i[\mathbf{d}_i]_i \tag{2.16}$$

where $\mathbf{R}_i$ is the rotation matrix of the frame $\mathcal{F}_i$ with respect to the inertial frame, while $\mathbf{d}_i$ and $[\mathbf{d}_i]_i$ are the position vectors of point P_i in $\mathcal{F}_i$ coordinates expressed in $\mathcal{F}_0$- and $\mathcal{F}_i$-coordinates, respectively. Note that, $[\mathbf{d}_i]_i$ is defined in eq.(2.15).

The velocity of point P_i on link i is then obtained by differentiating both sides of eq.(2.16) with respect to time as

$$\dot{\mathbf{p}}_i = \dot{\mathbf{r}}_i + \dot{\mathbf{R}}_i[\mathbf{d}_i]_i + \mathbf{R}_i[\dot{\mathbf{d}}_i]_i \tag{2.17}$$

By differentiating both sides of eq.(2.15) with respect to time and recalling that the first component of $[\mathbf{d}_i]_i$ is constant, $[\dot{\mathbf{d}}_i]_i$ can be expressed as

$$[\dot{\mathbf{d}}_i]_i = \mathbf{L}_i(P_{0i})\dot{\mathbf{u}}_i(t) \tag{2.18}$$

Moreover, by substituting $[\dot{\mathbf{d}}_i]_i$ from eq.(2.18) into eq.(2.17), $\dot{\mathbf{p}}_i$ can be expressed as

$$\dot{\mathbf{p}}_i = \dot{\mathbf{r}}_i + \dot{\mathbf{R}}_i[\mathbf{d}_i]_i + \mathbf{R}_i\mathbf{L}_i(P_{0i})\dot{\mathbf{u}}_i(t) \tag{2.19}$$

where $\dot{\mathbf{R}}_i[\mathbf{d}_i]_i$ can be written as

$$\dot{\mathbf{R}}_i[\mathbf{d}_i]_i \equiv \dot{\mathbf{R}}_i\mathbf{R}_i^T\mathbf{R}_i[\mathbf{d}_i]_i = \dot{\mathbf{R}}_i\mathbf{R}_i^T\mathbf{d}_i \tag{2.20}$$

Now, we use the above equation and take advantage of the relation

$$\dot{\mathbf{R}}_i\mathbf{R}_i^T = \mathbf{\Omega}_i \tag{2.21}$$

where $\mathbf{\Omega}_i$ is the cross-product matrix of the vector $\boldsymbol{\omega}_i$, that can be defined as

$$\mathbf{\Omega}_i \equiv \frac{\partial(\boldsymbol{\omega}_i \times \mathbf{c})}{\partial \mathbf{c}}, \quad \forall \quad \mathbf{c} \tag{2.22}$$

It is then possible to write $\dot{\mathbf{R}}_i[\mathbf{d}_i]_i$ as

$$\dot{\mathbf{R}}_i[\mathbf{d}_i]_i = \mathbf{\Omega}_i\mathbf{d}_i = \boldsymbol{\omega}_i \times \mathbf{d}_i \equiv -\mathbf{D}_i\boldsymbol{\omega}_i \tag{2.23}$$

where $\mathbf{D}_i$ is the cross-product matrix of vector $\mathbf{d}_i$.

Upon substitution of $\dot{\mathbf{R}}_i[\mathbf{d}_i]_i$ from the above equation into eq.(2.19), one obtains $\dot{\mathbf{p}}_i$ as

$$\dot{\mathbf{p}}_i = \dot{\mathbf{r}}_i - \mathbf{D}_i\boldsymbol{\omega}_i + \mathbf{R}_i\mathbf{L}_i(P_{0i})\dot{\mathbf{u}}_i(t) \tag{2.24}$$

Moreover, $\mathbf{D}_i$ in $\mathcal{F}_O$ takes the form

$$\mathbf{D}_i = \mathbf{R}_i[\mathbf{D}_i]_i\mathbf{R}_i^T \tag{2.25}$$

where $[\mathbf{D}_i]_i$ is the cross-product matrix of vector $[\mathbf{d}_i]_i$.

Thus, from eq.(2.24), $\dot{\mathbf{p}}_i$ can be written as a linear transformation of the flexible-twist vector, namely,

$$\dot{\mathbf{p}}_i = \mathbf{W}_i\mathbf{v}_i \tag{2.26}$$

where

$$\mathbf{W}_i = \begin{bmatrix} -\mathbf{D}_i & \mathbf{1}_{33} & \mathbf{R}_i\mathbf{L}_i(P_{0i}) \end{bmatrix} \tag{2.27}$$

$\mathbf{W}_i$ being a $3 \times m'_i$ matrix, while $\mathbf{1}_{33}$ is the 3×3 identity matrix; $\mathbf{v}_i$ is defined in eq.(2.2).

2.5 Formulation of the Kinematic Constraints

In the course of this thesis, it will be assumed that all links are coupled to each other by lower kinematic pairs of the rotational type. Hence, the constraint equations for the system at hand can be expressed in terms of generalized coordinates of the system, i.e, only holonomic systems are considered here. In addition, it is assumed that all joints are rigid. Moreover, the constraint equations are derived in linear homogeneous form in the flexible twists, with possibly time-dependent coefficients. In other words, there are no prescribed motions in the system, and so, the systems considered are assumed to be catastatic.

The twist-constraint equations of the multibody system at hand with kinematic loops, as shown in Fig. 2.1, can be expressed as

$$\mathbf{A}\mathbf{v} = \mathbf{0}_p \tag{2.28}$$

where $\mathbf{v}$ is the $m'(= \sum_{i=1}^{r} m'_i)$-dimensional vector of generalized flexible-twist, which is composed of the vectors of flexible twist of all moving links, namely,

$$\mathbf{v} = \begin{bmatrix} \boldsymbol{\omega}_1^T & \dot{\mathbf{r}}_1^T & \dot{\mathbf{u}}_1^T & \cdots & \boldsymbol{\omega}_r^T & \dot{\mathbf{r}}_r^T & \dot{\mathbf{u}}_r^T \end{bmatrix}^T \tag{2.29}$$

with r defined as the number of all moving links in the system, matrix $\mathbf{A}$ is the $p \times m'$ twist-constraint matrix, and $\mathbf{0}_p$ is the p-dimensional zero vector, with p defined as the number of kinematic constraint equations of the whole system.

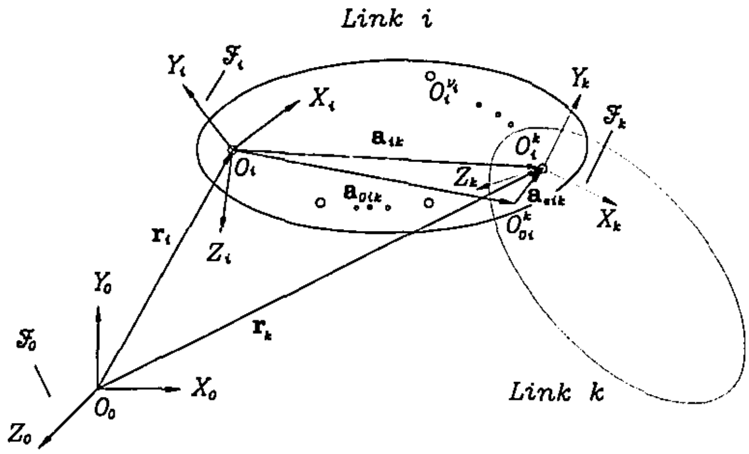

Figure 2.4: Kinematic coupling of links i and k

The twist-constraint matrix can be derived using the kinematic constraint equations of kinematic couplings of the links as a series of equations in terms of the flexible-twist vectors of all moving links.

As an example, we derive the kinematic constraint equations due to the kinematic coupling of links i and k of Fig. 2.1, that are coupled by a revolute joint, as depicted in Fig. 2.4.

The derivation below is the same for the kinematic coupling of link i and all other links. The position vector of point O_i^k, the origin of frame $\mathcal{F}_k$ $(X_k Y_k Z_k)$ attached to link k, as shown in Fig. 2.4, in $\mathcal{F}_0$, takes on the form

$$\mathbf{r}_k = \mathbf{r}_i + \mathbf{a}_{ik} = \mathbf{r}_i + \mathbf{R}_i[\mathbf{a}_{ik}]_i = \mathbf{r}_i + \mathbf{R}_i[\mathbf{a}_{0ik} + \mathbf{a}_{eik}]_i \tag{2.30}$$

where $[\mathbf{a}_{ik}]_i$ can be obtained using eq.(2.15) as

$$[\mathbf{a}_{ik}]_i = \mathbf{L}_i^o(O_{0i,k})\mathbf{u}_i^o + \mathbf{L}_i(O_{0i,k})\mathbf{u}_i(t) \tag{2.31}$$

Here, $\mathbf{L}_i(O_{0i,k})$ and $\mathbf{L}_i^o(O_{0i,k})$ are the same as defined in eqs.(2.10) and (2.14), but evaluated at point O_{0i}^k in the undeformed configuration of link i, and other quantities are as defined earlier.

Upon differentiating both sides of eq.(2.30) with respect to time, one obtains

$$\dot{\mathbf{r}}_k = \dot{\mathbf{r}}_i + \dot{\mathbf{R}}_i[\mathbf{a}_{ik}]_i + \mathbf{R}_i[\dot{\mathbf{a}}_{ik}]_i \tag{2.32}$$

Using eqs.(2.18) and (2.23) and replacing the position vector $[\mathbf{d}_i]_i$ with $[\mathbf{a}_{ik}]_i$, $\dot{\mathbf{r}}_k$ becomes

$$\dot{\mathbf{r}}_k = \dot{\mathbf{r}}_i + \boldsymbol{\omega}_i \times \mathbf{a}_{ik} + \mathbf{R}_i\mathbf{L}_i(O_{0i,k})\dot{\mathbf{u}}_i(t) \tag{2.33}$$

The kinematic constraint equations due to the coupling of links i and k can then be expressed, in light of eq.(2.33), as

$$\boldsymbol{\omega}_k = \boldsymbol{\omega}_i + \dot{\theta}_k\mathbf{z}_k + \mathbf{w}_{ik} \tag{2.34a}$$

$$\dot{\mathbf{r}}_k = \dot{\mathbf{r}}_i + \boldsymbol{\omega}_i \times \mathbf{a}_{ik} + \mathbf{R}_i\mathbf{L}_i(O_{0i,k})\dot{\mathbf{u}}_i(t) \tag{2.34b}$$

where $\boldsymbol{\omega}_k$ is the angular velocity of the frame $\mathcal{F}_k$ with respect to the inertial frame. Moreover, $\mathbf{w}_{ik}$ is the angular velocity of $\mathcal{F}_k$ with respect to $\mathcal{F}_i$, resulting from the elastic displacement of link i, while θ_k is the joint angle and $\mathbf{z}_k$ is the unit vector parallel to the joint axis Z_k.

There are six scalar linear homogeneous equations for each kinematic coupling of the two links, e.g., eqs.(2.34) for coupling of links i and k; it can be readily shown that these equations are linearly dependent (Saha, 1993). In fact, the number of dependent equations are related to the number of degree-of-freedom (DOF) of the kinematic pair, e.g., the number of dependent equations is one for a revolute joint that permits one DOF. Moreover, the general spatial six DOF of a rigid kinematic pair is restricted to one due to the five independent constraint equations for a revolute joint. Here, link i is connected to ν_i links, which leads to $6\nu_i$ kinematic constraint equations. Therefore, the number of twist-constraint equations p is 6ν, where ν is the number of all joints in the system at hand.

2.6 The Natural Orthogonal Complement

For a q-degree-of-freedom (DOF) system, the generalized flexible-twist $\mathbf{v}$ can be expressed as a linear transformation of $\dot{\boldsymbol{\theta}}_I$, which is defined as a q-dimensional vector of independent generalized speeds, namely,

$$\mathbf{v} = \mathbf{N}\dot{\boldsymbol{\theta}}_I \tag{2.35}$$

and $\mathbf{N}$ is an $m' \times q$ matrix.

Upon substitution of $\mathbf{v}$ from eq.(2.35) into eq.(2.28), one obtains

$$\mathbf{A}\mathbf{N}\dot{\boldsymbol{\theta}}_I = \mathbf{0}_p \tag{2.36}$$

Since all the components of $\dot{\boldsymbol{\theta}}_I$ are independent, the above equation holds if and only if

$$\mathbf{A}\mathbf{N} = \mathbf{O}_{pq} \tag{2.37}$$

where $\mathbf{O}_{pq}$ is the $p \times q$ zero matrix.

Therefore, from eq.(2.37), it is apparent that $\mathbf{N}$ is an orthogonal complement of $\mathbf{A}$, which was termed the natural orthogonal complement of $\mathbf{A}$ in (Angeles and Lee, 1988).

The DOF of the multibody mechanical system (Fig. (2.1)), q, is composed of two parts: the rigid-body DOF, q_r, plus the DOF associated with link flexibility, q_e, namely,

$$q = q_r + q_e \tag{2.38}$$

The rigid-body DOF for the system at hand is obtained using Chebyshev-Grübler-Kutzbach formula as

$$q_r = 6r - 5\nu \tag{2.39}$$

where r is defined just after eq.(2.29) and ν is defined already as the number of all joints in the system. It may be noted that the first part of the above equation, i.e, $6r$, determines the DOF for all moving links under no consideration of kinematic coupling of the links, while the second part determines the number of independent constraint equations that arises because of the kinematic joints, which are assumed to be all revolute. The DOF associated with link flexibility can be written as

$$q_e = \sum_{i=1}^{r_f} n_i \tag{2.40}$$

Here, n_i is defined just before eq.(2.1) and r_f is the number of all flexible links in the system. Therefore, upon substitution of eqs.(2.39) and (2.40) into eq.(2.38), one obtains the DOF of the system as

$$q = 6r - 5\nu + \sum_{i=1}^{r_f} n_i \tag{2.41}$$

2.7 Formulation of the Problem in Cartesian and in Joint Spaces

It is apparent from eq.(2.35) that the form of $\mathbf{N}$ depends on the definition of $\dot{\boldsymbol{\theta}}_I$. The vector of independent generalized speeds $\dot{\boldsymbol{\theta}}_I$ depends, in turn, on whether the system is being modelled in joint space or in Cartesian space. The formulation of the problem in joint and in Cartesian spaces are discussed in the subsections below.

2.7.1 Formulation of the Problem in Joint Space

In open-chain systems, vector $\dot{\boldsymbol{\theta}}_I$ is usually composed of joint speeds plus the generalized speeds associated with link flexibility. All joints are actuated and independent of each other so that they can be considered as components of the vector of independent generalized speeds. Therefore, the components of $\mathbf{v}$ can be specified in terms of $\dot{\boldsymbol{\theta}}_I$, which leads to $\mathbf{N}$ by using the equations constraining only the twists of the two coupled links, i.e, eqs.(2.34).

On the other hand, not all joints are actuated in systems with kinematic loops. Here, the ϑ-dimensional vector of generalized coordinates can be defined as

$$\boldsymbol{\theta} = \begin{bmatrix} \boldsymbol{\theta}_I^T & \boldsymbol{\theta}_D^T \end{bmatrix}^T \tag{2.42}$$

where $\boldsymbol{\theta}_I$ is the q-dimensional vector of independent generalized coordinates comprising the vector of actuated joint angles and generalized coordinates associated with link flexibility and $\boldsymbol{\theta}_D$ is the $(\vartheta - q)$-dimensional vector of dependent generalized coordinates consists of the vector of unactuated joint angles. The loop-constraint equations, which are usually nonlinear, allow one to solve numerically for the dependent generalized coordinates in terms of the independent ones. The form of the loop-constraint equations for different examples will be obtained later in detail.

Additionally, $\dot{\boldsymbol{\theta}}_D$ can be expressed in terms of $\dot{\boldsymbol{\theta}}_I$ as follows: Upon differentiating the loop-constraint equations with respect to time one obtains

$$\mathbf{N}_I\dot{\boldsymbol{\theta}}_I + \mathbf{N}_D\dot{\boldsymbol{\theta}}_D = \mathbf{0}_l \tag{2.43}$$

where $\mathbf{N}_I$ is an $l \times q$ matrix and $\mathbf{N}_D$ is an $l \times (\vartheta - q)$ matrix, with l denoting the number of loop-constraint equations, while $\mathbf{0}_l$ is the l-dimensional zero vector. Note that, usually, $l = \vartheta - q$, i.e, the number of loop-constraint equations equals the number of dependent joint angles in the system. Hence, $\dot{\boldsymbol{\theta}}_D$ can be expressed as a linear transformation of $\dot{\boldsymbol{\theta}}_I$, namely,

$$\dot{\boldsymbol{\theta}}_D = -\mathbf{N}_D^{-1}\mathbf{N}_I\dot{\boldsymbol{\theta}}_I \tag{2.44}$$

The components of vector $\mathbf{v}$ from eq.(2.29) can now be expressed in terms of the independent generalized speeds by substituting $\dot{\boldsymbol{\theta}}_D$ from eq.(2.44) into the kinematic constraint equations, i.e., eqs.(2.34). Finally, using eq.(2.35) leads to $\mathbf{N}$, which is the linear transformation mapping the independent generalized speeds into the generalized flexible-twist.

This procedure, however, needs some time-consuming kinematical analysis, e.g., the direct kinematics solution in case of a parallel manipulator. Nevertheless, we will show that there is no need for this task in formulating the problem in Cartesian space.

2.7.2 Formulation of the Problem in Cartesian Space

Vector $\dot{\boldsymbol{\theta}}_I$ can be defined, in Cartesian space, as the array containing the end-effector flexible-twist plus the generalized speeds associated with link flexibility, namely,

$$\dot{\boldsymbol{\theta}}_I = \begin{bmatrix} \boldsymbol{\omega}_r^T & \dot{\mathbf{r}}_r^T & \dot{\mathbf{u}}_r^T & \dot{\mathbf{u}}_1^T & \dot{\mathbf{u}}_2^T & \cdots & \dot{\mathbf{u}}_{r-1}^T \end{bmatrix}^T \tag{2.45}$$

where $\boldsymbol{\omega}_r$, $\dot{\mathbf{r}}_r$ and $\dot{\mathbf{u}}_r$ are the end-effector flexible-twist. The formulation of the problem in Cartesian space is possible when the end-effector motion is prescribed, as is the case in many applications. Matrix $\mathbf{N}$ can then be evaluated using the equations expressing vector $\mathbf{v}$ in terms of $\dot{\boldsymbol{\theta}}_I$ and resorting to the linear relations between the flexible twists of the links and $\dot{\boldsymbol{\theta}}_I$. Then, using the kinematic constraint equations and rearranging the expressions thus resulting, one obtains expressions for all components of $\mathbf{v}$, eq.(2.29), in terms of $\dot{\boldsymbol{\theta}}_I$. Therefore, vector $\mathbf{v}$ can be specified as a linear transformation of $\dot{\boldsymbol{\theta}}_I$, which leads to $\mathbf{N}$.

The approaches explained in Subsections 2.7.1 and 2.7.2 will be examined later in detail with different examples to show how $\dot{\boldsymbol{\theta}}_I$ and matrix $\mathbf{N}$ are derived for robotic manipulators with kinematic loops.

Chapter 3

Dynamics of Multibody Systems with Kinematic Loops and Flexible Links

3.1 Introduction

As mentioned in Chapter 1, many methods for modelling the dynamics of robotic mechanical systems have been reported, namely, Newton-Euler, Lagrange equations, virtual-work principle, Hamilton's principle, and Kane's method, also known as Lagrange's form of d'Alembert's principle. Among them, the Lagrange equations (Nagarajan and Turcic, 1990-a; Bricout et al., 1990; Serna and Bayo, 1989; Cyril et al., 1991), and Kane's method (Kane and Levinson, 1983; Everett, 1989; Ider and Amirouche, 1989–b; Banerjee and Lemak, 1991) have been found to be more efficient for modelling the dynamics of mechanical systems with flexible links.

Some researchers derived the equations of motion of an individual body first and then obtained the model of the mechanical system by assembling all the bodies together (Sunada and Dubowsky, 1983; Nagrajan and Turcic, 1990; Cyril et al, 1991). The drawback of this method is to consider the kinematic-constraint forces which should be eliminated from the equations of motion. On the other hand, other investigators considered the mechanical system as a whole and derived the equations of motion for the whole system. As an example, Lieh (1991) used the virtual-work principle to derive directly the equations of motion of flexible-link manipulators for the whole system. The drawback of this approach is that it leads to lengthy, and cumbersome equations.

In this chapter, the equations of motion of an individual link are first derived for an uncoupled body using the Lagrange equations. Here, nodal coordinates are transformed into modal coordinates to reduce the number of generalized coordinates associated with the link flexibility. The effect of geometric nonlinearities in the elastic displacements is considered by adding a term to the elastic strain energy which requires introduction of a geometric stiffness matrix in addition to the conventional one. This consideration results in compensating for the errors caused by the use of finite-element analyses and modal coordinates together with the classical theory of elasticity in high-speed operations, as mentioned in the previous chapter. Thus, large rigid-body motions can be considered even in high-speed operations.

Then, the governing equations of motion of the entire mechanical system is obtained by assembling all the links together. The method of the natural orthogonal complement, applied previously to systems with open-chain or single-closed chain structures, is used to eliminate the constraint forces and to derive the minimum number of equations of motion.

3.2 Dynamics of Link i

Basic to any modelling of a mechanical system is the understanding of the dynamics of each link. To this end, the position and velocity vectors of any point on link i, which were obtained in the previous chapter, are used to model link i. First, an expression for the kinetic energy of the link is derived in terms of the link mass matrix. Then, the elastic strain energy due to the elastic displacements of the link is obtained in terms of the conventional stiffness matrix plus the geometric stiffness matrix. Next, the nodal coordinates are transformed to modal coordinates in order to reduce the number of the generalized coordinates. Finally, the Lagrange equations of motion for link i are derived without consideration of kinematic couplings.

3.2.1 Kinetic Energy of Link i

The kinetic energy of link i is given by

$$T_i = \int_{v_i} \frac{1}{2}\dot{\mathbf{p}}_i^T\dot{\mathbf{p}}_i\rho_i dv_i \tag{3.1}$$

where ρ_i and v_i are the mass density and volume of the i^{th} link, respectively. It may be pointed out that the expression inside the integral is integrated over the entire volume of all the elements of link i. Moreover, for each element, the proper value of $\dot{\mathbf{p}}_i$ should be chosen from eq.(2.26), in light of eqs.(2.27) and (2.10).

Introducing the values of $\dot{\mathbf{p}}_i$ from eq.(2.26) into eq.(3.1) yields

$$T_i = \int_{v_i} \frac{1}{2}\mathbf{v}_i^T\mathbf{W}_i^T\mathbf{W}_i\mathbf{v}_i\rho_i dv_i \tag{3.2}$$

The kinetic energy can thus be written as a quadratic form in the flexible twist, namely,

$$T_i = \frac{1}{2}\mathbf{v}_i^T\mathbf{M}_i\mathbf{v}_i \tag{3.3}$$

where $\mathbf{M}_i$ is the $m_i' \times m_i'$ positive-definite and symmetric mass matrix of link i, defined as

$$\mathbf{M}_i = \int_{v_i} \rho_i \mathbf{W}_i^T \mathbf{W}_i dv_i \tag{3.4}$$

Matrix $\mathbf{M}_i$ can be obtained by inserting $\mathbf{W}_i$ from eq.(2.27) into eq.(3.4), namely,

$$\mathbf{M}_i = \int_{v_i} \begin{bmatrix} -\mathbf{D}_i^2 & \mathbf{D}_i & \mathbf{D}_i\mathbf{R}_i\mathbf{L}_i(P_{0i}) \\ -\mathbf{D}_i & \mathbf{1}_{33} & \mathbf{R}_i\mathbf{L}_i(P_{0i}) \\ -\mathbf{L}_i^T(P_{0i})\mathbf{R}_i^T\mathbf{D}_i & \mathbf{L}_i^T(P_{0i})\mathbf{R}_i^T & \mathbf{L}_i^T(P_{0i})\mathbf{L}_i(P_{0i}) \end{bmatrix} \rho_i dv_i \tag{3.5a}$$

in which all quantities were defined in eq.(2.27).

Thus, $\mathbf{M}_i$ can be written in block form as

$$\mathbf{M}_i = \begin{bmatrix} \mathbf{M}_i^{rr} & \mathbf{M}_i^{rd} & \mathbf{M}_i^{re} \\ \mathbf{M}_i^{dr} & \mathbf{M}_i^{dd} & \mathbf{M}_i^{de} \\ \mathbf{M}_i^{er} & \mathbf{M}_i^{ed} & \mathbf{M}_i^{ee} \end{bmatrix} \tag{3.5b}$$

where

$$\mathbf{M}_i^{rr} \equiv -\int_{v_i} \rho_i \mathbf{D}_i^2 dv_i \tag{3.5c}$$

$$\mathbf{M}_i^{rd} = (\mathbf{M}_i^{dr})^T \equiv \int_{v_i} \rho_i \mathbf{D}_i dv_i \tag{3.5d}$$

$$\mathbf{M}_i^{re} = (\mathbf{M}_i^{er})^T \equiv \int_{v_i} \rho_i \mathbf{D}_i\mathbf{R}_i\mathbf{L}_i(P_{0i}) dv_i \tag{3.5e}$$

$$\mathbf{M}_i^{dd} \equiv \int_{v_i} \rho_i \mathbf{1}_{33} dv_i \tag{3.5f}$$

$$\mathbf{M}_i^{de} = (\mathbf{M}_i^{ed})^T \equiv \int_{v_i} \rho_i \mathbf{R}_i\mathbf{L}_i(P_{0i}) dv_i \tag{3.5g}$$

$$\mathbf{M}_i^{ee} \equiv \int_{v_i} \rho_i \mathbf{L}_i^T(P_{0i})\mathbf{L}_i(P_{0i}) dv_i \tag{3.5h}$$

in which $\mathbf{M}_i^{rr}$, $\mathbf{M}_i^{rd}$ and $\mathbf{M}_i^{dd}$ are all 3×3 matrices, while $\mathbf{M}_i^{de}$ and $\mathbf{M}_i^{re}$ are $3 \times n_i$ matrices and $\mathbf{M}_i^{ee}$ is an $n_i \times n_i$ matrix, with n_i as defined in eq.(2.1). Moreover, $\mathbf{1}_{33}$ is the 3×3 identity matrix.

Inserting $\mathbf{D}_i$ from eq.(2.25) into eq.(3.5c) and noting that

$$[\mathbf{D}_i]_i = -[\mathbf{D}_i]_i^T \tag{3.6}$$

with the understanding that the rotation matrix of link i, $\mathbf{R}_i$, is not a function of v_i, matrix $\mathbf{M}_i^{rr}$ can be written as

$$\mathbf{M}_i^{rr} = \mathbf{R}_i \mathbf{V}_i^{rr} \mathbf{R}_i^T \tag{3.7}$$

In the foregoing equation, $\mathbf{V}_i^{rr}$ is the 3×3 symmetric matrix defined as

$$\mathbf{V}_i^{rr} \equiv \int_{v_i} [\mathbf{D}_i]_i^T [\mathbf{D}_i]_i \rho_i dv_i \tag{3.8}$$

where $[\mathbf{D}_i]_i^T[\mathbf{D}_i]_i$ can be expressed in terms of vector $[\mathbf{d}_i]_i$ as

$$[\mathbf{D}_i]_i^T [\mathbf{D}_i]_i = \|[\mathbf{d}_i]_i\|^2 \mathbf{1}_{33} - [\mathbf{d}_i]_i [\mathbf{d}_i]_i^T \equiv \|\mathbf{d}_i\|^2 \mathbf{1}_{33} - [\mathbf{d}_i \mathbf{d}_i^T]_i \tag{3.9}$$

The last equality follows because the Euclidean norm is frame-invariant. Moreover, the components of vector $[\mathbf{d}_i]_i$ are

$$d_j = \mathbf{l}_j^T \mathbf{u}_i(t) + (\mathbf{l}_j^o)^T \mathbf{u}_i^o \quad j = 1,2,3 \tag{3.10}$$

where d_j is the j^{th} component of $[\mathbf{d}_i]_i$, while $\mathbf{l}_j^T$ and $(\mathbf{l}_j^o)^T$ are j^{th} rows of matrices $\mathbf{L}_i(P_{0i})$ and $\mathbf{L}_i^o(P_{0i})$, defined in eqs.(2.10) and (2.14), respectively. Furthermore, $\mathbf{u}_i(t)$ and $\mathbf{u}_i^o$ are n_i- and m_i-dimensional vectors, as defined in eqs.(2.6) and (2.12). Now, we introduce 27 constant matrices, namely,

$$\mathbf{C}_{kj}^{i3} = \int_{v_i} \mathbf{l}_j \mathbf{l}_k^T \rho_i dv_i \tag{3.11a}$$

$$\mathbf{C}_{kj}^{i4} = \int_{v_i} \mathbf{l}_j^o (\mathbf{l}_k^o)^T \rho_i dv_i \tag{3.11b}$$

$$\mathbf{C}_{kj}^{i5} = \int_{v_i} \mathbf{l}_j (\mathbf{l}_k^o)^T \rho_i dv_i \tag{3.11c}$$

in which $k = 1,2,3$ and $j = 1,2,3$. It is then possible to express the components of $\mathbf{V}_i^{rr}$ as

$$v_i^{11} = \mathbf{u}_i^T(t)(\mathbf{C}_{22}^{i3} + \mathbf{C}_{33}^{i3})\mathbf{u}_i(t) + 2\mathbf{u}_i^T(t)(\mathbf{C}_{22}^{i5} + \mathbf{C}_{33}^{i5})\mathbf{u}_i^o + \mathbf{u}_i^{oT}(\mathbf{C}_{22}^{i4} + \mathbf{C}_{33}^{i4})\mathbf{u}_i^o \tag{3.12a}$$

$$v_i^{12} = v_i^{21} = -\left[\mathbf{u}_i^T(t)\mathbf{C}_{12}^{i3}\mathbf{u}_i(t) + \mathbf{u}_i^T(t)\left(\mathbf{C}_{12}^{i5} + \mathbf{C}_{21}^{i5}\right)\mathbf{u}_i^o + \mathbf{u}_i^{oT}\mathbf{C}_{12}^{i4}\mathbf{u}_i^o\right] \tag{3.12b}$$

while other components are obtained by using suitable permutations. Here, $\mathbf{C}_{kj}^{i3}$, $\mathbf{C}_{kj}^{i4}$ and $\mathbf{C}_{kj}^{i5}$ are $n_i \times n_i$, $m_i \times m_i$ and $n_i \times m_i$ matrices, respectively.

Upon substitution of $\mathbf{D}_i$ from eq.(2.25), into $\mathbf{M}_i^{rd}$ and expanding the equation thus resulting, one obtains

$$\mathbf{M}_i^{rd} = \int_{v_i} \mathbf{R}_i[\mathbf{D}_i]_i \mathbf{R}_i^T \rho_i dv_i = \mathbf{R}_i \left\{ \int_{v_i} \frac{\partial}{\partial \mathbf{c}}([\mathbf{d}_i]_i \times \mathbf{c})\rho_i dv_i \right\} \mathbf{R}_i^T \quad \forall \mathbf{c} \quad (3.13)$$

Using eq.(2.15) for $[\mathbf{d}_i]_i$ and noting that $\mathbf{u}_i(t)$ and $\mathbf{u}_i^o$ are not functions of v_i, $\mathbf{M}_i^{rd}$ can be written as

$$\mathbf{M}_i^{rd} = \mathbf{R}_i \mathbf{V}_i^{rd} \mathbf{R}_i^T \quad (3.14a)$$

in which $\mathbf{V}_i^{rd}$ is the cross-product matrix of vector $\mathbf{v}_i^{rd}$, defined, in turn, as

$$\mathbf{v}_i^{rd} = \mathbf{C}^{i1}\mathbf{u}_i(t) + \mathbf{C}^{i2}\mathbf{u}_i^o \quad (3.14b)$$

where $\mathbf{C}^{i1}$ and $\mathbf{C}^{i2}$ are $3 \times n_i$ and $3 \times m_i$ constant matrices, defined as

$$\mathbf{C}^{i1} \equiv \int_{v_i} \mathbf{L}_i(P_{0i})\rho_i dv_i \quad (3.15a)$$

$$\mathbf{C}^{i2} \equiv \int_{v_i} \mathbf{L}_i^o(P_{0i})\rho_i dv_i \quad (3.15b)$$

Moreover, $\mathbf{L}_i(P_{0i})$ and $\mathbf{L}_i^o(P_{0i})$ are defined in eqs.(2.10) and (2.14), respectively.

Finally, expanding eqs.(3.5e), (3.5g) and (3.5h), $\mathbf{M}_i^{re}$, $\mathbf{M}_i^{de}$ and $\mathbf{M}_i^{ee}$ are obtained as

$$\mathbf{M}_i^{re} = \mathbf{R}_i \mathbf{V}_i^{re} \quad (3.16a)$$

$$\mathbf{M}_i^{de} = \mathbf{R}_i \mathbf{C}^{i1} \quad (3.16b)$$

$$\mathbf{M}_i^{ee} = \mathbf{C}_{11}^{i3} + \mathbf{C}_{22}^{i3} + \mathbf{C}_{33}^{i3} \quad (3.16c)$$

in which

$$\mathbf{V}_i^{re} = \begin{bmatrix} \mathbf{u}_i^T(t)\,(\mathbf{C}_{32}^{i3} - \mathbf{C}_{23}^{i3}) + \mathbf{u}_i^{oT}\,(\mathbf{C}_{23}^{i5} - \mathbf{C}_{32}^{i5})^T \\ \mathbf{u}_i^T(t)\,(\mathbf{C}_{13}^{i3} - \mathbf{C}_{31}^{i3}) + \mathbf{u}_i^{oT}\,(\mathbf{C}_{31}^{i5} - \mathbf{C}_{13}^{i5})^T \\ \mathbf{u}_i^T(t)\,(\mathbf{C}_{21}^{i3} - \mathbf{C}_{12}^{i3}) + \mathbf{u}_i^{oT}\,(\mathbf{C}_{12}^{i5} - \mathbf{C}_{21}^{i5})^T \end{bmatrix} \quad (3.16d)$$

It may be noted that all constant integrals can be calculated off-line and the results can then be used to develop the mass matrix of link i.

3.2.2 Potential Energy of Link i

The potential energy of link i comprises two parts: the elastic strain energy and the potential energy due to other sources such as gravity. The latter will be considered later in this chapter. The elastic strain energy of the element j of link i, as shown in Fig. 2.3, can be written as

$$V_{ij} = V_{ij}^{e} + V_{ij}^{gn} \tag{3.17}$$

where V_{ij}^{e} is the standard elastic strain energy of the element j of link i (Cook, 1981; Zienkiewicz, 1979), namely,

$$V_{ij}^{e} = \frac{1}{2}\mathbf{u}_{ij}^{T}(t)\mathbf{K}_{ij}^{e}\mathbf{u}_{ij}(t) \tag{3.18}$$

where $\mathbf{u}_{ij}(t)$ is defined in eq.(2.5) and $\mathbf{K}_{ij}^{e}$ is the $n_{ij} \times n_{ij}$ conventional stiffness matrix of element j of link i, and can be obtained for different types of elements from the literature, e.g. (Przemieniecki, 1967), or from direct integration formulas (Cook, 1981). The elastic strain energy V_{ij}^{gn} arises because of the effect of geometric nonlinearities in the elastic displacements of element j of link i, namely,

$$V_{ij}^{gn} = \frac{1}{2}\mathbf{u}_{ij}^{T}(t)\mathbf{K}_{ij}^{gn}\mathbf{u}_{ij}(t) \tag{3.19}$$

where $\mathbf{K}_{ij}^{gn}$ is the geometric stiffness matrix, to be obtained in Subsection 3.2.3.

Introducing V_{ij}^{e} and V_{ij}^{gn} from eqs.(3.18) and (3.19) into eq.(3.17), one obtains

$$V_{ij} = \frac{1}{2}\mathbf{u}_{i}^{T}(t)\mathbf{K}_{ij}\mathbf{u}_{i}(t) \tag{3.20}$$

in which

$$\mathbf{K}_{ij} = \mathbf{K}_{ij}^{e} + \mathbf{K}_{ij}^{gn} \tag{3.21}$$

Therefore, the stiffness matrix $\mathbf{K}_{ij}$ can be thought of as composed of two parts: the conventional stiffness matrix, which is constant, plus a geometric stiffness matrix, which is configuration-dependent.

The elastic strain energy can be written for link i by assembling the stiffness matrices of all elements as

$$V_i = \frac{1}{2}\mathbf{u}_i^T(t)\mathbf{K}_i^f\mathbf{u}_i(t) \tag{3.22}$$

where $\mathbf{u}_i(t)$ was defined in eq.(2.6), while the $n_i \times n_i$ stiffness matrix $\mathbf{K}_i^f$ of link i is a matrix defined as

$$\mathbf{K}_i^f = \sum_{j=1}^{\kappa_i}\mathbf{\Phi}_{ij}^T\mathbf{K}_{ij}\mathbf{\Phi}_{ij} \tag{3.23}$$

where $\mathbf{\Phi}_{ij}$ was defined in eq.(2.6) and κ_i is the number of elements of link i.

It is also possible to write the elastic strain energy in terms of the flexible pose $\mathbf{q}_i$ of link i, namely,

$$V_i = \frac{1}{2}\mathbf{q}_i^T\mathbf{K}_i\mathbf{q}_i \tag{3.24}$$

in which $\mathbf{K}_i$, the $n_i' \times n_i'$ stiffness matrix of link i, is defined as

$$\mathbf{K}_i = \begin{bmatrix} \mathbf{O}_{44} & \mathbf{O}_{43} & \mathbf{O}_{4n_i} \\ \mathbf{O}_{34} & \mathbf{O}_{33} & \mathbf{O}_{3n_i} \\ \mathbf{O}_{n_i4} & \mathbf{O}_{n_i3} & \mathbf{K}_i^f \end{bmatrix} \tag{3.25}$$

Here, $\mathbf{O}_{mn}$ is the $m \times n$ zero matrix.

3.2.3 Effect of Geometric Nonlinearities in the Elastic Displacements

High-speed operations give rise to significant coupling of the longitudinal and transverse displacements of the flexible links of multibody systems. This coupling results from consideration of the effect of geometric nonlinearities in the elastic displacements of the flexible links. As a simple example, in a laterally loaded beamed-shaped link, it accounts for the fact that axial compression tends to increase the transverse displacement and, thus, decrease transverse stiffness, while axial tension tends to decrease the transverse displacement and, thus, increase the transverse stiffness. This is the effect of geometric stiffening that has been introduced for the modelling of the rotating beams by Likins (1974).

The effect of geometric nonlinearities in the elastic displacements of the flexible links arises because of a term that should be added to the standard elastic strain energy of the element j of link i, i.e., V_{ij}^{gn}. This term can be written as

$$V_{ij}^{gn} = \int_{v_{ij}} [\epsilon^{nl}]_{ij}^T [\boldsymbol{\sigma}]_{ij} dv_{ij} \tag{3.26}$$

in which $[\boldsymbol{\sigma}]_{ij}$ and $[\epsilon^{nl}]_{ij}$ are 6-dimensional vectors of state stress because of the inertia loading and nonlinear terms in Green's strain tensor (Novozhilov, 1961), respectively, i.e.,

$$[\boldsymbol{\sigma}]_{ij} = \begin{bmatrix} \sigma_{XX} & \sigma_{YY} & \sigma_{ZZ} & \sigma_{XY} & \sigma_{XZ} & \sigma_{YZ} \end{bmatrix}_{ij}^T \tag{3.27a}$$

$$\left[\epsilon^{nl}\right]_{ij} = \begin{bmatrix} \epsilon_{XX} & \epsilon_{YY} & \epsilon_{ZZ} & \epsilon_{XY} & \epsilon_{XZ} & \epsilon_{YZ} \end{bmatrix}_{ij}^T \tag{3.27b}$$

Here,

$$[\epsilon_{XX}]_{ij} = \frac{1}{2}\left[(\frac{\partial u}{\partial X})^2 + (\frac{\partial v}{\partial X})^2 + (\frac{\partial w}{\partial X})^2\right]_{ij} \tag{3.27c}$$

$$[\epsilon_{YY}]_{ij} = \frac{1}{2}\left[(\frac{\partial u}{\partial Y})^2 + (\frac{\partial v}{\partial Y})^2 + (\frac{\partial w}{\partial Y})^2\right]_{ij} \tag{3.27d}$$

$$[\epsilon_{ZZ}]_{ij} = \frac{1}{2}\left[(\frac{\partial u}{\partial Z})^2 + (\frac{\partial v}{\partial Z})^2 + (\frac{\partial w}{\partial Z})^2\right]_{ij} \tag{3.27e}$$

$$[\epsilon_{XY}]_{ij} = \left[\frac{\partial u}{\partial X}\frac{\partial u}{\partial Y} + \frac{\partial v}{\partial X}\frac{\partial v}{\partial Y} + \frac{\partial w}{\partial X}\frac{\partial w}{\partial Y}\right]_{ij} \tag{3.27f}$$

$$[\epsilon_{XZ}]_{ij} = \left[\frac{\partial u}{\partial X}\frac{\partial u}{\partial Z} + \frac{\partial v}{\partial X}\frac{\partial v}{\partial Z} + \frac{\partial w}{\partial X}\frac{\partial w}{\partial Z}\right]_{ij} \tag{3.27g}$$

$$[\epsilon_{YZ}]_{ij} = \left[\frac{\partial u}{\partial Y}\frac{\partial u}{\partial Z} + \frac{\partial v}{\partial Y}\frac{\partial v}{\partial Z} + \frac{\partial w}{\partial Y}\frac{\partial w}{\partial Z}\right]_{ij} \tag{3.27h}$$

where u_{ij}, v_{ij} and w_{ij} are the three components of the elastic displacements $[\mathbf{d}_{ei}]_{ij}$ from eq.(2.5). Moreover, X_{ij}, Y_{ij} and Z_{ij} are three orthogonal axes, as shown in Fig. 2.3. Furthermore, the state stress vector $[\boldsymbol{\sigma}]_{ij}$ is the same as explained in

Banerjee and Lemak (1991), i.e., it is a 6-dimensional array containing the distinct entries of the stress tensor.

Using the same approach as in Zienkiewicz (1979), V_{ij}^{gn} can be written as

$$V_{ij}^{gn} = \frac{1}{2}\mathbf{u}_{ij}^T\mathbf{K}_{ij}^{gn}\mathbf{u}_{ij} \tag{3.28}$$

Hence, $\mathbf{K}_{ij}^{gn}$ can be obtained as

$$\mathbf{K}_{ij}^{gn} = \int_{v_{ij}} \mathbf{H}_{ij}^T\mathbf{\Sigma}_{ij}\mathbf{H}_{ij}dv_{ij} \tag{3.29}$$

in which $\mathbf{\Sigma}_{ij}$ is the 9×9 matrix defined as

$$\mathbf{\Sigma}_{ij} = \begin{bmatrix} (\sigma_{XX})_{ij}\mathbf{1}_{33} & (\sigma_{XY})_{ij}\mathbf{1}_{33} & (\sigma_{XZ})_{ij}\mathbf{1}_{33} \\ (\sigma_{XY})_{ij}\mathbf{1}_{33} & (\sigma_{YY})_{ij}\mathbf{1}_{33} & (\sigma_{YZ})_{ij}\mathbf{1}_{33} \\ (\sigma_{XZ})_{ij}\mathbf{1}_{33} & (\sigma_{YZ})_{ij}\mathbf{1}_{33} & (\sigma_{ZZ})_{ij}\mathbf{1}_{33} \end{bmatrix} \tag{3.30}$$

with $\mathbf{H}_{ij}$ being the $9 \times n_{ij}$ matrix defined, in turn, as

$$\mathbf{H}_{ij} = \begin{bmatrix} \partial\mathbf{L}_{ij}(P_{0i})/\partial X_{ij} \\ \partial\mathbf{L}_{ij}(P_{0i})/\partial Y_{ij} \\ \partial\mathbf{L}_{ij}(P_{0i})/\partial Z_{ij} \end{bmatrix} \tag{3.31}$$

where $\mathbf{L}_{ij}(P_{0i})$ is the $3 \times n_{ij}$ matrix defined in eq.(2.5), and $\mathbf{1}_{33}$ is the 3×3 identity matrix. The form of $\mathbf{K}_{ij}^{gn}$ will be obtained later for links that can be modelled as beams. An empirical speed limit can be used as a condition where the effect of geometric nonlinearities in elastic displacements of the flexible links becomes significant. This limit can be defined as follows: if the ratio of the rigid-body angular rates to the lowest natural frequency of the system be of the order 0.1 or more, the effect of geometric nonlinearities should be considered.

3.2.4 Modal Coordinates

In large mechanical systems, using finite elements results in quite a large dimension of the flexible-pose $\mathbf{q}_i$ and the flexible-twist $\mathbf{v}_i$ of link i, because of the number of nodal coordinates of the same link. The number of nodal coordinates can be reduced by changing the nodal coordinates to modal coordinates, using the standard component-mode technique (Hurty, 1965), as explained below.

The n_i-dimensional vector of nodal coordinates $\mathbf{u}_i(t)$, as defined in eq.(2.6), and the l_i-dimensional vector of modal coordinates of link i, $\mathbf{u}_i^m(t)$, can be related as:

$$\mathbf{u}_i(t) = \mathbf{\Psi}_{im}\mathbf{u}_i^m(t) \tag{3.32}$$

where $\mathbf{\Psi}_{im}$ is the $n_i \times l_i$ modal matrix, which can be evaluated by computing the normal modes of link i. The n_i normal modes of the elastic displacement of the same link can be evaluated by solving the eigenvalue problem derived from the model, namely,

$$\mathbf{M}_i^{ee}\ddot{\mathbf{u}}_i(t) + \mathbf{K}_i^f\mathbf{u}_i(t) = \mathbf{0}_{n_i} \tag{3.33}$$

where $\mathbf{0}_{n_i}$ is the n_i-dimensional zero vector and $\mathbf{M}_i^{ee}$ was defined in eq.(3.5h). Moreover, $\mathbf{K}_i^f$ is the same as given in eq.(3.23), unless only the conventional stiffness matrix $\mathbf{K}_{ij}^e$ is used to derive $\mathbf{K}_{ij}$.

By choosing the first l_i eigenvectors (mode shapes) of the above model, $\mathbf{\Psi}_{im}$ takes on the form

$$\mathbf{\Psi_{im}} = \begin{bmatrix} \psi^1 & \psi^2 & \dots & \psi^{l_i} \end{bmatrix}_i \tag{3.34}$$

where ψ_i^j, the j^{th} column of $\mathbf{\Psi}_{im}$, is an n_i-dimensional eigenvector. The value of l_i is chosen based on the desired accuracy for the computation and also the CPU time. It will be shown later how l_i is chosen for different numerical examples.

Upon substitution of $\mathbf{u}_i(t)$ from eq.(3.32) into eq.(2.9), the elastic displacement of any point P_i of link i, $[\mathbf{d}_{ei}]_i$, can be written in terms of modal coordinates as

$$[\mathbf{d}_{ei}]_i = \mathbf{L}_i^m(P_{0i})\mathbf{u}_i^m(t) \tag{3.35}$$

with

$$\mathbf{L}_i^m(P_{0i}) \equiv \mathbf{L}_i(P_{0i})\mathbf{\Psi}_{\mathbf{im}} \tag{3.36}$$

where $\mathbf{L}_i(P_{0i})$ is the same as defined in eq.(2.10), while $\mathbf{L}_i^m(P_{0i})$ is a $3 \times l_i$ matrix.

The above transformation should be carried out in order to use modal coordinates. This transformation leads to modifications in the definitions of the vector of flexible-pose, $\mathbf{q}_i$, as well as the vector of the flexible-twist of link i, $\mathbf{v}_i$, as defined in eqs.(2.1) and (2.2), respectively. The n_i-dimensional nodal coordinates $\mathbf{u}_i(t)$ and its time-rate of change, $\dot{\mathbf{u}}_i(t)$, should be replaced by the l_i-dimensional modal coordinates $\mathbf{u}_i^m(t)$ and $\dot{\mathbf{u}}_i^m(t)$, respectively. To this end, the dimension of vectors $\mathbf{q}_i$ and $\mathbf{v}_i$ are changed from $n_i'(= 7 + n_i)$ and $m_i'(= 6 + n_i)$ to $n_i'(= 7 + l_i)$ and $m_i'(= 6 + l_i)$, respectively.

3.2.5 Lagrange Equations of Motion of Link i

Having the expressions for the kinetic and the elastic strain energies, the Lagrange equations of motion of link i are written as

$$\frac{d}{dt}(\frac{\partial T_i}{\partial \dot{\mathbf{q}}_i}) - \frac{\partial T_i}{\partial \mathbf{q}_i} + \frac{\partial V_i}{\partial \mathbf{q}_i} = \mathbf{f}_i \tag{3.37}$$

where T_i and V_i are the kinetic and the elastic strain energies of the link i, as given in eqs.(3.3) and (3.24), respectively, and $\mathbf{q}_i$ is the vector of flexible-pose of link i, given in eq.(2.1). Moreover, $\mathbf{f}_i$ is the n_i'-dimensional vector of generalized forces, decomposed as

$$\mathbf{f}_i = \mathbf{f}_i^E + \mathbf{f}_i^A + \mathbf{f}_i^D + \mathbf{f}_i^K + \mathbf{f}_i^G \tag{3.38}$$

where $\mathbf{f}_i^E$, $\mathbf{f}_i^A$, $\mathbf{f}_i^D$, $\mathbf{f}_i^K$ and $\mathbf{f}_i^G$ are generalized-force vectors accounting for external wrenches, algebraic constraint wrenches, dissipative wrenches, kinematic-constraint wrenches, and gravity forces, respectively. The wrench $\mathbf{f}_i^A$ arises due to the algebraic constraint among the components of the Euler parameters, while $\mathbf{f}_i^K$ results from the kinematic coupling of the links.

The gravity wrench $\mathbf{f}_i^G$ can be evaluated, in turn, as

$$\mathbf{f}_i^G = \frac{\partial \Pi_i^G}{\partial \dot{\mathbf{q}}_i} \tag{3.39}$$

where Π_i^G is the power developed by gravity forces and is defined as

$$\Pi_i^G = \dot{\mathbf{p}}_{C_i} \cdot \mathbf{g}_i = \mathbf{g}_i^T \dot{\mathbf{p}}_{C_i} \tag{3.40}$$

in which $\mathbf{g}_i$ is the 3-dimensional vector representing the gravity force acting on link i and $\dot{\mathbf{p}}_{C_i}$ is the velocity of the centre of mass C_i of the same link, with respect to the inertial frame. Inserting Π_i^G from eq.(3.40) into eq.(3.39) and differentiating the result with respect to $\dot{\mathbf{q}}_i$, with the understanding that $\mathbf{g}_i$ is not a function of $\dot{\mathbf{q}}_i$, one obtains

$$\mathbf{f}_i^G = \frac{\partial \left(\mathbf{g}_i^T \dot{\mathbf{p}}_{C_i}\right)}{\partial \dot{\mathbf{q}}_i} = \frac{\partial \dot{\mathbf{p}}_{C_i}^T}{\partial \dot{\mathbf{q}}_i} \mathbf{g}_i \tag{3.41}$$

Now, using eq.(2.26), $\dot{\mathbf{p}}_{C_i}$ can be written as

$$\dot{\mathbf{p}}_{C_i} = \mathbf{W}_{C_i} \mathbf{v}_i \tag{3.42}$$

where

$$\mathbf{W}_{C_i} = \begin{bmatrix} -\mathbf{D}_{C_i} & \mathbf{1}_{33} & \mathbf{R}_i \mathbf{L}_i(C_{0i}) \end{bmatrix} \tag{3.43}$$

in which $\mathbf{D}_{C_i}$ and $\mathbf{L}_i(C_{0i})$ are evaluated at point C_i, while other quantities are defined in eq.(2.27). Introducing $\dot{\mathbf{p}}_{C_i}$ from eq.(3.42) into eq.(3.41) and recalling that $\mathbf{W}_{C_i}$ is not a function of $\dot{\mathbf{q}}_i$, one obtains

$$\mathbf{f}_i^G = \frac{\partial \mathbf{v}_i^T}{\partial \dot{\mathbf{q}}_i} \mathbf{W}_{C_i}^T \mathbf{g}_i \tag{3.44}$$

Inserting $\mathbf{v}_i$ from eq.(2.3a) into the above equation, and noting that $\mathbf{\Gamma}_i = \mathbf{\Gamma}_i(\mathbf{q}_i, t)$ is not a function of $\dot{\mathbf{q}}_i$, leads to

$$\mathbf{f}_i^G = \mathbf{\Gamma}_i^T \mathbf{W}_{C_i}^T \mathbf{g}_i \tag{3.45}$$

The external wrench $\mathbf{f}_i^E$ can be derived, in turn, as

$$\mathbf{f}_i^E = \frac{\partial \Pi_i^E}{\partial \dot{\mathbf{q}}_i} \tag{3.46}$$

where Π_i^E is the power developed by the external wrench and is defined as

$$\Pi_i^E = \mathbf{v}_i \cdot \mathbf{w}_i^E = (\mathbf{w}_i^E)^T \mathbf{v}_i \tag{3.47}$$

provided that all external wrenches $\mathbf{w}_i^E$ are applied at the joints. Using the same procedure as in deriving $\mathbf{f}_i^G$, one may readily show that

$$\mathbf{f}_i^E = \mathbf{\Gamma}_i^T \mathbf{w}_i^E \tag{3.48}$$

Upon substitution of eq.(2.3a) into eq.(3.3), the form of the kinetic energy is obtained in terms of the time-rate of change of the flexible-pose of link i as

$$T_i = \frac{1}{2}\dot{\mathbf{q}}_i^T \mathbf{\Gamma}_i^T \mathbf{M}_i \mathbf{\Gamma}_i \dot{\mathbf{q}}_i \tag{3.49}$$

Now, the inertia matrix $\mathbf{I}_i$ of link i is defined as

$$\mathbf{I}_i \equiv \mathbf{\Gamma}_i^T \mathbf{M}_i \mathbf{\Gamma}_i \tag{3.50}$$

which is a positive-definite $n_i' \times n_i'$ matrix. Thus,

$$T_i = \frac{1}{2}\dot{\mathbf{q}}_i^T \mathbf{I}_i \dot{\mathbf{q}}_i \tag{3.51}$$

By differentiating the kinetic energy, eq.(3.51), with respect to $\dot{\mathbf{q}}_i$ and then with respect to time, $d(\partial T_i/\partial \dot{\mathbf{q}}_i)/dt$ can be obtained as

$$\frac{d}{dt}\left(\frac{\partial T_i}{\partial \dot{\mathbf{q}}_i}\right) = \frac{d}{dt}(\mathbf{I}_i \dot{\mathbf{q}}_i) = \dot{\mathbf{I}}_i \dot{\mathbf{q}}_i + \mathbf{I}_i \ddot{\mathbf{q}}_i \tag{3.52}$$

Similarly, $\partial T_i/\partial \mathbf{q}_i$ is obtained by differentiating the kinetic energy given by eq.(3.51) with respect to $\mathbf{q}_i$ as

$$\frac{\partial T_i}{\partial \mathbf{q}_i} = \frac{\partial}{\partial \mathbf{q}_i}\left(\frac{1}{2}\dot{\mathbf{q}}_i^T \mathbf{I}_i \dot{\mathbf{q}}_i\right) \tag{3.53}$$

Introducing $d(\partial T_i/\partial \dot{\mathbf{q}}_i)/dt$ and $\partial T_i/\partial \mathbf{q}_i$ from above equations into eq.(3.37), the dynamics model of link i is obtained as

$$\mathbf{I}_i \ddot{\mathbf{q}}_i = \mathbf{f}_i^S + \mathbf{f}_i \tag{3.54}$$

where the *system wrench* of link i is defined as

$$\mathbf{f}_i^S = \frac{\partial}{\partial \mathbf{q}_i}(\frac{1}{2}\dot{\mathbf{q}}_i^T \mathbf{I}_i \dot{\mathbf{q}}_i) - \dot{\mathbf{I}}_i \dot{\mathbf{q}}_i - \frac{\partial V_i}{\partial \mathbf{q}_i} \tag{3.55}$$

while $\mathbf{f}_i$ is as defined in eq.(3.38).

Moreover, the dynamics model can be expressed in terms of the flexible twist as follows: Introducing $\mathbf{I}_i$ from eq.(3.50) into eq.(3.54) and multiplying both sides of the equations thus obtained by $\mathbf{\Lambda}_i^T$, with $\mathbf{\Lambda}_i$ as defined in eq.(2.3b), one obtains

$$\mathbf{\Lambda}_i^T \mathbf{\Gamma}_i^T \mathbf{M}_i \mathbf{\Gamma}_i \ddot{\mathbf{q}}_i = \mathbf{\Lambda}_i^T \mathbf{f}_i^S + \mathbf{\Lambda}_i^T \mathbf{f}_i \tag{3.56}$$

Differentiating eq.(2.3a) with respect to time leads to

$$\dot{\mathbf{v}}_i = \mathbf{\Gamma}_i \ddot{\mathbf{q}}_i + \dot{\mathbf{\Gamma}}_i \dot{\mathbf{q}}_i \tag{3.57}$$

Therefore, substituting $\mathbf{\Gamma}_i \ddot{\mathbf{q}}_i$ from above equation into eq.(3.56) and, in light of eq.(A.10), one obtains the m_i'-dimensional vector of the dynamics model of link i in terms of flexible twist as

$$\mathbf{M}_i \dot{\mathbf{v}}_i = \mathbf{\Lambda}_i^T \mathbf{f}_i^S + \mathbf{M}_i \dot{\mathbf{\Gamma}}_i \dot{\mathbf{q}}_i + \mathbf{\Lambda}_i^T \mathbf{f}_i \tag{3.58a}$$

or

$$\mathbf{M}_i \dot{\mathbf{v}}_i = \mathbf{b}_i^S + \mathbf{b}_i^E + \mathbf{b}_i^D + \mathbf{b}_i^K + \mathbf{b}_i^G \tag{3.58b}$$

where

$$\mathbf{b}_i^S = \mathbf{\Lambda}_i^T \mathbf{f}_i^S + \mathbf{M}_i \dot{\mathbf{\Gamma}}_i \dot{\mathbf{q}}_i \tag{3.58c}$$

$$\mathbf{b}_i^E = \mathbf{\Lambda}_i^T \mathbf{f}_i^E \tag{3.58d}$$

$$\mathbf{b}_i^D = \mathbf{\Lambda}_i^T \mathbf{f}_i^D \tag{3.58e}$$

$$\mathbf{b}_i^K = \mathbf{\Lambda}_i^T \mathbf{f}_i^K \tag{3.58f}$$

$$\mathbf{b}_i^G = \mathbf{\Lambda}_i^T \mathbf{f}_i^G \tag{3.58g}$$

Here, introducing $\mathbf{f}_i^G$ and $\mathbf{f}_i^E$ from eqs.(3.45) and (3.48) into eqs.(3.58g) and (3.58d), in light of eq.(A.10), $\mathbf{b}_i^G$ and $\mathbf{b}_i^E$ can be written as

$$\mathbf{b}_i^G = \mathbf{\Lambda}_i^T \mathbf{\Gamma}_i^T \mathbf{W}_{C_i}^T \mathbf{g}_i = \mathbf{W}_{C_i}^T \mathbf{g}_i \tag{3.58h}$$

$$\mathbf{b}_i^E = \mathbf{\Lambda}_i^T \mathbf{\Gamma}_i^T \mathbf{w}_i^E = \mathbf{w}_i^E \tag{3.58i}$$

Moreover, if all links are connected by revolute joints, the external wrench $\mathbf{b}_i^E$ can be decomposed as

$$\mathbf{b}_i^E = \begin{bmatrix} \boldsymbol{\tau}_i^T & \mathbf{0}_3^T & \mathbf{0}_{n_i}^T \end{bmatrix}^T \tag{3.58j}$$

where $\boldsymbol{\tau}_i$ is the 3-dimensional vector of external torque applied at joint i.

For most structures, the exact form of the damping matrix is unknown, since the mechanisms of energy loss are complicated. For structural damping it is generally assumed that the existence of damping does not cause coupling of the undamped natural modes of vibration. In this thesis, structural damping is approximated by a suitable viscous damping coefficient for different modes as in Midha et al. (1979) and Turcic and Midha (1984–a).

It may be noted that $\mathbf{\Lambda}_i^T \mathbf{f}_i^A$ vanishes (Cyril et al., 1991), i.e.,

$$\mathbf{\Lambda}_i^T \mathbf{f}_i^A = \mathbf{0}_{m_i'} \tag{3.59}$$

where $\mathbf{0}_{m_i'}$ is the m_i'-dimensional zero vector.

Determination of the System Wrench $\mathbf{b}_i^S$

The system wrench $\mathbf{b}_i^S$ given in eq.(3.58c), in light of eq.(3.55), can be simplified as (Cyril et al, 1991)

$$\mathbf{b}_i^S = \frac{1}{2}\mathbf{\Lambda}_i^T \left[\frac{\partial}{\partial \mathbf{q}_i}(\mathbf{v}_i^T \mathbf{M}_i \mathbf{v}_i)\right] - \mathbf{\Lambda}_i^T(\frac{\partial V_i}{\partial \mathbf{q}_i}) - 2\mathbf{\Lambda}_i^T \dot{\mathbf{\Gamma}}_i^T \mathbf{M}_i \mathbf{v}_i - \dot{\mathbf{M}}_i \mathbf{v}_i \tag{3.60}$$

The first term of $\mathbf{b}_i^S$ is written in this form providing that the derivative of $(\mathbf{v}_i^T \mathbf{M}_i \mathbf{v}_i)$ with respect to $\mathbf{q}_i$ is only applied on $\mathbf{M}_i$. In other words, it is assumed that $\mathbf{v}_i$ is not a function of $\mathbf{q}_i$. This modification is applied to ease partial-derivative computation, namely, by taking the partial derivatives of a scalar and a vector, instead of a matrix, with respect to $\mathbf{q}_i$. The latter leads to Christoffel symbols in tensor analysis which we try to avoid. Expressing the flexible-pose vector $\mathbf{q}_i$ in terms of components, $\partial(\mathbf{v}_i^T\mathbf{M}_i\mathbf{v}_i)/\partial\mathbf{q}_i$ obtains as

$$\frac{\partial}{\partial\mathbf{q}_i}(\mathbf{v}_i^T\mathbf{M}_i\mathbf{v}_i) = \begin{bmatrix} \partial(\mathbf{v}_i^T\mathbf{M}_i\mathbf{v}_i)/\partial\hat{\mathbf{q}}_i \\ \partial(\mathbf{v}_i^T\mathbf{M}_i\mathbf{v}_i)/\partial\mathbf{r}_i \\ \partial(\mathbf{v}_i^T\mathbf{M}_i\mathbf{v}_i)/\partial\mathbf{u}_i \end{bmatrix} \tag{3.61}$$

Using eqs.(3.5) and (2.2) and expanding the result thus obtained, $\mathbf{v}_i^T\mathbf{M}_i\mathbf{v}_i$ is evaluated as

$$\mathbf{v}_i^T\mathbf{M}_i\mathbf{v}_i = 2\boldsymbol{\omega}_i^T\mathbf{M}_i^{rd}\dot{\mathbf{r}}_i + \boldsymbol{\omega}_i^T\mathbf{M}_i^{rr}\boldsymbol{\omega}_i + 2\boldsymbol{\omega}_i^T\mathbf{M}_i^{re}\dot{\mathbf{u}}_i + \dot{\mathbf{r}}_i^T\mathbf{M}_i^{dd}\dot{\mathbf{r}}_i + 2\dot{\mathbf{r}}_i^T\mathbf{M}_i^{de}\dot{\mathbf{u}}_i + \dot{\mathbf{u}}_i^T\mathbf{M}_i^{ee}\dot{\mathbf{u}}_i \tag{3.62}$$

Using the above relation and eliminating the terms which are not functions of $\mathbf{q}_i$, in light of eqs.(3.5), the components of eq.(3.61) are given by

$$\frac{\partial}{\partial\hat{\mathbf{q}}_i}(\mathbf{v}_i^T\mathbf{M}_i\mathbf{v}_i) = 2\frac{\partial}{\partial\hat{\mathbf{q}}_i}(\boldsymbol{\omega}_i^T\mathbf{M}_i^{rd}\dot{\mathbf{r}})_i + 2\frac{\partial}{\partial\hat{\mathbf{q}}_i}(\dot{\mathbf{r}}_i^T\mathbf{M}_i^{de}\dot{\mathbf{u}}_i) + 2\frac{\partial}{\partial\hat{\mathbf{q}}_i}(\boldsymbol{\omega}_i^T\mathbf{M}_i^{re}\dot{\mathbf{u}}_i) + \frac{\partial}{\partial\hat{\mathbf{q}}_i}(\boldsymbol{\omega}_i^T\mathbf{M}_i^{rr}\boldsymbol{\omega}_i) \tag{3.63a}$$

$$\frac{\partial}{\partial\mathbf{r}_i}(\mathbf{v}_i^T\mathbf{M}_i\mathbf{v}_i) = \mathbf{0}_3 \tag{3.63b}$$

$$\frac{\partial}{\partial\mathbf{u}_i}(\mathbf{v}_i^T\mathbf{M}_i\mathbf{v}_i) = 2\frac{\partial}{\partial\mathbf{u}_i}(\boldsymbol{\omega}_i^T\mathbf{M}_i^{rd}\dot{\mathbf{r}}_i) + 2\frac{\partial}{\partial\mathbf{u}_i}(\boldsymbol{\omega}_i^T\mathbf{M}_i^{re}\dot{\mathbf{u}}_i) + \frac{\partial}{\partial\mathbf{u}_i}(\boldsymbol{\omega}_i^T\mathbf{M}_i^{rr}\boldsymbol{\omega}_i) \tag{3.63c}$$

The detailed derivation of eqs.(3.63a) and (3.63c) are included in Appendices B and C, respectively.

$\dot{\mathbf{M}}_i$ is obtained by differentiating $\mathbf{M}_i$ given in eq.(3.5) with respect to time. We now take advantage of the relations

$$\dot{\mathbf{R}}_i = \boldsymbol{\Omega}_i\mathbf{R}_i \tag{3.64a}$$

$$\dot{\mathbf{R}}_i^T = \mathbf{R}_i^T\boldsymbol{\Omega}_i^T = -\mathbf{R}_i^T\boldsymbol{\Omega}_i \tag{3.64b}$$

where $\mathbf{\Omega}_i$ is cross-product matrix of $\boldsymbol{\omega}_i$ as defined in eq.(2.22); hence, the components of matrix $\dot{\mathbf{M}}_i$ can be identified as

$$\dot{\mathbf{M}}_i^{rr} = \mathbf{\Omega}_i\mathbf{M}_i^{rr} - \mathbf{M}_i^{rr}\mathbf{\Omega}_i + \mathbf{R}_i\dot{\mathbf{V}}_i^{rr}\mathbf{R}_i^T \tag{3.65a}$$

$$\dot{\mathbf{M}}_i^{rd} = (\dot{\mathbf{M}}_i^{dr})^T = \mathbf{\Omega}_i\mathbf{M}_i^{rd} - \mathbf{M}_i^{rd}\mathbf{\Omega}_i + \mathbf{R}_i\dot{\mathbf{V}}_i^{rd}\mathbf{R}_i^T \tag{3.65b}$$

$$\dot{\mathbf{M}}_i^{re} = (\dot{\mathbf{M}}_i^{er})^T = \mathbf{\Omega}_i\mathbf{M}_i^{re} + \mathbf{R}_i\dot{\mathbf{V}}_i^{re} \tag{3.65c}$$

$$\dot{\mathbf{M}}_i^{dd} = \mathbf{O}_{33} \tag{3.65d}$$

$$\dot{\mathbf{M}}_i^{de} = (\dot{\mathbf{M}}_i^{ed})^T = \mathbf{\Omega}_i\mathbf{M}_i^{de} \tag{3.65e}$$

$$\dot{\mathbf{M}}_i^{ee} = \mathbf{O}_{n_in_i} \tag{3.65f}$$

where $\dot{\mathbf{V}}_i^{rd}$ is the cross-product matrix of vector $\dot{\mathbf{v}}_i^{rd}$, while $\dot{\mathbf{v}}_i^{rd}$ is obtained by differentiating $\mathbf{v}_i^{rd}$ from eq.(3.14b) with respect to time as

$$\dot{\mathbf{v}}_i^{rd} = \mathbf{C}^{i1}\dot{\mathbf{u}}_i(t) \tag{3.65g}$$

and $\dot{\mathbf{V}}_i^{re}$ can be evaluated by differentiating eq.(3.16d) with respect to time, namely,

$$\dot{\mathbf{V}}_i^{re} = \begin{bmatrix} \dot{\mathbf{u}}_i^T(t)\,(\mathbf{C}_{32}^{i3} - \mathbf{C}_{23}^{i3}) \\ \dot{\mathbf{u}}_i^T(t)\,(\mathbf{C}_{13}^{i3} - \mathbf{C}_{31}^{i3}) \\ \dot{\mathbf{u}}_i^T(t)\,(\mathbf{C}_{21}^{i3} - \mathbf{C}_{12}^{i3}) \end{bmatrix} \tag{3.65h}$$

Moreover, differentiating the components of $\mathbf{V}_i^{rr}$ given in eq.(3.12) with respect to time leads to $\dot{\mathbf{V}}_i^{rr}$, namely,

$$\dot{v}_i^{11} = 2\dot{\mathbf{u}}_i^T(t)\left(\mathbf{C}_{22}^{i3} + \mathbf{C}_{33}^{i3}\right)\mathbf{u}_i(t) + 2\dot{\mathbf{u}}_i^T(t)\left(\mathbf{C}_{22}^{i5} + \mathbf{C}_{33}^{i5}\right)\mathbf{u}_i^o \tag{3.65i}$$

$$\dot{v}_i^{12} = -\left[2\dot{\mathbf{u}}_i^T(t)\mathbf{C}_{12}^{i3}\mathbf{u}_i(t) + \dot{\mathbf{u}}_i^T(t)\mathbf{C}_{12}^{i5}\mathbf{u}_i^o + \dot{\mathbf{u}}_i^T(t)\mathbf{C}_{21}^{i5}\mathbf{u}_i^o\right] \tag{3.65j}$$

with other components of $\dot{\mathbf{V}}_i^{rr}$ obtained by suitable permutations.

Finally, inserting $\partial(\mathbf{v}_i^T\mathbf{M}_i\mathbf{v}_i)/\partial\mathbf{q}_i$ from eqs.(3.63) into eq.(3.60), expanding $\mathbf{\Lambda}_i^T\dot{\mathbf{\Gamma}}_i^T$ using eqs.(A.8), and substituting the result thus obtained into eq.(3.60), vector $\mathbf{b}_i^S$ can be decomposed into rotational, translational and elastic parts as follows:

$$\mathbf{b}_i^S = \begin{bmatrix} (\mathbf{b}_i^S)_R \\ (\mathbf{b}_i^S)_T \\ (\mathbf{b}_i^S)_E \end{bmatrix} \tag{3.66a}$$

where $(\mathbf{b}_i^S)_R$ and $(\mathbf{b}_i^S)_T$ are 3-dimensional vectors, while $(\mathbf{b}_i^S)_E$ is n_i-dimensional. These vectors are defined as

$$\begin{aligned}(\mathbf{b}_i^S)_R = {} & \frac{1}{4}\mathbf{G}_i[2\frac{\partial}{\partial \hat{\mathbf{q}}_i}(\boldsymbol{\omega}_i^T\mathbf{M}_i^{rd}\dot{\mathbf{r}}_i) + 2\frac{\partial}{\partial \hat{\mathbf{q}}_i}(\dot{\mathbf{r}}_i^T\mathbf{M}_i^{de}\dot{\mathbf{u}}_i) + 2\frac{\partial}{\partial \hat{\mathbf{q}}_i}(\boldsymbol{\omega}_i^T\mathbf{M}_i^{re}\dot{\mathbf{u}}_i) + \\ & \frac{\partial}{\partial \hat{\mathbf{q}}_i}(\boldsymbol{\omega}_i^T\mathbf{M}_i^{rr}\boldsymbol{\omega}_i)] - 2\mathbf{G}_i\dot{\mathbf{G}}_i^T[\mathbf{M}_i^{rd}\dot{\mathbf{r}}_i + \mathbf{M}_i^{rr}\boldsymbol{\omega}_i + \\ & \mathbf{M}_i^{re}\dot{\mathbf{u}}_i] - \left(\dot{\mathbf{M}}_i^{rd}\dot{\mathbf{r}}_i + \dot{\mathbf{M}}_i^{rr}\boldsymbol{\omega}_i + \dot{\mathbf{M}}_i^{re}\dot{\mathbf{u}}_i\right) \end{aligned} \tag{3.66b}$$

$$(\mathbf{b}_i^S)_T = -\left(\dot{\mathbf{M}}_i^{dd}\dot{\mathbf{r}}_i + \dot{\mathbf{M}}_i^{dr}\boldsymbol{\omega}_i + \dot{\mathbf{M}}_i^{de}\dot{\mathbf{u}}_i\right) \tag{3.66c}$$

$$\begin{aligned}(\mathbf{b}_i^S)_E = {} & \frac{\partial}{\partial \mathbf{u}_i}\left(\boldsymbol{\omega}_i^T\mathbf{M}_i^{rd}\dot{\mathbf{r}}_i\right) + \frac{\partial}{\partial \mathbf{u}_i}\left(\boldsymbol{\omega}_i^T\mathbf{M}_i^{re}\dot{\mathbf{u}}_i\right) + \frac{1}{2}\frac{\partial}{\partial \mathbf{u}_i}\left(\boldsymbol{\omega}_i^T\mathbf{M}_i^{rr}\boldsymbol{\omega}_i\right) \\ & -\mathbf{K}_i^f\mathbf{u}_i - \left(\dot{\mathbf{M}}_i^{ed}\dot{\mathbf{r}}_i + \dot{\mathbf{M}}_i^{er}\boldsymbol{\omega}_i + \dot{\mathbf{M}}_i^{ee}\dot{\mathbf{u}}_i\right)\end{aligned} \tag{3.66d}$$

where the components of $\dot{\mathbf{M}}_i$ are defined, in turn, in eqs.(3.65), while $\mathbf{K}_i^f$ and $\mathbf{G}_i$ are defined in eqs.(3.23) and (A.4a), respectively.

3.3 Dynamics of the Entire Mechanical System

The dynamics model of the overall mechanical system is obtained by assembling the dynamics models of all links, represented by eqs.(3.58), thereby obtaining

$$\mathbf{M}\dot{\mathbf{v}} = \mathbf{b}^S + \mathbf{b}^E + \mathbf{b}^D + \mathbf{b}^K + \mathbf{b}^G \tag{3.67}$$

where $\mathbf{v}$ is the m'-dimensional vector of generalized flexible twist defined in eq.(2.29) and $\mathbf{M}$ is the $m' \times m'$ generalized extended mass matrix of the system, given by

$$\mathbf{M} = \operatorname{diag}\begin{pmatrix} \mathbf{M}_1 & \mathbf{M}_2 & \cdots & \mathbf{M}_r \end{pmatrix} \tag{3.68}$$

Here, $\mathbf{M}_i$ is the $m_i' \times m_i'$ extended mass matrix of link i defined in eqs.(3.5), while $\mathbf{b}^S$, $\mathbf{b}^K$, $\mathbf{b}^E$, $\mathbf{b}^D$ and $\mathbf{b}^G$ are m'-dimensional generalized-force vectors accounting for system wrenches, kinematic-constraint wrenches, external wrenches, damping or dissipative wrenches and gravity forces, respectively. Moreover, $\mathbf{b}^E$, $\mathbf{b}^G$ and $\mathbf{b}^S$ can be written by assembling external wrenches, gravity forces and system wrenches of all links as

$$\mathbf{b}^E = \begin{bmatrix} (\mathbf{b}_1^E)^T & (\mathbf{b}_2^E)^T & \cdots & (\mathbf{b}_r^E)^T \end{bmatrix}^T \tag{3.69}$$

$$\mathbf{b}^G = \begin{bmatrix} (\mathbf{b}_1^G)^T & (\mathbf{b}_2^G)^T & \cdots & (\mathbf{b}_r^G)^T \end{bmatrix}^T \tag{3.70}$$

$$\mathbf{b}^S = \begin{bmatrix} (\mathbf{b}_1^S)^T & (\mathbf{b}_2^S)^T & \cdots & (\mathbf{b}_r^S)^T \end{bmatrix}^T \tag{3.71}$$

where $\mathbf{b}_i^E$, $\mathbf{b}_i^G$ and $\mathbf{b}_i^S$ are as defined in eqs.(3.58i), (3.58h) and(3.66), respectively.

By definition, the power Π^K developed by the nonworking kinematic constraint wrench $\mathbf{b}^K$ vanishes, i.e.,

$$\Pi^K = \mathbf{v}^T\mathbf{b}^K = 0 \tag{3.72}$$

Upon substitution of $\mathbf{v}$ from eq.(2.35) into eq.(3.72), one obtains

$$\Pi^K = \dot{\boldsymbol{\theta}}_I^T\mathbf{N}^T\mathbf{b}^K = 0 \tag{3.73}$$

Since all components of $\dot{\boldsymbol{\theta}}_I$ are independent, the above equation leads to

$$\mathbf{N}^T\mathbf{b}^K = \mathbf{0}_{m'} \tag{3.74}$$

where $\mathbf{0}_{m'}$ is the m'-dimensional zero vector, i.e., $\mathbf{b}^K$ lies in the nullspace of $\mathbf{N}^T$.

Upon multiplication of both sides of eq.(3.67) by $\mathbf{N}^T$, the vector of nonworking constraint wrenches is eliminated from the dynamical equations of motion. Thus, the dynamics model of the mechanical system is given by

$$\mathbf{N}^T\mathbf{M}\dot{\mathbf{v}} = \mathbf{N}^T\mathbf{b}^S + \mathbf{N}^T\mathbf{b}^E + \mathbf{N}^T\mathbf{b}^D + \mathbf{N}^T\mathbf{b}^G \tag{3.75}$$

Moreover, differentiation of eq.(2.35) with respect to time yields

$$\dot{\mathbf{v}} = \dot{\mathbf{N}}\dot{\boldsymbol{\theta}}_I + \mathbf{N}\ddot{\boldsymbol{\theta}}_I \tag{3.76}$$

Upon substitution of $\dot{\mathbf{v}}$ from eq.(3.76) into eq.(3.75), q independent dynamical equations of the mechanical system, which are the minimum number of equations, are derived as

$$\hat{\mathbf{M}}\ddot{\boldsymbol{\theta}}_I = \mathbf{N}^T\mathbf{b}^S + \mathbf{N}^T\mathbf{b}^E + \mathbf{N}^T\mathbf{b}^D + \mathbf{N}^T\mathbf{b}^G - \mathbf{N}^T\mathbf{M}\dot{\mathbf{N}}\dot{\boldsymbol{\theta}}_I \tag{3.77}$$

where $\hat{\mathbf{M}}$ is the $q \times q$ positive-definite matrix of generalized inertia, defined as

$$\hat{\mathbf{M}} = \mathbf{N}^T\mathbf{M}\mathbf{N} \tag{3.78}$$

Therefore, it has been shown that using the methodology of NOC leads to the elimination of the nonworking kinematic-constraint wrenches as well as to the derivation of the minimum number of equations.

3.4 Simulation

The dynamics model of the manipulator represented by eq.(3.77) involves highly nonlinear coupled ordinary differential equations defining an initial-value problem that is solved with Gear's method (Gear, 1971) for numerical integration, as available in the DIVPAG package from IMSL.

The dynamic simulation can be performed using the following steps:

- Off-line computations
  - compute constant matrices $\mathbf{C}^{i1}$, $\mathbf{C}^{i2}$, $\mathbf{C}^{i3}_{kj}$, $\mathbf{C}^{i4}_{kj}$ and $\mathbf{C}^{i5}_{kj}$ using eqs.(3.15) and (3.11);

- Compute conventional stiffness matrix of each element of a link using expressions available in the literature (Przemieniecki, 1968) or direct integration formulas (Cook, 1981).

- On-line computation

  Give initial values for $\boldsymbol{\theta}_I$ and $\dot{\boldsymbol{\theta}}_I$ as well as the time history of the actuated joint torques.

  For $i = 1, \cdots, r$ do

  - Compute $\mathbf{p}_i$ and $\mathbf{r}_k$ using eqs.(2.16) and (2.30), respectively;
  - Compute $\dot{\mathbf{p}}_i$, $\boldsymbol{\omega}_k$ and $\dot{\mathbf{r}}_k$ using eqs.(2.26), (2.34a) and (2.34b), respectively;
  - Compute the mass matrix $\mathbf{M}_i$ and its time-rate of change, $\dot{\mathbf{M}}_i$, using eqs.(2.5) and (3.65), respectively;
  - Compute the geometric stiffness matrix $\mathbf{K}_{ij}^{gn}$ of each element of the ith link using eq.(3.29);
  - Compute the stiffness matrix of link i, $\mathbf{K}_i$, using eq.(3.25);
  - Compute the system wrenches $\mathbf{b}_i^S$, $\mathbf{b}_i^E$ and $\mathbf{b}_i^G$ using eqs.(3.66), (3.58i) and (3.58h), respectively;

  end do

  - Compute $\mathbf{b}^E$, $\mathbf{b}^G$ and $\mathbf{b}^S$ using eqs.(3.69), (3.70) and (3.71), respectively;
  - Compute $\mathbf{M}$ using eq.(3.68);
  - The following steps depend on whether the formulation of the problem is in joint or in Cartesian space.

    Formulation of the problem in joint space:

* Compute $\boldsymbol{\theta}_D$ as described in Subsection 2.7.1;
* Compute $\dot{\boldsymbol{\theta}}_D$ using eq.(2.44);
* Compute NOC matrix $\mathbf{N}$ as described in Subsection 2.7.1;

Formulation of the problem in Cartesian space:

* Compute $\boldsymbol{\theta}_D$ and $\dot{\boldsymbol{\theta}}_D$ as described in Subsection 2.7.2;
* Compute NOC matrix $\mathbf{N}$ as described in Subsection 2.7.2;

- Compute $\hat{\mathbf{M}}$ using eq.(3.78);
- Compute $\ddot{\boldsymbol{\theta}}_I$ using eq.(3.77);
- Compute the state-space vector $\mathbf{y}$ (change $\ddot{\boldsymbol{\theta}}_I$ to first order derivatives) as

$$\mathbf{y} = \begin{bmatrix} \mathbf{y}_1 \\ \mathbf{y}_2 \end{bmatrix} = \begin{bmatrix} \boldsymbol{\theta}_I \\ \dot{\boldsymbol{\theta}}_I \end{bmatrix} \tag{3.79a}$$

and

$$\dot{\mathbf{y}} = \begin{bmatrix} \dot{\mathbf{y}}_1 \\ \dot{\mathbf{y}}_2 \end{bmatrix} = \begin{bmatrix} \dot{\boldsymbol{\theta}}_I \\ \ddot{\boldsymbol{\theta}}_I \end{bmatrix} \tag{3.79b}$$

- Use a direct numerical integration scheme (Gear method) to compute the state vector for a new step in time, i.e, $t \leftarrow t + \Delta t$.

The inverse dynamics can be carried out by rearranging the dynamical equations of the mechanical system represented by eq.(3.77), namely,

$$\mathbf{N}^T\mathbf{b}^E = \hat{\mathbf{M}}\ddot{\boldsymbol{\theta}}_I - \mathbf{N}^T\mathbf{b}^S - \mathbf{N}^T\mathbf{b}^D - \mathbf{N}^T\mathbf{b}^G + \mathbf{N}^T\mathbf{M}\dot{\mathbf{N}}\dot{\boldsymbol{\theta}}_I \tag{3.80}$$

The time history of motion of the mechanical system, namely, $\boldsymbol{\theta}_I(t)$, $\dot{\boldsymbol{\theta}}_I(t)$ and $\ddot{\boldsymbol{\theta}}_I(t)$, is given, while $\mathbf{M}$, $\mathbf{N}$ and $\hat{\mathbf{M}}$ are computed as explained in the simulation algorithm. However, all computations are carried out by setting to zero the generalized coordinates associated with link flexibility, namely, $\mathbf{u}_i(t)$ and $\dot{\mathbf{u}}_i(t)$.

Therefore, using eq.(3.80), in light of eqs.(3.69) and (3.58i), the time histories of the actuated joint torques can be derived for the rigid-link model.

Chapter 4

Dynamics of Two Cooperating Flexible-link Manipulators–Planar Case

4.1 Introduction

Cooperating serial and multi-armed manipulators are expected to be used in many situations, especially in space applications. This has prompted research work in this area. Some researchers have studied the dynamics of multi-armed manipulators with rigid links (Lilly and Orin, 1994; McMillan et al., 1992; Zheng and Luh, 1989). However, long and light-weight links, high-speed, and accurate manoeuvres are some important features of space systems, requiring consideration of link flexibility in the corresponding models. Cooperating manipulators can be modelled as multibody systems with kinematic loops. Hence, the modelling formulations described in Chapters 2 and 3 can be used for modelling these manipulators. As an example, the dynamics simulation of two planar cooperating manipulators is considered here using for both rigid and flexible-link models to show the effect of link flexibility. It may be easier to develop the dynamical equations of motion for planar systems starting from the beginning instead of using the general ones developed earlier. Therefore, modelling of the planar system at hand is first carried out. The formulation of the problem is usually carried out in Cartesian space, since the end-effector motion is prescribed in many applications for cooperating manipulators. On the other hand, the formulation of the problem in joint space is also conducted to compare the speeds of operation for the two formulations. In addition, the effect of structural damping on the simulation results is also considered. The chapter concludes with the comparison of the results of the formulation in Cartesian and joint spaces in order to show the consistency of the simulation scheme.

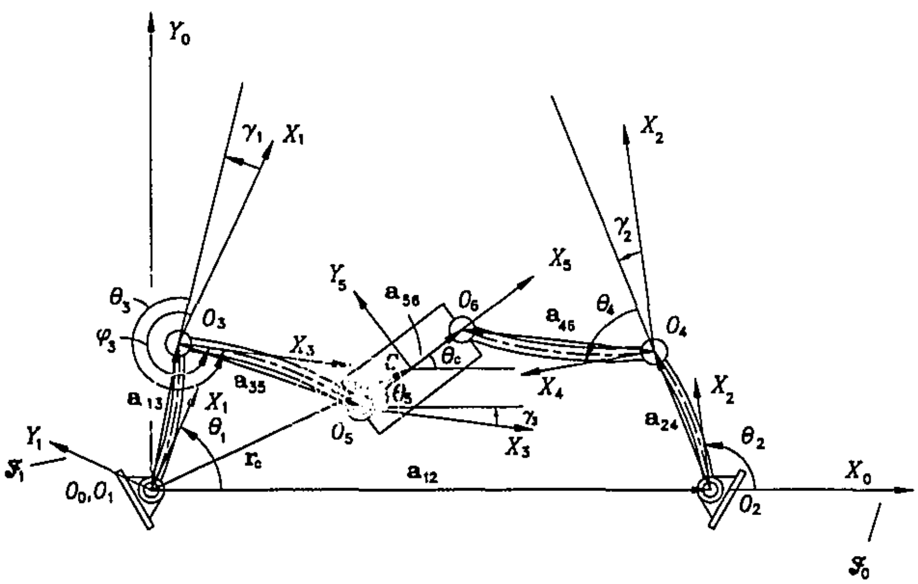

Figure 4.1: Two cooperative flexible-link manipulators

Figure 4.1 shows two identical planar manipulators separately mounted on the same base structure and participating in changing the position and orientation of a rigid object coupled to the manipulators via revolute joints of centres O_5 and O_6. The two manipulators have four flexible links O_iO_{i+2}, for $i = 1, \ldots, 4$, which are connected to each other by revolute joints. The DOF of this example can be obtained by rewriting eq.(2.41) for planar systems, namely,

$$q = 3r - 2\nu + \sum_{i=1}^{r_f} n_i \tag{4.1}$$

where

r=number of moving links=5,

ν= number of joints =6,

r_f= number of flexible links=4,

and n_i determining the number of nodal coordinates of link i associated with link flexibility. Inserting the above relations into eq.(4.1), one obtains the DOF of the system at hand as

$$q = 3 + \sum_{i=1}^{4} n_i \tag{4.2}$$

Hence, this example has three rigid DOF. Four motors, located at O_1, O_2, O_3 and O_4, drive the joints. However, the motor at joint O_4 becomes idle by using a clutch when the two manipulators are participating in a coordinated activity, which gives rise to a manipulator with a kinematic loop. Moreover, θ_i, for $i = 1, \ldots, 5$, is the angle of rotation of the joint at O_i, while θ_c and $\mathbf{r}_c$ describe the orientation of the manipulated object and the position vector of its centre of mass, respectively.

4.2 Modelling of the Flexible Links

The approach for modelling the dynamics of link i is similar to that described in Sections 2.3, 2.4 and 3.2. However, some modifications are applied on some of the definitions, in order to ease the modelling for the planar systems as follows:

The $m_i'(= 3 + n_i)$-dimensional vector of *flexible-pose* of link i is defined as

$$\mathbf{q}_i = \begin{bmatrix} \phi_i & \mathbf{r}_i^T & \mathbf{u}_i(t)^T \end{bmatrix}^T \tag{4.3}$$

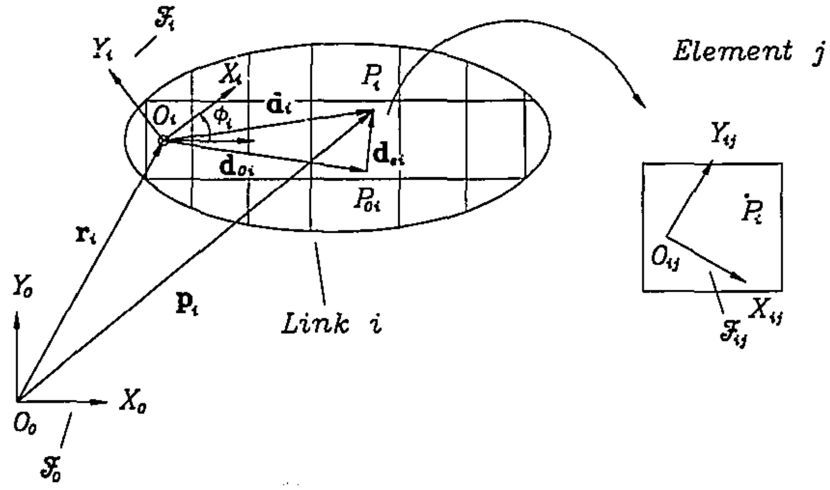

Figure 4.2: Modelling of the planar flexible links

while the m_i'-dimensional vector of *flexible-twist*, $\mathbf{v}_i$, of the same link is defined, for this particular case of planar motion, simply as the time-derivative of $\dot{\mathbf{q}}_i$, i.e.,

$$\mathbf{v}_i \equiv \dot{\mathbf{q}}_i \tag{4.4}$$

With reference to Fig. 4.2, O_i is the origin of the coordinate frame X_iY_i ($\mathcal{F}_i$) fixed to link i, $\mathbf{r}_i$ is the 2-dimensional position vector of O_i in the inertial frame X_0Y_0 ($\mathcal{F}_0$), ϕ_i is the angle of orientation of X_i with respect to X_0 and $\mathbf{u}_i(t)$ is the n_i-dimensional vector of generalized coordinates associated with link flexibility, with n_i determining the number of nodal elastic displacement of link i. The 2-dimensional position vector, in $\mathcal{F}_0$ coordinates, of any point P_i of link i can be written from Fig. 4.2 as

$$\mathbf{p}_i = \mathbf{r}_i + \mathbf{d}_i = \mathbf{r}_i + \mathbf{R}_i[\mathbf{d}_i]_i \tag{4.5}$$

where $\mathbf{R}_i$ is the rotation matrix of frame $\mathcal{F}_i$ with respect to the inertial frame, while $\mathbf{d}_i$ and $[\mathbf{d}_i]_i$ denote the position vector of point P_i, of frame $\mathcal{F}_i$, expressed in the inertial frame $\mathcal{F}_0$ and in frame $\mathcal{F}_i$, respectively. The position vector $[\mathbf{d}_i]_i$ can be obtained using eq.(2.15). Here, it may be noted that $\mathbf{L}_i(P_{0i})$ and $\mathbf{L}_i^o(P_{0i})$ are $2 \times n_i$ and $2 \times m_i$ matrices, as defined in eqs. (2.10) and (2.14), respectively.

The velocity of any point P_i of link i can then be written as

$$\dot{\mathbf{p}}_i = \dot{\mathbf{r}}_i + \dot{\mathbf{R}}_i[\mathbf{d}_i]_i + \mathbf{R}_i\mathbf{L}_i(P_{0i})\dot{\mathbf{u}}_i(t) \tag{4.6}$$

where $\dot{\mathbf{R}}_i[\mathbf{d}_i]_i$ can be written for planar systems as

$$\dot{\mathbf{R}}_i[\mathbf{d}_i]_i = \omega_i\mathbf{E}\mathbf{d}_i = \mathbf{E}\mathbf{d}_i\omega_i = \mathbf{E}\mathbf{R}_i[\mathbf{d}_i]_i\omega_i \tag{4.7}$$

while $\omega_i = \dot{\phi}_i$ is the scalar angular velocity of the frame $\mathcal{F}_i$ of link i with respect to the inertial frame and $\mathbf{E}$ is the 2×2 orthogonal matrix that rotates vectors through 90° counterclockwise, namely,

$$\mathbf{E} = \begin{bmatrix} 0 & -1 \\ 1 & 0 \end{bmatrix} \tag{4.8}$$

It is then possible to write $\dot{\mathbf{p}}_i$ as

$$\dot{\mathbf{p}}_i = \dot{\mathbf{r}}_i + \mathbf{E}\mathbf{d}_i\omega_i + \mathbf{R}_i\mathbf{L}_i(P_{0i})\dot{\mathbf{u}}_i(t) \tag{4.9}$$

Thus, from eq.(4.9), $\dot{\mathbf{p}}_i$ can be written as a linear transformation of the vector of flexible twist, namely,

$$\dot{\mathbf{p}}_i = \mathbf{W}_i\mathbf{v}_i \tag{4.10}$$

where $\mathbf{W}_i$ is a $2 \times m_i'$ matrix, namely,

$$\mathbf{W}_i = \begin{bmatrix} \mathbf{E}\mathbf{d}_i & \mathbf{1}_{22} & \mathbf{R}_i\mathbf{L}_i(P_{0i}) \end{bmatrix} \tag{4.11}$$

while $\mathbf{1}_{22}$ is the 2×2 identity matrix.

Now one can derive an expression for the kinetic energy of link i as

$$T_i = \frac{1}{2}\mathbf{v}_i^T\mathbf{M}_i\mathbf{v}_i, \quad \text{with} \quad \mathbf{M}_i = \int_{v_i} \rho_i\mathbf{W}_i^T\mathbf{W}_i dv_i \tag{4.12}$$

where ρ_i and v_i are the mass density and volume of the link i, respectively. Moreover, $\mathbf{M}_i$ is the $m_i' \times m_i'$ mass matrix of link i derived by introducing $\mathbf{W}_i$ from eq.(4.11) into the above equation, and is given by

$$\mathbf{M}_i = \int_{v_i} \begin{bmatrix} \mathbf{d}_i^T\mathbf{d}_i & \mathbf{d}_i^T\mathbf{E}^T & \mathbf{d}_i^T\mathbf{E}^T\mathbf{R}_i\mathbf{L}_i(P_{0i}) \\ \mathbf{E}\mathbf{d}_i & \mathbf{1}_{22} & \mathbf{R}_i\mathbf{L}_i(P_{0i}) \\ \mathbf{L}_i^T(P_{0i})\mathbf{R}_i^T\mathbf{E}\mathbf{d}_i & \mathbf{L}_i^T(P_{0i})\mathbf{R}_i^T & \mathbf{L}_i^T(P_{0i})\mathbf{L}_i(P_{0i}) \end{bmatrix} \rho_i dv_i \tag{4.13}$$

Finally, the Lagrange equations of motion for link i can be derived from

$$\frac{d}{dt}\left(\frac{\partial T_i}{\partial \dot{\mathbf{q}}_i}\right) - \frac{\partial T_i}{\partial \mathbf{q}_i} + \frac{\partial V_i}{\partial \mathbf{q}_i} = \mathbf{f}_i \tag{4.14}$$

in which T_i and V_i are the kinetic and elastic strain energies of link i, eqs.(4.12) and (3.24), respectively, while $\mathbf{f}_i$ is the m_i'-dimensional vector of generalized forces, defined as

$$\mathbf{f}_i = \mathbf{f}_i^E + \mathbf{f}_i^D + \mathbf{f}_i^K + \mathbf{f}_i^G \tag{4.15}$$

in which $\mathbf{f}_i^E$, $\mathbf{f}_i^D$, $\mathbf{f}_i^K$ and $\mathbf{f}_i^G$ are the contributions to the generalized forces from the external forces and torques, dissipative or damping forces, nonworking kinematic constraint forces resulting from kinematic coupling of the links, and gravity forces, respectively. Upon substitution of eqs.(4.4) and (4.12) into eq.(4.14), the dynamics model of link i is obtained as

$$\mathbf{M}_i\dot{\mathbf{v}}_i = \mathbf{f}_i^S + \mathbf{f}_i \tag{4.16}$$

where the *system wrench* of link i, $\mathbf{f}_i^S$, is defined as

$$\mathbf{b}_i^S \equiv \frac{\partial}{\partial \mathbf{q}_i}\left(\frac{1}{2}\mathbf{v}_i^T\mathbf{M}_i\mathbf{v}_i\right) - \dot{\mathbf{M}}_i\mathbf{v}_i - \frac{\partial V_i}{\partial \mathbf{q}_i} \tag{4.17}$$

4.3 Formulation of the Kinematic Constraints

The $m' = \sum_{i=1}^{5} m_i'$-dimensional vector of generalized flexible-twist is obtained for this example by using eq.(2.29) as

$$\mathbf{v} = \begin{bmatrix} \omega_1 & \dot{\mathbf{r}}_1^T & \dot{\mathbf{u}}_1^T & \cdots & \omega_4 & \dot{\mathbf{r}}_4^T & \dot{\mathbf{u}}_4^T & \omega_c & \dot{\mathbf{r}}_c^T \end{bmatrix}^T \tag{4.18}$$

where $\omega_c = \dot{\theta}_c$ is the angular velocity of the manipulated object and $\dot{\mathbf{r}}_c$ is the velocity of the centre of mass of the manipulated object. The position vector of point $O_{i,i+2}$ of $\mathcal{F}_i$, expressed in the inertial frame, as shown in Fig. 4.1, takes on the form

$$\mathbf{a}_{i,i+2} = \mathbf{R}_i[\mathbf{a}_{i,i+2}]_i = \mathbf{R}_i[\mathbf{a}_{0i,i+2}]_i + \mathbf{R}_i[\mathbf{a}_{ei,i+2}]_i, \quad i = 1,\ldots,4 \tag{4.19}$$

where $[\mathbf{a}_{0i,i+2}]_i$ and $[\mathbf{a}_{ei,i+2}]_i$ are, respectively, the position vector of point O_{i+2} in the undeformed configuration of link i and the elastic displacement of point O_{i+2}, expressed in link i. Differentiating $\mathbf{a}_{i,i+2}$ with respect to time leads to

$$\dot{\mathbf{a}}_{i,i+2} = \omega_i \mathbf{E}\mathbf{a}_{i,i+2} + \mathbf{R}_i \mathbf{L}_i(O_{0i,i+2})\dot{\mathbf{u}}_i(t), \quad i = 1, \ldots, 4 \tag{4.20}$$

where eqs. (4.6) and (4.7) are recalled and $\mathbf{L}_i(O_{0i,i+2})$ is the $2 \times n_i$ shape-function matrix evaluated at point O_{i+2} in the undeformed configuration of link i, as defined in eq.(2.31). Hence, the components of $\mathbf{v}$ are computed by using eqs.(2.34) for planar systems, in light of eq.(4.20), as

$$\omega_i = \dot{\theta}_i \tag{4.21a}$$

$$\dot{\mathbf{r}}_i = \mathbf{0}_2 \tag{4.21b}$$

$$\omega_{i+2} = \omega_i + \dot{\theta}_{i+2} + w_{i,i+2} \tag{4.21c}$$

$$\dot{\mathbf{r}}_{i+2} = \dot{\mathbf{r}}_i + \mathbf{E}\mathbf{a}_{i,i+2}\omega_i + \mathbf{R}_i \mathbf{L}_i(O_{0i,i+2})\dot{\mathbf{u}}_i(t) \tag{4.21d}$$

$$\omega_c = \dot{\theta}_1 + \dot{\theta}_3 + w_{13} + w_{35} + \dot{\theta}_5 \tag{4.21e}$$

$$\dot{\mathbf{r}}_c = \dot{\mathbf{r}}_3 + \frac{1}{2}\omega_c \mathbf{E}\mathbf{a}_{56} + \mathbf{E}\mathbf{a}_{35}\omega_3 + \mathbf{R}_3 \mathbf{L}_3(O_{03,5})\dot{\mathbf{u}}_3(t) \tag{4.21f}$$

where $i = 1, 2$, and $w_{i,i+2}$ is the angular velocity of the frame $\mathcal{F}_{i+2}$ with respect to $\mathcal{F}_i$, resulting from the elastic displacement of link i, that can be written for small displacements as

$$w_{i,i+2} = \mathbf{x}_i^T \dot{\mathbf{u}}_i(t) = \left(\mathbf{l}_i^T / \|\mathbf{a}_{0i,i+2}\|\right) \dot{\mathbf{u}}_i(t) \tag{4.21g}$$

Here, $\mathbf{x}_i$ is an n_i-dimensional vector, while $\mathbf{l}_i^T$ is defined as the second row of $\mathbf{L}_i(O_{0i,i+2})$ and $\|.\|$ is the Euclidean norm of the vector $(\cdot)$.

4.4 Formulation in Joint Space

The approach explained in Subsection 2.7.1 is now applied to this example. The $(q+2)$-dimensional vector of generalized coordinates is obtained as

$$\boldsymbol{\theta} = \begin{bmatrix} \boldsymbol{\theta}_I^T & \boldsymbol{\theta}_D^T \end{bmatrix}^T \tag{4.22a}$$

where $\boldsymbol{\theta}_I$ is the q-dimensional vector of independent generalized coordinates, defined as

$$\boldsymbol{\theta}_I = \begin{bmatrix} \theta_1 & \theta_2 & \theta_3 & \mathbf{u}_1^T(t) & \mathbf{u}_2^T(t) & \mathbf{u}_3^T(t) & \mathbf{u}_4^T(t) \end{bmatrix}^T \tag{4.22b}$$

Here, θ_i, for $i = 1, 2, 3$, is the actuated joint angle and $\mathbf{u}_i(t)$ is defined in eq.(4.3). Moreover, $\boldsymbol{\theta}_D$ is the 2-dimensional vector of dependent generalized coordinates, defined as

$$\boldsymbol{\theta}_D = \begin{bmatrix} \theta_4 & \theta_5 \end{bmatrix}^T \tag{4.22c}$$

in which θ_j, for $j = 4, 5$, is the unactuated joint angle, as shown in Fig. 4.1 The loop-constraint equation for the problem at hand can be derived using Fig. 4.1, as

$$\mathbf{a}_{13} + \mathbf{a}_{35} + \mathbf{a}_{56} - \mathbf{a}_{46} - \mathbf{a}_{24} - \mathbf{a}_{12} = \mathbf{0}_2 \tag{4.23}$$

It is possible to write the above equation in terms of local coordinates as

$$\mathbf{R}_1[\mathbf{a}_{13}]_1 + \mathbf{R}_3[\mathbf{a}_{35}]_3 + \mathbf{R}_5[\mathbf{a}_{56}]_5 - \mathbf{R}_4[\mathbf{a}_{46}]_4 - \mathbf{R}_2[\mathbf{a}_{24}]_2 - \mathbf{a}_{12} = \mathbf{0}_2 \tag{4.24}$$

with $\mathbf{R}_j$, the rotation matrix of frame $\mathcal{F}_j$ with respect to the inertial frame, given as

$$\mathbf{R}_i = \mathbf{Q}_i \qquad \text{for} \quad i = 1, 2 \tag{4.25a}$$

$$\mathbf{R}_{i+2} = \mathbf{R}_i \mathbf{F}_i \mathbf{Q}_{i+2} \qquad \text{for} \quad i = 1, 2, 3 \tag{4.25b}$$

where

$$\mathbf{Q}_j = \begin{bmatrix} \cos(\theta_j) & -\sin(\theta_j) \\ \sin(\theta_j) & \cos(\theta_j) \end{bmatrix} \qquad \text{for} \quad i = 1, \ldots, 5 \tag{4.25c}$$

Moreover, $\mathbf{F}_i$ is the rotation matrix associated with the flexibility of link i, which can be written for small displacements as

$$\mathbf{F}_i = \begin{bmatrix} 1 & -\gamma_i \\ \gamma_i & 1 \end{bmatrix} \tag{4.25d}$$

where γ_i is the joint angle associated with the link flexibility, as depicted in Fig. 4.1, and is given by

$$\gamma_i = \tan^{-1}\left(\frac{([\mathbf{a}_{ei,i+2}]_i)_2}{\|\mathbf{a}_{0i,i+2}\|}\right) \tag{4.25e}$$

Here, $[\mathbf{a}_{ei,i+2}]_i$ and $\mathbf{a}_{0i,i+2}$ are defined in eq.(4.19), while $(\cdot)_2$ is the second component of vector $(\cdot)$. Introducing $\mathbf{R}_j$ from eqs.(4.25) into eq.(4.24) and expanding the equation thus resulting, one obtains two nonlinear scalar equations that should be solved numerically to obtain the dependent generalized coordinates $\boldsymbol{\theta}_D$ in terms of the independent ones, $\boldsymbol{\theta}_I$. The Newton-Raphson method is used to solve the above-mentioned equations.

The vector of dependent generalized speeds $\dot{\boldsymbol{\theta}}_D$ can be expressed in terms of $\dot{\boldsymbol{\theta}}_I$ by differentiating both sides of eq.(4.23) with respect to time and applying eqs.(4.20)–(4.21) and $\dot{\mathbf{a}}_{56} = \omega_c \mathbf{E}\mathbf{a}_{56}$, namely,

$$\begin{aligned} &\mathbf{R}_1\mathbf{L}_1(O_{01,3})\dot{\mathbf{u}}_1(t) + \dot{\theta}_1\mathbf{E}\mathbf{a}_{13} + \mathbf{R}_3\mathbf{L}_3(O_{03,5})\dot{\mathbf{u}}_3(t) + [\dot{\theta}_1 + \dot{\theta}_3 + \\ &\mathbf{x}_1^T\dot{\mathbf{u}}_1(t)]\mathbf{E}\mathbf{a}_{35} + [\dot{\theta}_1 + \dot{\theta}_3 + \dot{\theta}_5 + \mathbf{x}_1^T\dot{\mathbf{u}}_1(t) + \mathbf{x}_3^T\dot{\mathbf{u}}_3(t)]\mathbf{E}\mathbf{a}_{56} - \dot{\theta}_2\mathbf{E}\mathbf{a}_{24} \\ &-\mathbf{R}_2\mathbf{L}_2(O_{02,4})\dot{\mathbf{u}}_2(t) - [\dot{\theta}_2 + \dot{\theta}_4 + \mathbf{x}_2^T\dot{\mathbf{u}}_2(t)]\mathbf{E}\mathbf{a}_{46} - \mathbf{R}_4\mathbf{L}_4(O_{04,6})\dot{\mathbf{u}}_4(t) = \mathbf{0}_2 \end{aligned} \tag{4.26}$$

The above equation can be written in compact form as

$$\mathbf{N}_I\dot{\boldsymbol{\theta}}_I + \mathbf{N}_D\dot{\boldsymbol{\theta}}_D = \mathbf{0}_2 \tag{4.27}$$

where $\mathbf{N}_I$ is the $2 \times q$ matrix defined as

$$\mathbf{N}_I = \begin{bmatrix} \mathbf{c}_1 & \mathbf{c}_2 & \mathbf{c}_3 & \mathbf{C}_4 & \mathbf{C}_5 & \mathbf{C}_6 & \mathbf{C}_7 \end{bmatrix} \tag{4.28}$$

with further definitions, as follows:

$$\mathbf{c}_1 = \mathbf{E}(\mathbf{a}_{13} + \mathbf{a}_{35} + \mathbf{a}_{56}) \tag{4.29a}$$

$$\mathbf{c}_2 = -\mathbf{E}(\mathbf{a}_{46} + \mathbf{a}_{24}) \tag{4.29b}$$

$$\mathbf{c}_3 = \mathbf{E}(\mathbf{a}_{35} + \mathbf{a}_{56}) \tag{4.29c}$$

$$\mathbf{C}_4 = \mathbf{R}_1\mathbf{L}_1 + \mathbf{E}(\mathbf{a}_{35} + \mathbf{a}_{56})\mathbf{x}_1^T \tag{4.29d}$$

$$\mathbf{C}_5 = -\mathbf{R}_2\mathbf{L}_2 - \mathbf{E}\mathbf{a}_{46}\mathbf{x}_2^T \tag{4.29e}$$

$$\mathbf{C}_6 = \mathbf{R}_3\mathbf{L}_3 + \mathbf{E}\mathbf{a}_{56}\mathbf{x}_3^T \tag{4.29f}$$

$$\mathbf{C}_7 = -\mathbf{R}_4\mathbf{L}_4 \tag{4.29g}$$

In addition, $\mathbf{N}_D$ is a 2×2 matrix, namely,

$$\mathbf{N}_D = \begin{bmatrix} -\mathbf{E}\mathbf{a}_{46} & \mathbf{E}\mathbf{a}_{56} \end{bmatrix} \tag{4.30}$$

Now, use of eq.(4.27) leads to

$$\dot{\boldsymbol{\theta}}_D = -\mathbf{N}_D^{-1}\mathbf{N}_I\dot{\boldsymbol{\theta}}_I \tag{4.31}$$

Here, the inverse of the 2×2 matrix $\mathbf{N}_D$ can be readily computed as

$$\mathbf{N}_D^{-1} = \frac{1}{\Delta}\begin{bmatrix} (\mathbf{E}\mathbf{a}_{56})^T \\ -(\mathbf{E}\mathbf{a}_{46})^T \end{bmatrix}\mathbf{E} \equiv \frac{1}{\Delta}\begin{bmatrix} \mathbf{a}_{56}^T \\ -\mathbf{a}_{46}^T \end{bmatrix} \tag{4.32}$$

with $\Delta \equiv -\mathbf{a}_{56}^T\mathbf{E}\mathbf{a}_{46}$.

Upon substitution of $\mathbf{N}_D^{-1}$ from eq.(4.32) into $\dot{\boldsymbol{\theta}}_D$, one obtains the dependent generalized speeds in terms of independent generalized speeds as

$$\dot{\boldsymbol{\theta}}_D = \begin{bmatrix} \dot{\theta}_4 \\ \dot{\theta}_5 \end{bmatrix} = \begin{bmatrix} -\frac{1}{\Delta}\mathbf{a}_{56}^T\mathbf{N}_I\dot{\boldsymbol{\theta}}_I \\ \frac{1}{\Delta}\mathbf{a}_{46}^T\mathbf{N}_I\dot{\boldsymbol{\theta}}_I \end{bmatrix} \tag{4.33}$$

Introducing $\dot{\vartheta}_D$ from the above equation into eqs.(4.21), the components of $\mathbf{v}$ can then be expressed in terms of the independent generalized speeds $\dot{\boldsymbol{\theta}}_I$, which leads to the $m' \times q$ NOC matrix $\mathbf{N}$, in light of eq.(2.35), as follows:

$$\mathbf{N} = \begin{bmatrix} \mathbf{n}_0 & \mathbf{O}_{2q}^T & \mathbf{N}_0^T & \mathbf{O}_{2q}^T & \mathbf{N}_1^T & \mathbf{n}_1 & \mathbf{N}_2^T & \mathbf{n}_2 & \mathbf{N}_3^T \end{bmatrix}^T \tag{4.34}$$

while the q-dimensional row vectors $\mathbf{n}_0^T$, $\mathbf{n}_1^T$, and $\mathbf{n}_2^T$ together with other matrices are given by

$$\mathbf{n}_0^T = \begin{bmatrix} 1 & 0 & 0 & \mathbf{0}_{n_1}^T & \mathbf{0}_{n_2}^T & \mathbf{0}_{n_3}^T & \mathbf{0}_{n_4}^T \end{bmatrix} \tag{4.35a}$$

$$\mathbf{n}_1^T = \begin{bmatrix} 0 & 1 & 0 & \mathbf{0}_{n_1}^T & \mathbf{x}_2^T & \mathbf{0}_{n_3}^T & \mathbf{0}_{n_4}^T \end{bmatrix} - \frac{1}{\Delta}\mathbf{a}_{56}^T\mathbf{N}_I \tag{4.35b}$$

$$\mathbf{n}_2^T = \begin{bmatrix} 1 & 0 & 1 & \mathbf{x}_1^T & \mathbf{0}_{n_2}^T & \mathbf{x}_3^T & \mathbf{0}_{n_4}^T \end{bmatrix} + \frac{1}{\Delta}\mathbf{a}_{46}^T\mathbf{N}_I \tag{4.35c}$$

$$\mathbf{N}_0 = \begin{bmatrix} \mathbf{0}_{n_1} & \mathbf{0}_{n_1} & \mathbf{0}_{n_1} & \mathbf{1}_{n_1n_1} & \mathbf{O}_{n_1n_2} & \mathbf{O}_{n_1n_3} & \mathbf{O}_{n_1n_4} \\ 1 & 0 & 0 & \mathbf{0}_{n_1}^T & \mathbf{0}_{n_2}^T & \mathbf{0}_{n_3}^T & \mathbf{0}_{n_4}^T \end{bmatrix} \tag{4.35d}$$

$$\mathbf{N}_1 = \begin{bmatrix} \mathbf{0}_{n_2} & \mathbf{0}_{n_2} & \mathbf{0}_{n_2} & \mathbf{O}_{n_2n_1} & \mathbf{1}_{n_2n_2} & \mathbf{O}_{n_2n_3} & \mathbf{O}_{n_2n_4} \\ 1 & 0 & 1 & \mathbf{x}_1^T & \mathbf{0}_{n_2}^T & \mathbf{0}_{n_3}^T & \mathbf{0}_{n_4}^T \\ \mathbf{E}\mathbf{a}_{13} & \mathbf{0}_2 & \mathbf{0}_2 & \mathbf{R}_1\mathbf{L}_1 & \mathbf{O}_{2n_2} & \mathbf{O}_{2n_3} & \mathbf{O}_{2n_4} \\ \mathbf{0}_{n_3} & \mathbf{0}_{n_3} & \mathbf{0}_{n_3} & \mathbf{O}_{n_3n_1} & \mathbf{O}_{n_3n_2} & \mathbf{1}_{n_3n_3} & \mathbf{O}_{n_3n_4} \end{bmatrix} \tag{4.35e}$$

$$\mathbf{N}_2 = \begin{bmatrix} \mathbf{0}_2 & \mathbf{E}\mathbf{a}_{24} & \mathbf{0}_2 & \mathbf{O}_{2n_1} & \mathbf{R}_2\mathbf{L}_2 & \mathbf{O}_{2n_3} & \mathbf{O}_{2n_4} \\ \mathbf{0}_{n_4} & \mathbf{0}_{n_4} & \mathbf{0}_{n_4} & \mathbf{O}_{n_4n_1} & \mathbf{O}_{n_4n_2} & \mathbf{O}_{n_4n_3} & \mathbf{1}_{n_4n_4} \end{bmatrix} \tag{4.35f}$$

$$\begin{aligned}\mathbf{N}_3 = [\ & \mathbf{E}(\mathbf{a}_{13} + \mathbf{a}_{35} + \tfrac{1}{2}\mathbf{a}_{56}) \quad 0 \quad \mathbf{E}(\mathbf{a}_{35} + \tfrac{1}{2}\mathbf{a}_{56}) \quad \mathbf{E}(\mathbf{a}_{35} + \tfrac{1}{2}\mathbf{a}_{56})\mathbf{x}_1^T + \mathbf{R}_1\mathbf{L}_1 \\ & \mathbf{O}_{2n_2} \quad \tfrac{1}{2}\mathbf{E}\mathbf{a}_{56}\mathbf{x}_3^T + \mathbf{R}_3\mathbf{L}_3 \quad \mathbf{O}_{2n_4}\ ] + \frac{1}{2\Delta}\mathbf{E}\mathbf{a}_{56}\mathbf{a}_{46}^T\mathbf{N}_I\end{aligned} \tag{4.35g}$$

where $\mathbf{0}_j$ is the j-dimensional zero vector, $\mathbf{O}_{ij}$ is the $i \times j$ zero matrix and $\mathbf{1}_{jj}$ is the $j \times j$ identity matrix. Moreover, $\mathbf{N}_I$ is as given in eq.(4.28), while $\mathbf{L}_i \equiv \mathbf{L}_i(O_{0i,i+2})$ is defined just after eq.(4.20).

4.5 Formulation in Cartesian Space

The approach explained in Subsection 2.7.2 is used for the problem at hand. The q-dimensional vector of independent generalized speeds $\dot{\boldsymbol{\theta}}_I$ can be defined in Cartesian space as

$$\dot{\boldsymbol{\theta}}_I = \begin{bmatrix} \omega_c & \dot{\mathbf{r}}_c^T & \dot{\mathbf{u}}_1^T(t) & \dot{\mathbf{u}}_2^T(t) & \dot{\mathbf{u}}_3^T(t) & \dot{\mathbf{u}}_4^T(t) \end{bmatrix}^T \tag{4.36}$$

The NOC matrix $\mathbf{N}$ is obtained by resorting to the linear relations between the flexible twists of the links and $\dot{\boldsymbol{\theta}}_I$ as follows. The position vector $\mathbf{r}_c$ can be obtained using two different paths in Fig. 4.1 as

$$\mathbf{r}_c = \mathbf{a}_{13} + \mathbf{a}_{35} + \frac{1}{2}\mathbf{a}_{56} \tag{4.37a}$$

$$\mathbf{r}_c = \mathbf{a}_{12} + \mathbf{a}_{24} + \mathbf{a}_{46} - \frac{1}{2}\mathbf{a}_{56} \tag{4.37b}$$

Differentiating eqs.(4.37) with respect to time and introducing $\dot{\mathbf{a}}_{i,i+2}$ from eqs.(4.20) and $\dot{\mathbf{a}}_{56} = \omega_c \mathbf{E}\mathbf{a}_{56}$ into the equations thus obtained yields

$$\dot{\mathbf{r}}_c = \omega_1 \mathbf{E}\mathbf{a}_{13} + \mathbf{R}_1\mathbf{L}_1\dot{\mathbf{u}}_1(t) + \omega_3\mathbf{E}\mathbf{a}_{35} + \mathbf{R}_3\mathbf{L}_3\dot{\mathbf{u}}_3(t) + \frac{1}{2}\dot{\omega}_c\mathbf{E}\mathbf{a}_{56} \tag{4.38a}$$

$$\dot{\mathbf{r}}_c = \omega_2 \mathbf{E}\mathbf{a}_{24} + \mathbf{R}_2\mathbf{L}_2\dot{\mathbf{u}}_2(t) + \omega_4\mathbf{E}\mathbf{a}_{46} + \mathbf{R}_4\mathbf{L}_4\dot{\mathbf{u}}_4(t) - \frac{1}{2}\dot{\omega}_c\mathbf{E}\mathbf{a}_{56} \tag{4.38b}$$

The scalar angular velocity ω_j, for $j = 1, \ldots, 4$, is obtained in terms of $\dot{\boldsymbol{\theta}}_I$ by rearranging eqs.(4.38) as

$$\begin{bmatrix} \omega_i \\ \omega_{i+2} \end{bmatrix} = \mathbf{Y}_{i,i+2}\dot{\boldsymbol{\theta}}_I \quad \text{for} \quad i = 1, 2 \tag{4.39a}$$

where $\mathbf{Y}_{i,i+2}$ is the $2 \times q$ matrix given by

$$\mathbf{Y}_{i,i+2} \equiv \begin{bmatrix} \mathbf{E}\mathbf{a}_{i,i+2} & \mathbf{E}\mathbf{a}_{i+2,i+4} \end{bmatrix} \mathbf{X}_{i,i+2} \tag{4.39b}$$

and

$$\mathbf{X}_{13} = \begin{bmatrix} -\frac{1}{2}\mathbf{E}\mathbf{a}_{56} & \mathbf{1}_{22} & -\mathbf{R}_1\mathbf{L}_1 & \mathbf{O}_{2n_2} & -\mathbf{R}_3\mathbf{L}_3 & \mathbf{O}_{2n_4} \end{bmatrix} \tag{4.39c}$$

$$\mathbf{X}_{24} = \begin{bmatrix} \frac{1}{2}\mathbf{E}\mathbf{a}_{56} & \mathbf{1}_{22} & \mathbf{O}_{2n_1} & -\mathbf{R}_2\mathbf{L}_2 & \mathbf{O}_{2n_3} & -\mathbf{R}_4\mathbf{L}_4 \end{bmatrix} \tag{4.39d}$$

Inserting ω_j from eqs.(4.39a) into eq.(4.21d), $\dot{\mathbf{r}}_{i+2}$ can also be expressed in terms of $\dot{\boldsymbol{\theta}}_I$ as

$$\dot{\mathbf{r}}_{i+2} = \mathbf{E}\mathbf{a}_{i,i+2}\mathbf{X}_{i,i+2}(i)\,\dot{\boldsymbol{\theta}}_I + \mathbf{R}_i\mathbf{L}_i\dot{\mathbf{u}}_i(t) \quad \text{for} \quad i = 1, 2 \tag{4.40}$$

where $(\cdot)(i)$ is i^{th} row of matrix $(\cdot)$. Hence, using eq.(2.35), the $m' \times q$ NOC matrix $\mathbf{N}$ takes on the form shown below:

$$\mathbf{N} = \begin{bmatrix} \mathbf{Y}_{13}^T(1) & \mathbf{O}_{2q}^T & \mathbf{N}_4^T & \mathbf{O}_{2q}^T & \mathbf{N}_5^T & \mathbf{N}_6^T & \mathbf{N}_7^T & \mathbf{N}_8^T & \mathbf{N}_9^T \end{bmatrix}^T \tag{4.41}$$

One has, additionally, the definitions given below:

$$\mathbf{N}_4 = \begin{bmatrix} \mathbf{0}_{n_1} & \mathbf{O}_{n_1 2} & \mathbf{1}_{n_1 n_1} & \mathbf{O}_{n_1 n_2} & \mathbf{O}_{n_1 n_3} & \mathbf{O}_{n_1 n_4} \\ & & & \mathbf{Y}_{24}(1) & & \end{bmatrix} \tag{4.42a}$$

$$\mathbf{N}_5 = \begin{bmatrix} \mathbf{0}_{n_2} & \mathbf{O}_{n_2 2} & \mathbf{O}_{n_2 n_1} & \mathbf{1}_{n_2 n_2} & \mathbf{O}_{n_2 n_3} & \mathbf{O}_{n_2 n_4} \\ & & & \mathbf{Y}_{13}(2) & & \end{bmatrix} \tag{4.42b}$$

$$\mathbf{N}_6 = \mathbf{E}\mathbf{a}_{13}\mathbf{X}_{13}(1) + \begin{bmatrix} \mathbf{0}_2 & \mathbf{O}_{22} & \mathbf{R}_1\mathbf{L}_1 & \mathbf{O}_{2n_2} & \mathbf{O}_{2n_3} & \mathbf{O}_{2n_4} \end{bmatrix} \tag{4.42c}$$

$$\mathbf{N}_7 = \begin{bmatrix} \mathbf{0}_{n_3} & \mathbf{O}_{n_3 2} & \mathbf{O}_{n_3 n_1} & \mathbf{O}_{n_3 n_2} & \mathbf{1}_{n_3 n_3} & \mathbf{O}_{n_3 n_4} \\ & & & \mathbf{Y}_{24}(2) & & \end{bmatrix} \tag{4.42d}$$

$$\mathbf{N}_8 = \mathbf{E}\mathbf{a}_{24}\mathbf{X}_{24}(1) + \begin{bmatrix} \mathbf{0}_2 & \mathbf{O}_{22} & \mathbf{O}_{2n_1} & \mathbf{R}_2\mathbf{L}_2 & \mathbf{O}_{2n_3} & \mathbf{O}_{2n_4} \end{bmatrix} \tag{4.42e}$$

$$\mathbf{N}_9 = \begin{bmatrix} \mathbf{0}_{n_4} & \mathbf{O}_{n_4 2} & \mathbf{O}_{n_4 n_1} & \mathbf{O}_{n_4 n_2} & \mathbf{O}_{n_4 n_3} & \mathbf{1}_{n_4 n_4} \\ 1 & \mathbf{0}_2^T & \mathbf{0}_{n_1}^T & \mathbf{0}_{n_2}^T & \mathbf{0}_{n_3}^T & \mathbf{0}_{n_4}^T \\ \mathbf{0}_2 & \mathbf{1}_{22} & \mathbf{O}_{2n_1} & \mathbf{O}_{2n_2} & \mathbf{O}_{2n_3} & \mathbf{O}_{2n_4} \end{bmatrix} \tag{4.42f}$$

while all quantities we already defined above.

The comparison of the two formulations shows that the formulations in joint space requires more computational work than the one in Cartesian space. The former needs the direct kinematic solution, which requires the solution of nonlinear equations. Moreover, the direct kinematic solution will be a very time-consuming task in case of systems with more than two cooperating manipulators. It will be shown later that the CPU time for simulation of a numerical example of the problem at hand, formulated in Cartesian space, is 75% of the one formulated in joint space.

4.6 Simulation Results

The equations of motion of the entire mechanical system are obtained by assembling all the individual link models together, as mentioned in Section 3.3.

Table 4.1: Physical parameters of two cooperative manipulators

Link	Length (metre)	Mass (Kg)	EI (Nm^2)
$1(O_1O_3)$, $2(O_2O_4)$	0.45	.0623	7.815
$3(O_3O_5)$, $4(O_4O_6)$	0.55	.0761	7.815
manipulated object(O_5O_6)	0.40	0.665	Rigid

The physical parameters of this example are given in Table 4.1. It may be noted that 2, 4, 6 and 8 beam elements for each flexible link are used to discretize the flexible links, the results in all cases being nearly the same. Hence, from now on, two beam elements for each flexible link are used to discretize the flexible links in our examples in order to reduce the simulation time. Similarly, it has been found that using the first two, four or six modes of each flexible link for defining modal coordinates leads to nearly the same results. In this example, two beam elements for each flexible link are used to discretize the flexible links as well, and the first two modes of each flexible link are used.

4.6.1 Comparison of the Simulation Results in Cartesian and Joint Spaces

The simulation of the problem at hand is performed for formulations in both Cartesian and joint spaces under the same conditions in order to compare the simulation results for both cases.

A prescribed *cycloidal* manoeuvre for the centre of mass of the manipulated object, which undergoes a horizontal translation, and the angle of orientation of the manipulated object, are chosen as follows:

$$x_c = 0.2 + 0.5\left(\frac{t}{T} - \frac{1}{2\pi}\sin\frac{2\pi t}{T}\right) \quad 0 \le t \le T$$

$$\theta_c = \frac{\pi}{6}\left(\frac{t}{T} - \frac{1}{2\pi}\sin\frac{2\pi t}{T}\right) \quad 0 \le t \le T$$

Here, x_c is a horizontal translation, i.e., the component of $\mathbf{r}_c$ along the X_0 axis, measured in metres, and θ_c is the angle of orientation, measured in radians, of the manipulated object, as shown in Fig. 4.1, while $T = 0.5$ s. Hence, one may carry out the simulation based on the prescribed motion of the manipulated object in Cartesian space. To this end, the inverse kinematics of the rigid-link model is used to derive the nominal actuated joint angles and their time-rates of change, which are shown in Fig. 4.3.

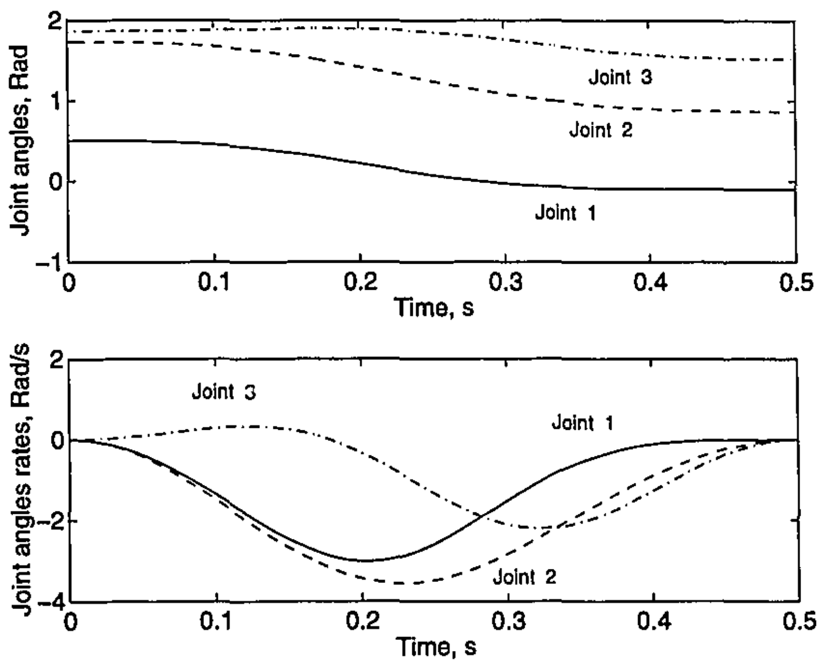

Figure 4.3: Actuated joint angles and their time-rates of change of the two cooperative manipulators

On the other hand, the joint trajectories shown in Fig. 4.3 are chosen for the prescribed manoeuvres of the actuated joints for the simulation in joint space. The actuated joint torques are then computed using inverse dynamics for formulations in both Cartesian and joint spaces, the results of which are depicted in Fig. 4.4. Next, the actual motion of the manipulated object, i.e., its orientation and translation, are computed by performing the simulation of the formulations in Cartesian space as obtained in Section 4.5. At the same time, the manipulated object motion is also computed based on the formulations in joint space using eqs.(4.21e) and (4.21f) for the actual model. The simulation results for both cases are depicted in Figs. 4.5 and 4.6. Given the manipulated object motion and joint angles γ_i associated with link flexibility, as depicted in Fig. 4.1, the total angles of rotation φ_i, as well as the joint angles θ_i and their time-rates of change are derived using the inverse kinematics for the model containing flexible links in Cartesian space. On the other hand, using the simulation of the model in joint space, as obtained in Section 4.4, joint angles and their time-rates of change are computed for the given joint torques using a model containing flexible links. The results for both formulations are shown in Figs. 4.7–4.9. Significant elastic displacements are observed in the flexible links, the results of which are shown for both cases in Figs. 4.10–4.13. The simulation results for both formulations are shown in the same plots in order to compare them. The overall results presented in the above-mentioned figures show that the simulation scheme is quite consistent for both formulations.

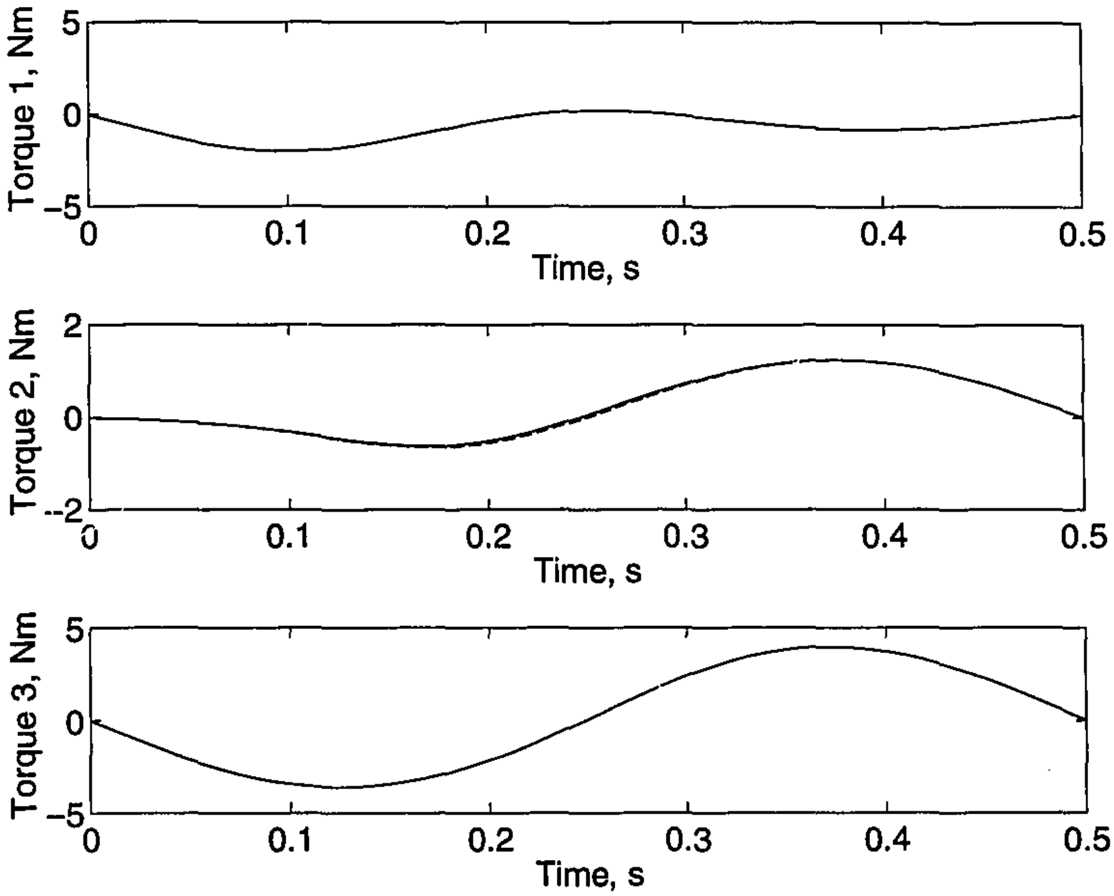

Figure 4.4: Actuated joint torques of the two cooperative manipulators (Cartesian —, joint – –)

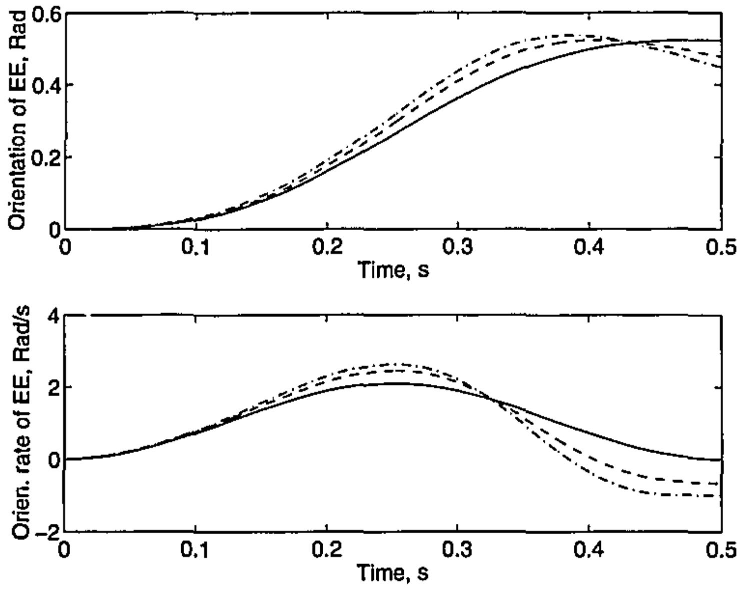

Figure 4.5: Orientation of the manipulated object and its time-rate of change of the two cooperative manipulators (rigid —, Cartesian – –, joint – · –)

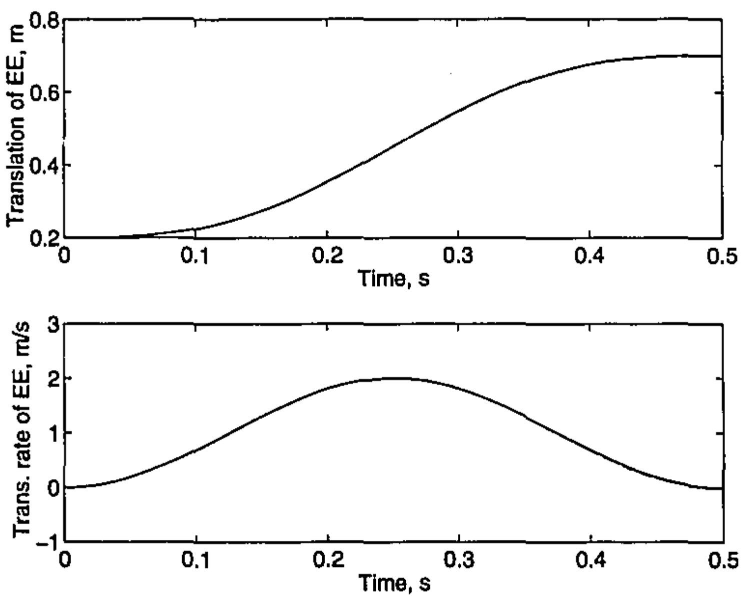

Figure 4.6: Translation of the manipulated object and its time-rate of change of the two cooperative manipulators (rigid —, Cartesian – –, joint – · –)

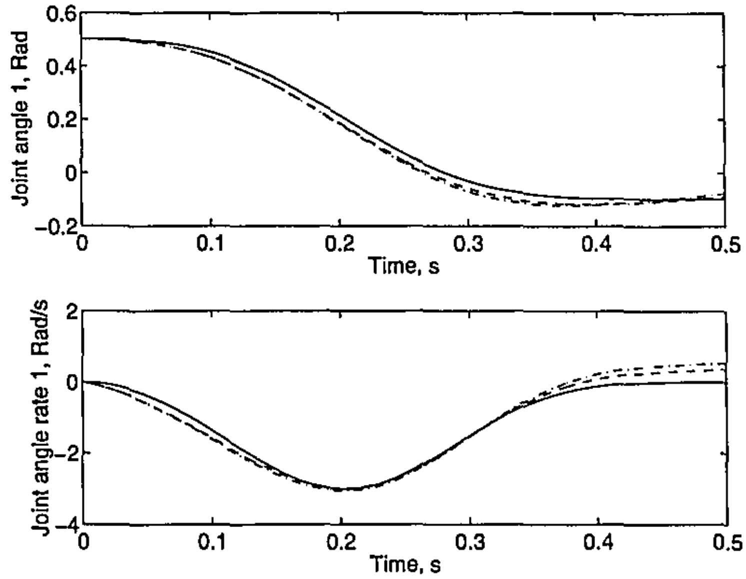

Figure 4.7: Joint angle 1 and its time-rate of change of the two cooperative manipulators (rigid —, Cartesian - -, joint — · —)

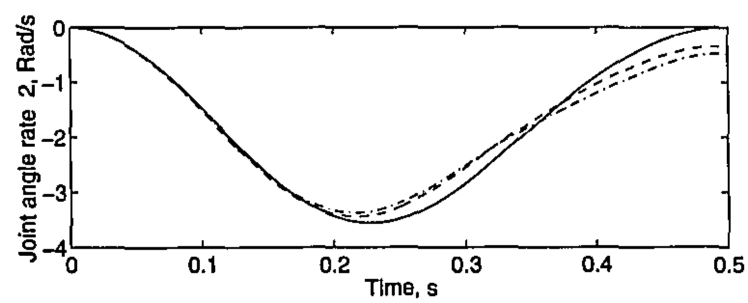

Figure 4.8: Joint angle 2 and its time-rate of change of the two cooperative manipulators (rigid —, Cartesian - -, joint — · —)

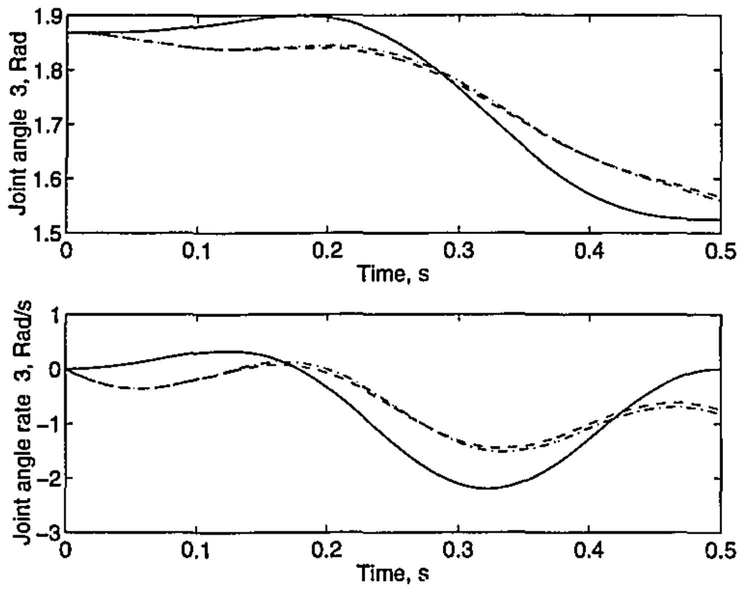

Figure 4.9: Joint angle 3 and its time-rate of change of the two cooperative manipulators (rigid —, Cartesian – –, joint – · –)

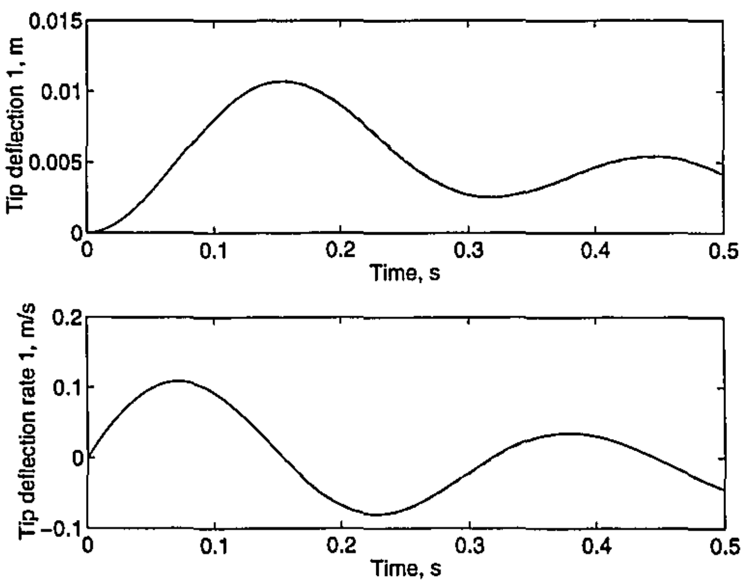

Figure 4.10: Tip deflection and its time-rate of change for link 1 of the two cooperative manipulators (Cartesian —, joint – –)

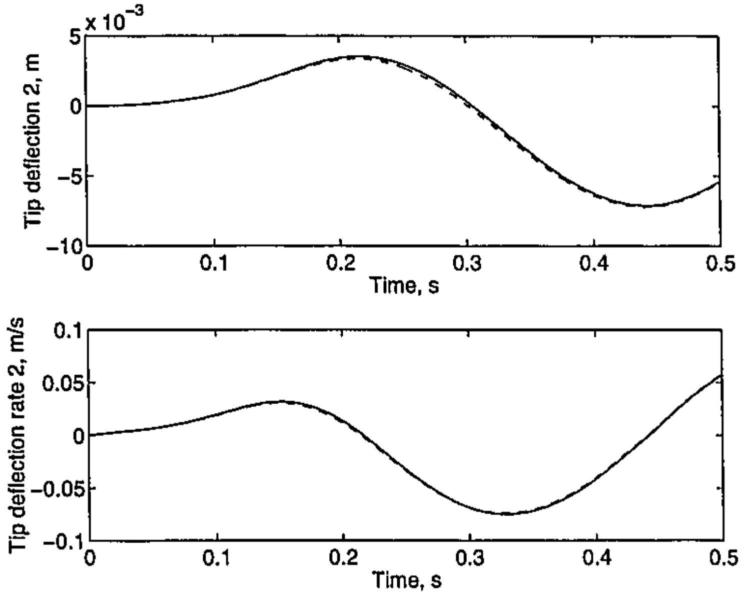

Figure 4.11: Tip deflection and its time-rate of change for link 2 of the two cooperative manipulators (Cartesian —, joint – –)

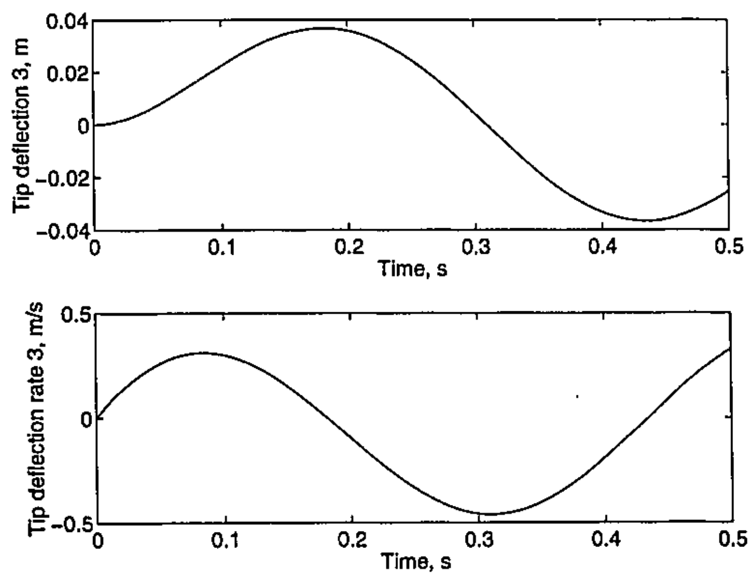

Figure 4.12: Tip deflection and its time-rate of change for link 3 of the two cooperative manipulators (Cartesian —, joint – –)

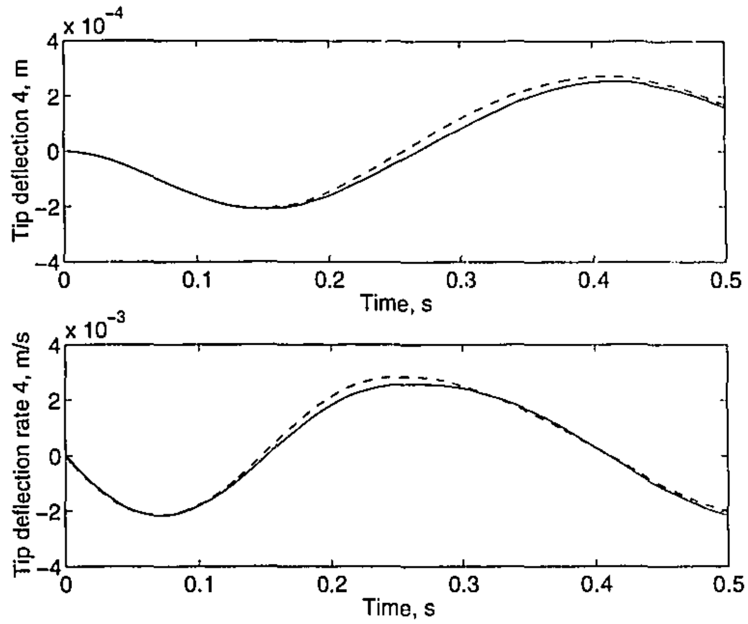

Figure 4.13: Tip deflection and its time-rate of change for link 4 of the two cooperative manipulators (Cartesian —, joint - -)

4.6.2 Structural Damping

In order to illustrate the effect of structural damping, simulations have been performed for two cases, one including structural damping and one without it. The damping coefficient for all the modes of the flexible links are taken equal to 1%. The simulation results for manipulated object motion, joint angles and tip deflections of the flexible links along with their time-rates of change are shown in the following figures. As it is apparent from the figures, the oscillations grow unbounded especially toward the end of the simulation, in the absence of structural damping. However, there is no source of energy in the system to explain the growth of the oscillations. Moreover, the smoothness of the trajectory for the actuated joint torques doesn't allow any initiation of real elastic oscillations. Hence, this growth is not due to physical reasons but rather numerical integration errors associated with discretization. On the other hand, consideration of structural damping does not allow the growth of spurious oscillations. It is evident from the results that consideration of structural damping leads to a reduction of the oscillations at the end of the simulation. Moreover, it is possible to increase the time step of the simulation time by including structural damping in the system. Furthermore, consideration of structural damping and small time step compensate for the errors that result from using the tabulated values of the actuated joint torques, computed based on a rigid-link model, to obtain the actual motion of the system at hand.

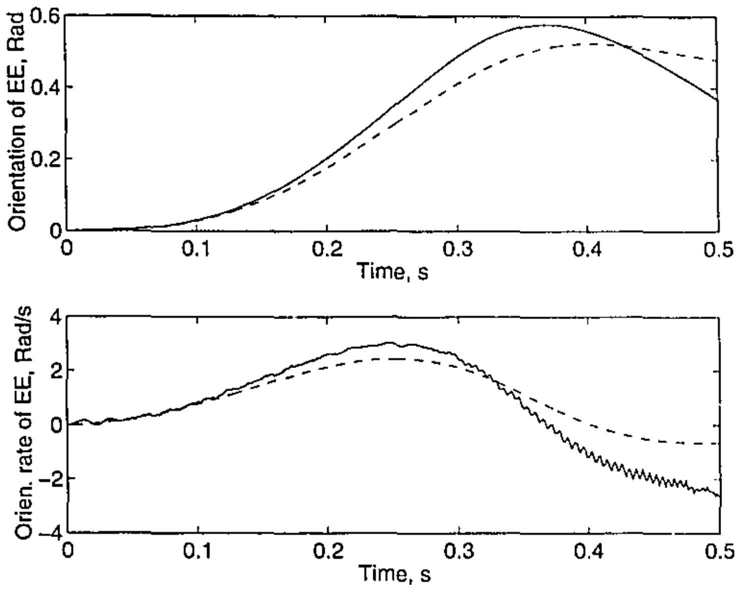

Figure 4.14: Orientation of manipulated object and its time-rate of change of the two cooperative manipulators (with damping – –, without damping —)

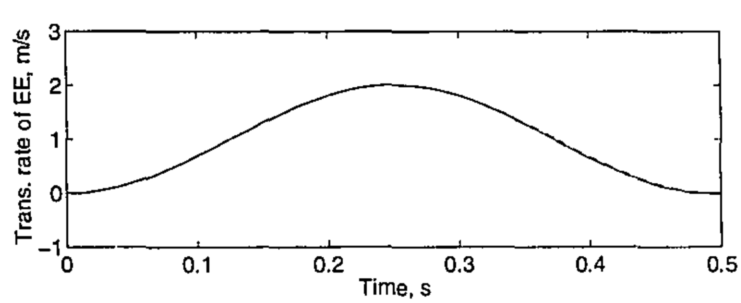

Figure 4.15: Translation of manipulated object and its time-rate of change of the two cooperative manipulators (with damping – –, without damping —)

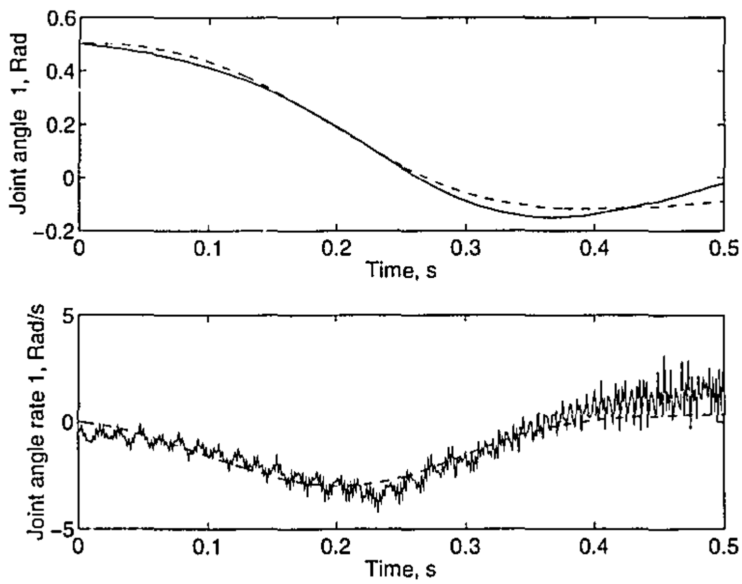

Figure 4.16: Joint angle 1 and its time-rate of change of the two cooperative manipulators (with damping – –, without damping —)

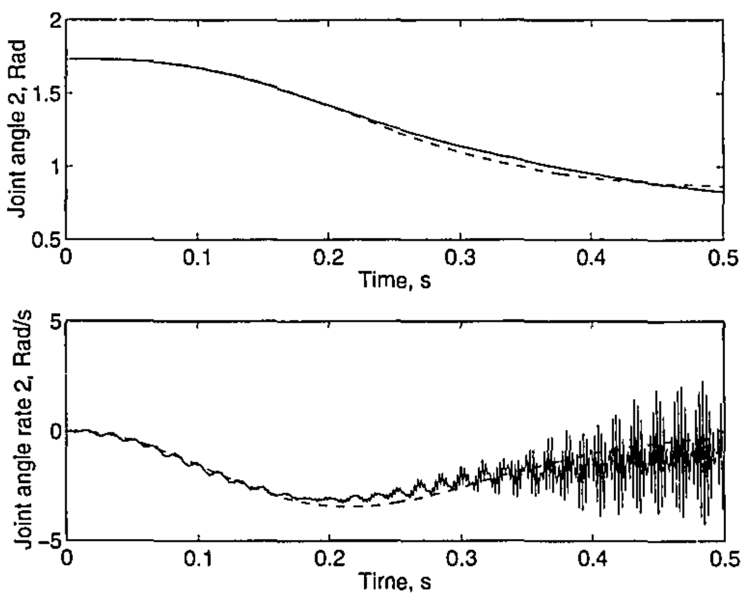

Figure 4.17: Joint angle 2 and its time-rate of change of the two cooperative manipulators (with damping – –, without damping —)

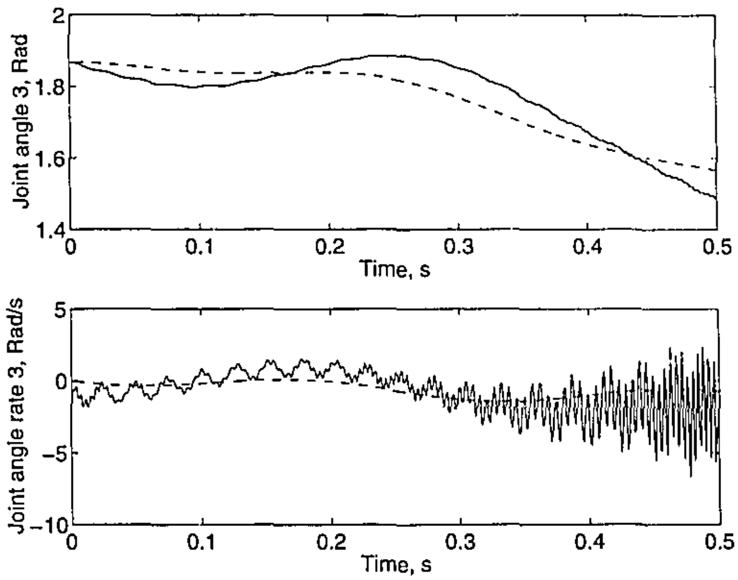

Figure 4.18: Joint angle 3 and its time-rate of change of the two cooperative manipulators (with damping – –, without damping —)

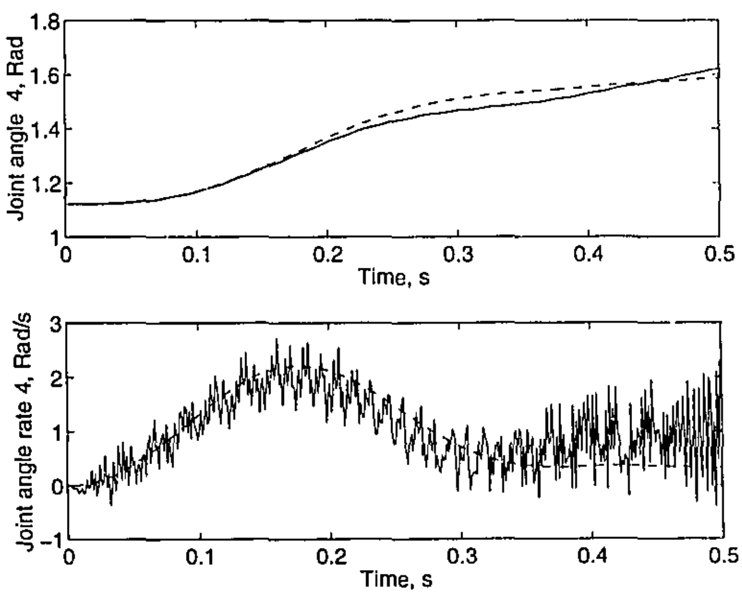

Figure 4.19: Joint angle 4 and its time-rate of change of the two cooperative manipulators (with damping – –, without damping —)

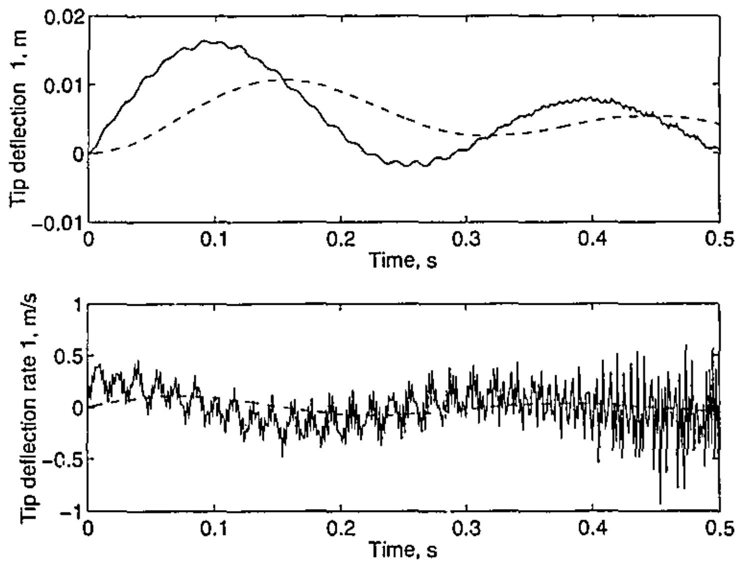

Figure 4.20: Tip deflection and its time-rate of change for link 1 of the two cooperative manipulators (with damping – –, without damping —)

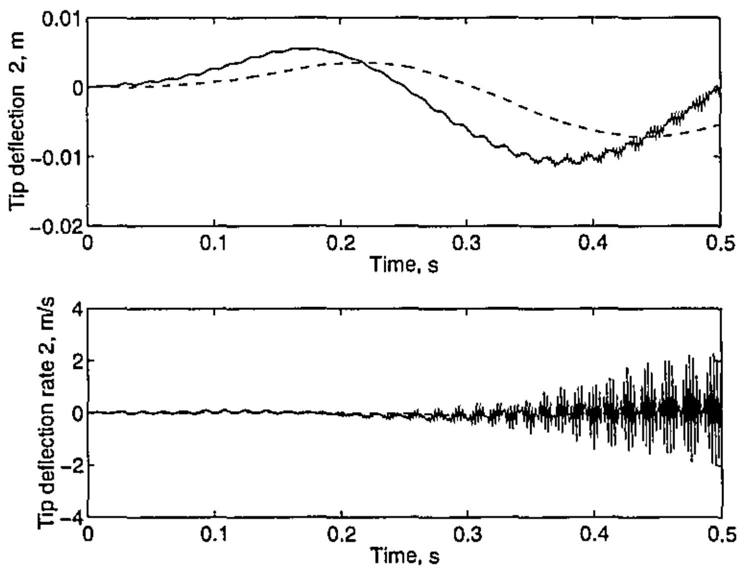

Figure 4.21: Tip deflection and its time-rate of change for link 2 of the two cooperative manipulators (with damping – –, without damping —)

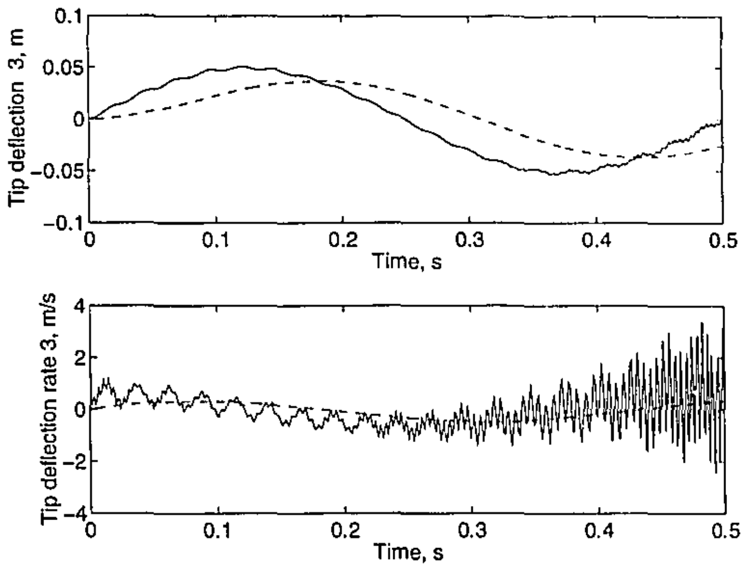

Figure 4.22: Tip deflection and its time-rate of change for link 3 of the two cooperative manipulators (with damping – –, without damping —)

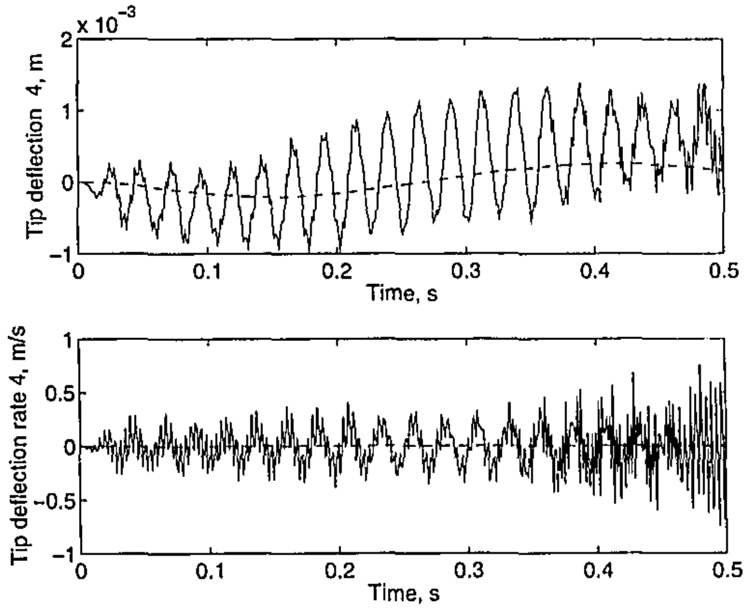

Figure 4.23: Tip deflection and its time-rate of change for link 4 of the two cooperative manipulators (with damping – –, without damping —)

Chapter 5

Dynamics of Planar Flexible-Link Parallel Manipulators

5.1 Introduction

In this chapter, another type of robotic manipulators with kinematic loops and flexible links, namely, planar parallel manipulators, is presented. Parallel manipulators are mechanical systems with multiple kinematic loops. They comprise two platforms, one fixed to the ground and one movable. The modelling formulations described in Chapters 2 and 3 are applied here to perform the simulation of the manipulators at hand. Some modifications in the modelling are made in order to simplify the formulation for planar systems, in the light of the modelling described in Section 4.2.

Figure 5.1 shows a planar parallel manipulator that contains flexible links and kinematic loops, the end-effector being assumed rigid. It has six flexible links, O_iO_{i+3}, for $i = 1, \ldots, 6$, and a rigid triangular end-effector, $O_7O_8O_9$.

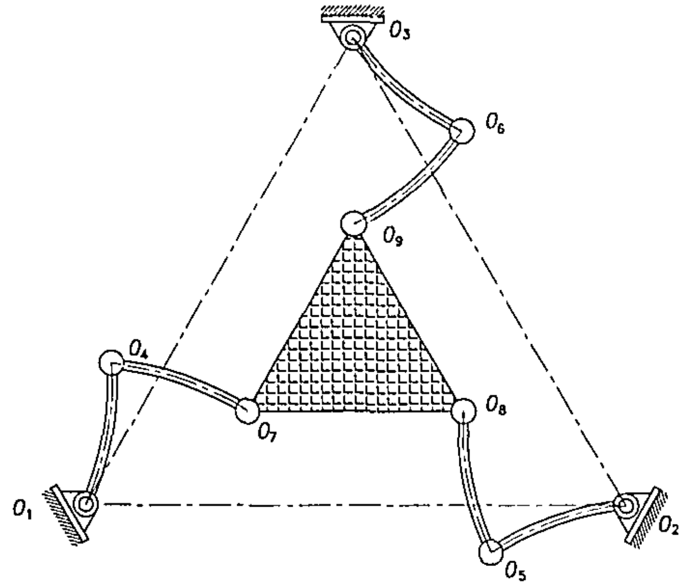

Figure 5.1: A planar flexible-link parallel manipulator

The DOF of the system at hand can be obtained by using eq.(4.1), namely,

$$q = 3 + \sum_{i=1}^{6} n_i = 3 + 6n \tag{5.1}$$

where the number of generalized coordinates associated with flexibility for all flexible links is assumed to be the same, i.e., all flexible links have the same number n of nodal coordinates. Equation (5.1) shows that the system has three rigid DOF. The motion of all links is planar and three motors, located at O_1, O_2 and O_3, drive the fixed joints.

If the end-effector motion is prescribed, the formulation of the problem in Cartesian space should be applied, which is discussed in Section 5.2. Here, to show the effect of geometric nonlinearities in the elastic displacements, a prescribed manoeuvre for the centre of mass of the end-effector is given with a very small time period T, in order to account for a high-speed operation. Structural damping is not considered in this example.

On the other hand, the formulation of the problem in joint space is used when the motion of the actuated joint angles and their time-rates of change are prescribed, which is studied in Section 5.3. In formulating the problem in joint space, the direct kinematic solution of the parallel manipulator, which is a very time-consuming task, is required. However, there is no need for this task in formulating the problem in Cartesian space.

5.2 Dynamics of the Planar Parallel Manipulator in Cartesian Space

The dynamics of the planar parallel manipulator, as shown in Fig. 5.2, in Cartesian space is modelled first. With reference to Fig. 5.2, γ_i is the joint angle associated with the flexibility of link i, while φ_i is the total angle of rotation of the joint centred at O_i, i.e., it is the sum of the joint angle, θ_i, and that due to the link flexibility. Using this model, some simulation results are obtained, and presented subsequently.

5.2.1 Modelling

The dynamical model of an individual beam-shaped link i, as shown in Fig. 5.3, is first formulated as an uncoupled body, as explained in Section 4.2. Then, the dynamical model of the entire system in Cartesian space is obtained by assembling all links together via their kinematic constraints, using the method of the natural orthogonal complement.

The twist-constraint equations of the holonomic system at hand can be expressed as

$$\mathbf{A}\mathbf{v} = \mathbf{0}_p \tag{5.2}$$

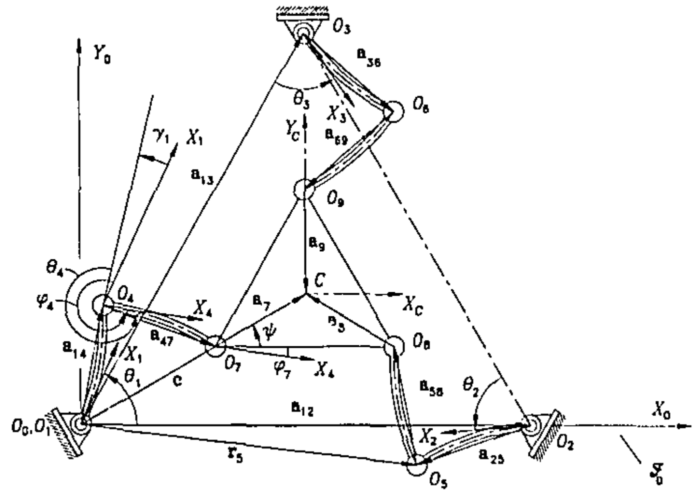

Figure 5.2: Geometric configuration of the planar parallel manipulator

where $\mathbf{v}$ is the $m'(=\sum_{i=1}^{r} m_i' + 3)$-dimensional vector of generalized twist, which is composed of the vectors of flexible twists of all moving links, which are the same as defined in eq.(4.4), plus the twist of the rigid end-effector, namely,

$$\mathbf{v} = \begin{bmatrix} \dot{\mathbf{r}}_1^T & \omega_1 & \dot{\mathbf{u}}_1^T & \ldots & \dot{\mathbf{r}}_r^T & \omega_r & \dot{\mathbf{u}}_r^T & \dot{\mathbf{c}}^T & \dot{\psi} \end{bmatrix}^T \tag{5.3}$$

With reference to Fig. 5.3, $\mathbf{r}_i$ is the 2-dimensional position vector of origin O_i with respect to the inertial frame and ω_i is the scalar angular velocity of the frame $\mathcal{F}_i(X_iY_i)$, attached to link i, with respect to the inertial frame. Moreover, ψ and $\mathbf{c}$ denote the angle of orientation of the end-effector and the position vector of the centre of mass of the end-effector with respect to the inertial frame, respectively, as shown in Fig. 5.2. In addition, r is the number of all moving links in the system, which is six here, and the matrix $\mathbf{A}$ appearing in eq.(5.2) is the $p \times m'$ twist-constraint matrix, while $\mathbf{0}_p$ is the p-dimensional zero vector, with p defined as the number of twist-constraint equations. Additionally, $\mathbf{u}_i \equiv \mathbf{u}_i(t)$ is the n-dimensional vector of generalized coordinates associated with the flexibility of link i. Vector $\mathbf{v}$, defined in eq.(5.3), can be expressed as a linear transformation of $\dot{\boldsymbol{\theta}}_I$, which is defined for a q-degree-of-freedom system as a q-dimensional vector of *independent* generalized speeds, namely,

$$\mathbf{v} = \mathbf{N}\dot{\boldsymbol{\theta}}_I \tag{5.4}$$

where $\mathbf{N}$ is the $m' \times q$ natural orthogonal complement (NOC) of matrix $\mathbf{A}$.

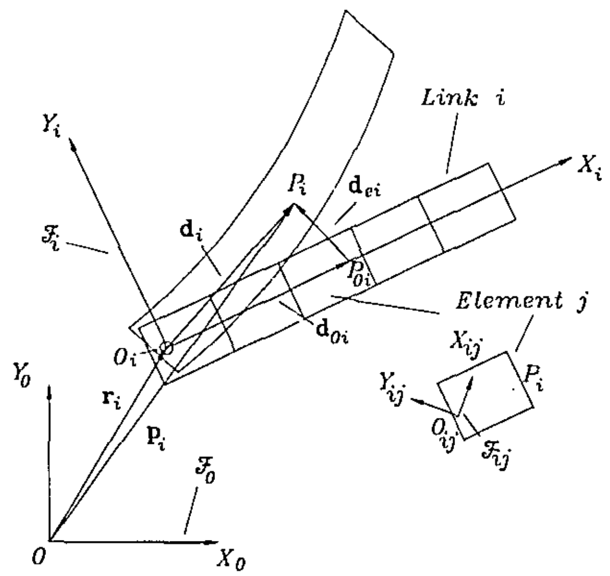

Figure 5.3: Modelling of the flexible beam-shaped link i

The form of $\dot{\boldsymbol{\theta}}_I$ depends on whether the system is being modelled in joint space or Cartesian space. Vector $\dot{\boldsymbol{\theta}}_I$ is usually composed of actuated joint speeds plus the generalized speeds associated with flexibility in joint space; while, in Cartesian space, $\dot{\boldsymbol{\theta}}_I$ can be defined as the array containing the end-effector twist plus the generalized speeds associated with flexibility. The $(3+6n)$-dimensional vector $\dot{\boldsymbol{\theta}}_I$, in the latter case, can be written as:

$$\dot{\boldsymbol{\theta}}_I = \begin{bmatrix} \dot{\psi} & \dot{\mathbf{c}}^T & \dot{\mathbf{u}}_1^T & \dot{\mathbf{u}}_2^T & \dot{\mathbf{u}}_3^T & \dot{\mathbf{u}}_4^T & \dot{\mathbf{u}}_5^T & \dot{\mathbf{u}}_6^T \end{bmatrix}^T \tag{5.5}$$

where all quantities are as defined just after eq.(5.3).

In formulating the problem in Cartesian space, using an expression for the position vector of the centre of mass of the end-effector, it is possible to express

$\mathbf{v}$ as a linear transformation of $\dot{\boldsymbol{\theta}}_I$, which leads to the NOC $\mathbf{N}$ as follows. Vector $\mathbf{c}$ can be determined using three different paths in Fig. 5.2, namely, $O_1O_4O_7C$, $O_1O_2O_5O_8C$ and $O_1O_3O_6O_9C$ to go from origin O_1 to C, the centre of mass of the end-effector, as shown in Fig. 5.2. These three paths then yield

$$\mathbf{c} = \mathbf{a}_{14} + \mathbf{a}_{47} + \mathbf{a}_7 \tag{5.6a}$$

$$\mathbf{c} = \mathbf{a}_{12} + \mathbf{a}_{25} + \mathbf{a}_{58} + \mathbf{a}_8 \tag{5.6b}$$

$$\mathbf{c} = \mathbf{a}_{13} + \mathbf{a}_{36} + \mathbf{a}_{69} + \mathbf{a}_9 \tag{5.6c}$$

where $\mathbf{a}_{i,i+3}$, for $i = 1, \ldots, 6$, is the position vector of point O_{i+3} in $\mathcal{F}_i$, and $\mathbf{a}_j$, for $j = 7, 8, 9$, is a vector on the end-effector $O_7O_8O_9$ from the origin O_j to point C, expressed in the inertial frame, as shown in Fig. 5.2, while vectors $\mathbf{a}_{12}$ and $\mathbf{a}_{13}$ are fixed. Using the same approach as in Section 4.3, the time derivative of vector $\mathbf{a}_{i,i+3}$ takes on the form

$$\dot{\mathbf{a}}_{i,i+3} = \omega_i \mathbf{E}\mathbf{a}_{i,i+3} + \mathbf{R}_i\mathbf{L}_i\dot{\mathbf{u}}_i(t), \quad i = 1, \ldots, 6 \tag{5.7}$$

where $\mathbf{L}_i \equiv \mathbf{L}_i(O_{0i,i+3})$ is the $2 \times n$ shape-function matrix evaluated at point O_{i+3} in the undeformed configuration of link i, as defined in eq.(2.31).

Differentiating eqs.(5.6) with respect to time and applying eqs.(5.7) for $\dot{\mathbf{a}}_{i,i+3}$ and using $\dot{\mathbf{a}}_j = \dot{\psi}\mathbf{E}\mathbf{a}_j$, for $j = 7, 8, 9$, one obtains

$$\dot{\mathbf{c}} = \omega_1\mathbf{E}\mathbf{a}_{14} + \mathbf{R}_1\mathbf{L}_1\dot{\mathbf{u}}_1 + \omega_4\mathbf{E}\mathbf{a}_{47} + \mathbf{R}_4\mathbf{L}_4\dot{\mathbf{u}}_4 + \dot{\psi}\mathbf{E}\mathbf{a}_7 \tag{5.8a}$$

$$\dot{\mathbf{c}} = \omega_2\mathbf{E}\mathbf{a}_{25} + \mathbf{R}_2\mathbf{L}_2\dot{\mathbf{u}}_2 + \omega_5\mathbf{E}\mathbf{a}_{58} + \mathbf{R}_5\mathbf{L}_5\dot{\mathbf{u}}_5 + \dot{\psi}\mathbf{E}\mathbf{a}_8 \tag{5.8b}$$

$$\dot{\mathbf{c}} = \omega_3\mathbf{E}\mathbf{a}_{36} + \mathbf{R}_3\mathbf{L}_3\dot{\mathbf{u}}_3 + \omega_6\mathbf{E}\mathbf{a}_{69} + \mathbf{R}_6\mathbf{L}_6\dot{\mathbf{u}}_6 + \dot{\psi}\mathbf{E}\mathbf{a}_9 \tag{5.8c}$$

Rearranging eqs.(5.8), ω_i is obtained in terms of $\dot{\boldsymbol{\theta}}_I$ as:

$$\begin{bmatrix} \omega_i \\ \omega_{i+3} \end{bmatrix} = \begin{bmatrix} \mathbf{E}\mathbf{a}_{i,i+3} & \mathbf{E}\mathbf{a}_{i+3,i+6} \end{bmatrix}^{-1} \mathbf{X}_{i,i+3}\dot{\boldsymbol{\theta}}_I \tag{5.9}$$

where $i = 1, 2, 3$, and $\mathbf{X}_{i,i+3}$ are $2 \times (3 + 6n)$ matrices defined as

$$\mathbf{X}_{14} = [-\mathbf{E}\mathbf{a}_7 \quad \mathbf{1}_{22} \quad -\mathbf{R}_1\mathbf{L}_1 \quad \mathbf{O}_{2n} \quad \mathbf{O}_{2n} \quad -\mathbf{R}_4\mathbf{L}_4 \quad \mathbf{O}_{2n} \quad \mathbf{O}_{2n}] \tag{5.10}$$

$$\mathbf{X}_{25} = [-\mathbf{E}\mathbf{a}_8 \quad \mathbf{1}_{22} \quad \mathbf{O}_{2n} \quad -\mathbf{R}_2\mathbf{L}_2 \quad \mathbf{O}_{2n} \quad \mathbf{O}_{2n} \quad -\mathbf{R}_5\mathbf{L}_5 \quad \mathbf{O}_{2n}] \tag{5.11}$$

$$\mathbf{X}_{36} = [-\mathbf{E}\mathbf{a}_9 \quad \mathbf{1}_{22} \quad \mathbf{O}_{2n} \quad \mathbf{O}_{2n} \quad -\mathbf{R}_3\mathbf{L}_3 \quad \mathbf{O}_{2n} \quad \mathbf{O}_{2n} \quad -\mathbf{R}_6\mathbf{L}_6] \tag{5.12}$$

with $\mathbf{1}_{22}$ defined already as the 2×2 identity matrix, while $\mathbf{O}_{2n}$ is the $2 \times n$ zero matrix. Here, the 2×2 inverse appearing in eq.(5.9) can be readily computed as

$$\begin{bmatrix} \mathbf{E}\mathbf{a}_{i,i+3} & \mathbf{E}\mathbf{a}_{i+3,i+6} \end{bmatrix}^{-1} = \frac{1}{\Delta} \begin{bmatrix} (\mathbf{E}\mathbf{a}_{i+3,i+6})^T \\ -(\mathbf{E}\mathbf{a}_{i,i+3})^T \end{bmatrix} \mathbf{E} \equiv \frac{1}{\Delta} \begin{bmatrix} \mathbf{a}_{i+3,i+6}^T \\ -\mathbf{a}_{i,i+3}^T \end{bmatrix} \tag{5.13}$$

with $\Delta \equiv -\mathbf{a}_{i+3,i+6}^T \mathbf{E}\mathbf{a}_{i,i+3}$.

Now, $\dot{\mathbf{r}}_i$, the velocity vector of O_i in the inertial frame, as shown in Fig. 5.2, can be derived, in light of eq.(5.7), as

$$\dot{\mathbf{r}}_i = \mathbf{0}_2, \tag{5.14a}$$

$$\dot{\mathbf{r}}_{i+3} = \omega_i \mathbf{E}\mathbf{a}_{i,i+3} + \mathbf{R}_i\mathbf{L}_i\dot{\mathbf{u}}_i(t) \tag{5.14b}$$

where $i = 1, 2, 3$, and $\mathbf{0}_2$ is the 2-dimensional zero vector, while other quantities have been defined already. Upon substitution of ω_i from eqs.(5.9) into eqs.(5.14), $\dot{\mathbf{r}}_{i+3}$ can also be expressed in terms of $\dot{\boldsymbol{\theta}}_I$. Therefore, substituting eqs.(5.9) and (5.14) into eq.(5.3), $\mathbf{v}$ can be expressed as a linear transformation of $\dot{\boldsymbol{\theta}}_I$, which leads to $\mathbf{N}$. Upon assembling the dynamics equations of all links and using the above modelling scheme for deriving the NOC $\mathbf{N}$, the model of the system at hand can be obtained by using eq.(3.77). It may be noted that, in this example, $m' = 21 + 6n$, while $q = 3 + 6n$.

Effect of Geometric Nonlinearities

As mentioned in Chapter 3, coupling of the longitudinal and transverse displacements of the beam-shaped links results from consideration of the effect of geometric nonlinearities in the elastic displacements. The latter arise, in turn, because of a term that should be added to the elastic strain energy of the beam element j

of link i in Fig. 5.3. This term can be obtained by using eq.(3.26) for planar beam-shaped links as

$$V_{ij}^{gn} = \frac{1}{2}\left[\int_v \epsilon_{XX}\sigma_{XX}dv\right]_{ij} \tag{5.15}$$

where the following assumptions for planar beam-shaped links are recalled.

$$[\sigma_{YY}]_{ij} = [\sigma_{ZZ}]_{ij} = [\sigma_{XY}]_{ij} = [\sigma_{XZ}]_{ij} = [\sigma_{YZ}]_{ij} = 0 \tag{5.16}$$

Introducing $[\epsilon_{XX}]_{ij}$ from eq.(3.27c) into eq.(5.15), one obtains

$$V_{ij}^{gn} = \frac{1}{2}\left[\int_0^l f(X,t)(\frac{\partial v}{\partial X})^2 dX\right]_{ij} \tag{5.17}$$

where l_{ij} is the length of the element j of link i and v_{ij} is its transverse displacement. Moreover, $f_{ij}(X,t)$ is the axial internal force, which can result from sources such as centrifugal effects associated with the angular velocity of link i. Equation (5.17) is obtained under the following assumptions: The beam has a constant cross-section throughout the element and the axial displacement can be ignored, i.e., the first term of eq.(3.27c) vanishes.

Then, using eqs. (3.28)–(3.31), one obtains $\mathbf{K}_{ij}^{gn}$ for the beam element j of link i as

$$\mathbf{K}_{ij}^{gn} = \left[\int_0^l f(X,t)(\frac{\partial \mathbf{L}}{\partial X})^T(\frac{\partial \mathbf{L}}{\partial X})dX\right]_{ij} \tag{5.18}$$

where $\mathbf{L}_{ij} \equiv \mathbf{L}_{ij}(P_{0i})$ is the $2 \times n_{ij}$ shape-function matrix of element j evaluated at any point P_i in the undeformed configuration of link i, as defined in eq.(2.5). If it is assumed that $f_{ij}(X,t)$ is constant along the element, the form of $\mathbf{K}_{ij}^{gn}$, for a given axial force, can be obtained from (Przemieniecki, 1967). Therefore, the stiffness matrix can be thought of as composed of two parts: the conventional stiffness matrix (Cook, 1981), which is constant, plus a geometric stiffness matrix, which is configuration-dependent, namely,

$$\mathbf{K}_{ij} = \mathbf{K}_{ij}^{e} + \mathbf{K}_{ij}^{gn} \tag{5.19}$$

Table 5.1: Physical parameters of the planar parallel manipulator

Link	Dimension (metre)	Mass (Kg)	EI (Nm^2)
$1(O_1O_4)$, $2(O_2O_5)$ and $3(O_3O_6)$	0.45	0.0623	7.815
$4(O_4O_7)$, $5(O_5O_8)$ and $6(O_6O_9)$	0.55	0.0761	7.815
End-effector($O_7O_8O_9$)	0.40	0.0959	Rigid

This expression is used to account for the effect of geometric nonlinearities, which lead to a coupling that has a considerable effect on the elastic displacements of beams in high-speed operations.

5.2.2 Simulation Results

The physical parameters used in this example are given in Table 5.1. In this example, two beam elements for each flexible link are used to discretize them and the first two modes of each flexible link are used for defining the modal coordinates.

A prescribed *cycloidal* manoeuvre for the centre of mass of the end-effector, which undergoes a horizontal translation, at a constant orientation, is given below:

$$x = \frac{1}{5} + \frac{1}{2}\left(\frac{t}{T} - \frac{1}{2\pi}\sin\frac{2\pi t}{T} \right) \tag{5.20}$$

Here, x is measured in metres and $T = 0.25$ s, which amounts to a high-speed operation. The inverse kinematics of the rigid-link model is used to obtain nominal joint angles and their time-rates of change. Actuated joint torques for the rigid-link model are then derived using inverse dynamics, the results of which are shown in Fig. 5.4. The actual end-effector motion and elastic displacements of the links are computed solving the equations of motion given by the the model

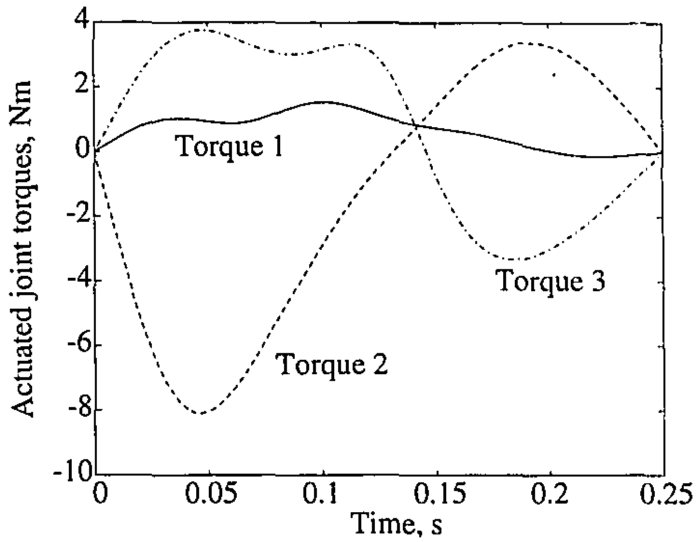

Figure 5.4: Actuated joint torques of the planar parallel manipulator

described in Section 5.2.1. Figure 5.5 displays the horizontal displacement of the centre of mass of the end-effector and its time-rate of change for the rigid-link model(dashed lines), as well as for the flexible-link model (solid lines). The joint angles and their time-rates of change for the model containing flexible links have also been calculated using the inverse kinematics of the parallel manipulator; as a sample, those for link 1 are shown in Fig. 5.6.

Finally, in order to illustrate the effect of the geometric nonlinearities, simulations for two cases have been performed, one including the above-mentioned effect (all the other results include this effect) and one without it. Tip deflections of links 1 and 4 and their time-rates of change for the two cases are shown in Figs. 5.7 and 5.8. One can observe from these figures that the simulation is unstable if geometric nonlinearities are not included. This is because the effect of geometric nonlinearities in the elastic displacements of flexible links is very crucial in high speed operations and without considering them, we could not obtain correct results.

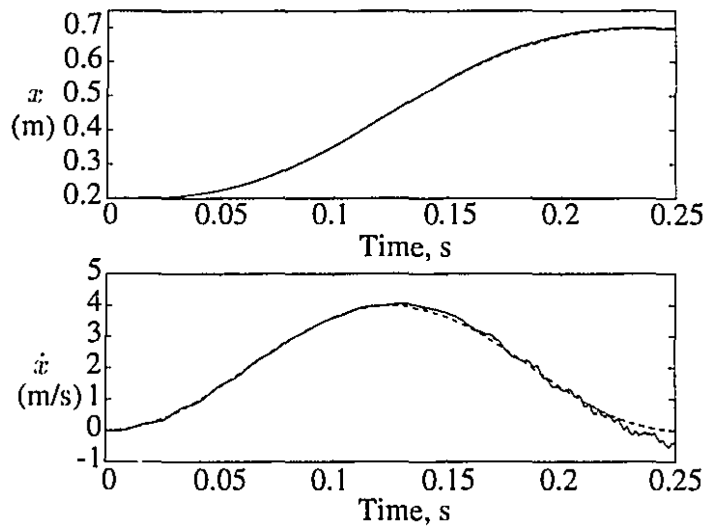

Figure 5.5: End-effector motion and its time-rate of change for the planar parallel manipulator (flexible —, rigid - - -)

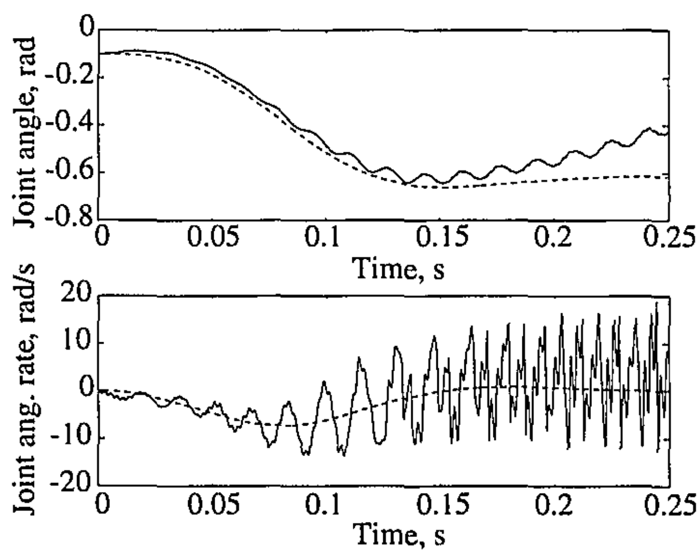

Figure 5.6: Joint angle and its time-rate for link 1 of the planar parallel manipulator (flexible —, rigid - - -)

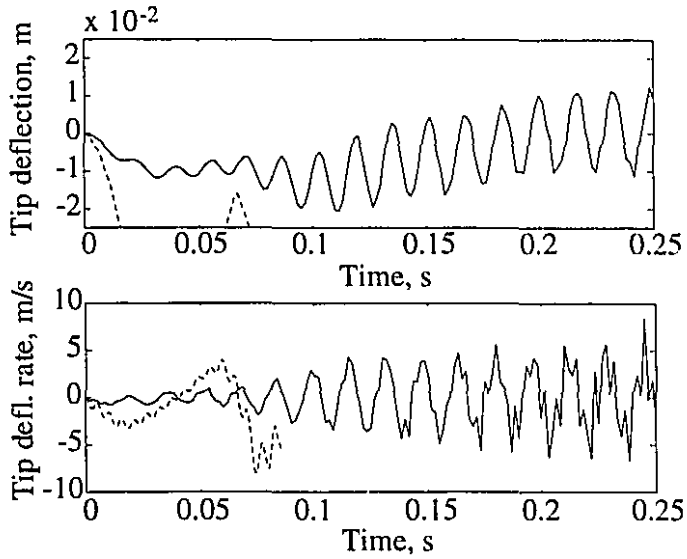

Figure 5.7: Tip deflection and its time-rate of change for link 1 of the planar parallel manipulator (with geometric nonlinearities —, without them - - -)

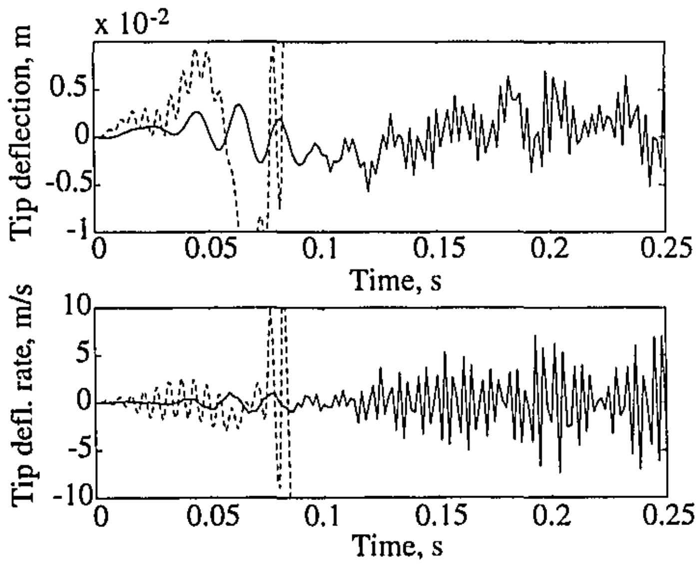

Figure 5.8: Tip deflection and its time-rate of change for link 4 of the planar parallel manipulator (with geometric nonlinearities —, without them - - -)

5.3 Dynamics of the Planar Parallel Manipulator in Joint Space

In this section, the modelling and simulation of the planar parallel manipulator, as shown in Fig. 5.1, in joint space is presented. The geometric configuration of the example at hand is shown in Fig. 5.9, while γ_i, φ_i and θ_i are the same as shown in Fig. 5.2. The vector of independent generalized speeds is composed of three time-rates of change of actuated joint angles plus the generalized speeds associated with link flexibility. The unactuated joint rates are the dependent generalized speeds. The model of an individual link is formulated in the same way as in Section 4.2. Then, the entire system is modelled by assembling all links together via their kinematic constraints. The kinematic constraints are formulated and the system dynamics for this example is simulated below.

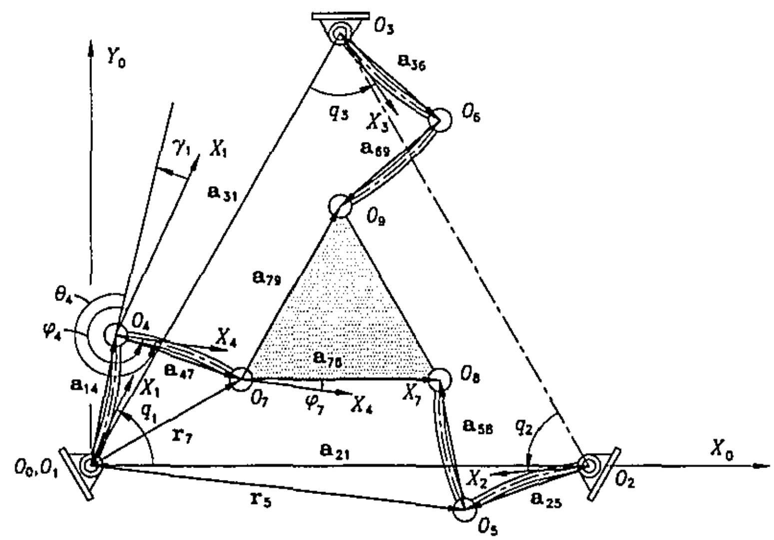

Figure 5.9: Geometric properties of the planar parallel manipulator

5.3.1 Formulation of Kinematic Constraints

In formulating the problem in joint space, for systems with kinematic loops, the NOC $\mathbf{N}$ can be evaluated using the equations constraining the twists of two coupled links as well as considering the loop-constraint equations of the system. This procedure needs the direct kinematics solution of the parallel manipulator.

The kinematic constraint equations of the parallel manipulator are derived using eqs.(2.34) for the planar systems, in light of eq.(4.20), which leads to

$$\omega_i = \dot{q}_i \tag{5.21a}$$

$$\dot{\mathbf{r}}_i = \mathbf{0}_2 \tag{5.21b}$$

$$\omega_{i+3} = \omega_i + \dot{\theta}_{i+3} + w_{i,i+3} \tag{5.21c}$$

$$\dot{\mathbf{r}}_{i+3} = \mathbf{E}\mathbf{a}_{i,i+3}\omega_i + \mathbf{R}_i\mathbf{L}_i\dot{\mathbf{u}}_i(t) \tag{5.21d}$$

$$\omega_7 = \omega_4 + \dot{\theta}_7 + w_{47} \tag{5.21e}$$

$$\dot{\mathbf{r}}_7 = \dot{\mathbf{r}}_4 + \mathbf{E}\mathbf{a}_{47}\omega_4 + \mathbf{R}_4\mathbf{L}_4\dot{\mathbf{u}}_4(t) \tag{5.21f}$$

where $i = 1, 2, 3$ and q_i is the actuated joint angle of the joint centred at O_i, while $\mathbf{L}_i \equiv \mathbf{L}_i(O_{0i,i+3})$ was defined in eq.(5.7). All other quantities are as defined earlier.

It is apparent from Fig. 5.9 that there are three loops in this parallel manipulator, namely, $O_1O_4O_7O_8O_5O_2O_1$, $O_1O_4O_7O_9O_6O_3O_1$ and $O_2O_5O_8O_9O_6O_3O_2$. However, from Euler's formula for graphs (Harary, 1969), only two of these three loops are independent. There is a 2-dimensional vector constraint equation for each loop, these equations taking on the forms

$$\mathbf{a}_{14} + \mathbf{a}_{47} + \mathbf{a}_{78} - \mathbf{a}_{58} - \mathbf{a}_{25} + \mathbf{a}_{21} = \mathbf{0}_2 \tag{5.22a}$$

$$\mathbf{a}_{14} + \mathbf{a}_{47} + \mathbf{a}_{79} - \mathbf{a}_{69} - \mathbf{a}_{36} + \mathbf{a}_{31} = \mathbf{0}_2 \tag{5.22b}$$

By differentiating the loop-constraint equations from eqs.(5.22) with respect to time, one obtains

$$\begin{aligned}\mathbf{R}_1\mathbf{L}_1\dot{\mathbf{u}}_1(t) + \dot{q}_1\mathbf{E}\mathbf{a}_{14} + \mathbf{R}_4\mathbf{L}_4\dot{\mathbf{u}}_4(t) + (\dot{q}_1 + \dot{\theta}_4 + \mathbf{x}_1^T\dot{\mathbf{u}}_1)& \\ \mathbf{E}\mathbf{a}_{47} + (\dot{q}_1 + \dot{\theta}_4 + \dot{\theta}_7 + \mathbf{x}_1^T\dot{\mathbf{u}}_1 + \mathbf{x}_4^T\dot{\mathbf{u}}_4)\mathbf{E}\mathbf{a}_{78} - \dot{q}_2\mathbf{E}\mathbf{a}_{25}& \\ -\mathbf{R}_2\mathbf{L}_2\dot{\mathbf{u}}_2(t) - (\dot{q}_2 + \dot{\theta}_5 + \mathbf{x}_2^T\dot{\mathbf{u}}_2)\mathbf{E}\mathbf{a}_{58} - \mathbf{R}_5\mathbf{L}_5\dot{\mathbf{u}}_5(t) = \mathbf{0}_2 &\end{aligned} \tag{5.23a}$$

$$\begin{aligned}\mathbf{R}_1\mathbf{L}_1\dot{\mathbf{u}}_1(t) + \dot{q}_1\mathbf{E}\mathbf{a}_{14} + \mathbf{R}_4\mathbf{L}_4\dot{\mathbf{u}}_4(t) + (\dot{q}_1 + \dot{\theta}_4 + \mathbf{x}_1^T\dot{\mathbf{u}}_1)& \\ \mathbf{E}\mathbf{a}_{47} + (\dot{q}_1 + \dot{\theta}_4 + \dot{\theta}_7 + \mathbf{x}_1^T\dot{\mathbf{u}}_1 + \mathbf{x}_4^T\dot{\mathbf{u}}_4)\mathbf{E}\mathbf{a}_{79} - \dot{q}_3\mathbf{E}\mathbf{a}_{36}& \\ -\mathbf{R}_3\mathbf{L}_3\dot{\mathbf{u}}_3(t) - (\dot{q}_3 + \dot{\theta}_6 + \mathbf{x}_3^T\dot{\mathbf{u}}_3)\mathbf{E}\mathbf{a}_{69} - \mathbf{R}_6\mathbf{L}_6\dot{\mathbf{u}}_6(t) = \mathbf{0}_2 &\end{aligned} \tag{5.23b}$$

where eqs.(5.7) and (5.21) have been recalled, while $\mathbf{x}_i$ is defined as $\mathbf{l}_i^T/\|\mathbf{a}_{0i(i+3)}\|$, with $\mathbf{l}_i^T$ defined, in turn, as the second row of $\mathbf{L}_i(O_{0i,i+3})$ of eq.(5.7) and $\|\mathbf{a}_{0i,i+3}\|$ is the Euclidean norm of the position vector of point O_{i+3} in the undeformed configuration of link i, as depicted in Fig. 5.9.

The above two equations can now be expressed in compact form as

$$\mathbf{N}_I\dot{\boldsymbol{\theta}}_I + \mathbf{N}_D\dot{\boldsymbol{\theta}}_D = \mathbf{0}_2 \tag{5.24}$$

where $\dot{\boldsymbol{\theta}}_I$ is the (3+6n)-dimensional vector of independent generalized speeds, and $\dot{\boldsymbol{\theta}}_D$ is the 4-dimensional vector of dependent generalized speeds, namely,

$$\dot{\boldsymbol{\theta}}_I = \begin{bmatrix} \dot{q}_1 & \dot{q}_2 & \dot{q}_3 & \dot{\mathbf{u}}_1^T & \dot{\mathbf{u}}_2^T & \dot{\mathbf{u}}_3^T & \dot{\mathbf{u}}_4^T & \dot{\mathbf{u}}_5^T & \dot{\mathbf{u}}_6^T \end{bmatrix}^T, \quad \dot{\boldsymbol{\theta}}_D = \begin{bmatrix} \dot{\theta}_4 & \dot{\theta}_5 & \dot{\theta}_6 & \dot{\theta}_7 \end{bmatrix}^T \tag{5.25}$$

while $\mathbf{N}_I$ is the $4 \times (3+6n)$ matrix defined as

$$\mathbf{N}_I = \begin{bmatrix} \mathbf{f}_1 & \mathbf{f}_2 & \mathbf{0}_2 & \mathbf{B}_1 & \mathbf{B}_2 & \mathbf{O}_{2n} & \mathbf{B}_3 & -\mathbf{R}_5\mathbf{L}_5 & \mathbf{O}_{2n} \\ \mathbf{g}_1 & \mathbf{0}_2 & \mathbf{g}_2 & \mathbf{G}_3 & \mathbf{O}_{2n} & \mathbf{G}_4 & \mathbf{G}_5 & \mathbf{O}_{2n} & -\mathbf{R}_6\mathbf{L}_6 \end{bmatrix} \tag{5.26}$$

Moreover, $\mathbf{O}_{2n}$ is the $2 \times n$ zero matrix. One has, additionally, further definitions, as follows:

$$\mathbf{f}_1 = \mathbf{E}(\mathbf{a}_{14} + \mathbf{a}_{47} + \mathbf{a}_{78}) \qquad \mathbf{f}_2 = -\mathbf{E}(\mathbf{a}_{58} + \mathbf{a}_{25}) \tag{5.27a}$$

$$\mathbf{B}_1 = \mathbf{R}_1\mathbf{L}_1 + \mathbf{E}(\mathbf{a}_{47} + \mathbf{a}_{78})\mathbf{x}_1^T \qquad \mathbf{B}_2 = -\mathbf{R}_2\mathbf{L}_2 - \mathbf{E}\mathbf{a}_{58}\mathbf{x}_2^T \tag{5.27b}$$

$$\mathbf{B}_3 = \mathbf{R}_4\mathbf{L}_4 + \mathbf{E}\mathbf{a}_{78}\mathbf{x}_4^T \qquad \mathbf{g}_1 = \mathbf{E}(\mathbf{a}_{14} + \mathbf{a}_{47} + \mathbf{a}_{79}) \tag{5.27c}$$

$$\mathbf{g}_2 = -\mathbf{E}(\mathbf{a}_{69} + \mathbf{a}_{36}) \qquad \mathbf{G}_3 = \mathbf{R}_1\mathbf{L}_1 + \mathbf{E}(\mathbf{a}_{47} + \mathbf{a}_{79})\mathbf{x}_1^T \tag{5.27d}$$

$$\mathbf{G}_4 = -\mathbf{R}_3\mathbf{L}_3 - \mathbf{E}\mathbf{a}_{69}\mathbf{x}_3^T \qquad \mathbf{G}_5 = \mathbf{R}_4\mathbf{L}_4 + \mathbf{E}\mathbf{a}_{79}\mathbf{x}_4^T \tag{5.27e}$$

while $\mathbf{N}_D$ in eq.(5.24) is a 4×4 matrix defined by

$$\mathbf{N}_D = \begin{bmatrix} \mathbf{E}(\mathbf{a}_{47} + \mathbf{a}_{78}) & -\mathbf{E}\mathbf{a}_{58} & \mathbf{0}_2 & \mathbf{E}\mathbf{a}_{78} \\ \mathbf{E}(\mathbf{a}_{47} + \mathbf{a}_{79}) & \mathbf{0}_2 & -\mathbf{E}\mathbf{a}_{69} & \mathbf{E}\mathbf{a}_{79} \end{bmatrix} \tag{5.28}$$

Therefore, from eq.(5.24), the dependent generalized speeds can be expressed in terms of the independent ones, as indicated below:

$$\dot{\theta}_4 = \frac{1}{\Delta^2\Delta_1}\left[(\Delta\Delta_1\mathbf{a}_{58} + \mu_1\mu_2\mathbf{a}_{58})^T\mathbf{h}_1 - \Delta\mu_1\mathbf{a}_{69}^T\mathbf{h}_2\right] \tag{5.29a}$$

$$\dot{\theta}_5 = \frac{1}{\Delta^2\Delta_1}\left\{[\Delta\Delta_1(\mathbf{a}_{47} + \mathbf{a}_{78}) + \mu_3\mu_2\mathbf{a}_{58}]^T\mathbf{h}_1 - \Delta\mu_3\mathbf{a}_{69}^T\mathbf{h}_2\right\} \tag{5.29b}$$

$$\dot{\theta}_6 = \frac{1}{\Delta\Delta_1}\left\{\mu_4\mathbf{a}_{58}^T\mathbf{h}_1 - [\Delta\mathbf{a}_{79} - \mu_1(\mathbf{a}_{47} + \mathbf{a}_{79})]^T\mathbf{h}_2\right\} \tag{5.29c}$$

$$\dot{\theta}_7 = \frac{1}{\Delta\Delta_1}\left(\mu_2\mathbf{a}_{58}^T\mathbf{h}_1 - \Delta\mathbf{a}_{69}^T\mathbf{h}_2\right) \tag{5.29d}$$

with

$$\Delta \equiv \mu_5 - \mu_1, \quad \Delta_1 \equiv \Delta\mu_1\mu_2 - \Delta^2\mu_6 \tag{5.30}$$

and

$$\mu_1 = \mathbf{a}_{58}^T\mathbf{E}\mathbf{a}_{78}, \quad \mu_2 = \mathbf{a}_{69}^T\mathbf{E}(\mathbf{a}_{47} + \mathbf{a}_{79}), \quad \mu_3 = (\mathbf{a}_{47} + \mathbf{a}_{78})^T\mathbf{E}\mathbf{a}_{78} \tag{5.31a}$$

$$\mu_4 = \mathbf{a}_{79}^T\mathbf{E}(\mathbf{a}_{47} + \mathbf{a}_{79}), \quad \mu_5 = \mathbf{a}_{47}^T\mathbf{E}\mathbf{a}_{58}, \quad \mu_6 = \mathbf{a}_{69}^T\mathbf{E}\mathbf{a}_{79} \tag{5.31b}$$

One has, additionally, the definitions given below:

$$\mathbf{h}_1 = \dot{q}_1\mathbf{f}_1 + \dot{q}_2\mathbf{f}_2 + \mathbf{B}_1\dot{\mathbf{u}}_1 + \mathbf{B}_2\dot{\mathbf{u}}_2 + \mathbf{B}_3\dot{\mathbf{u}}_4 - \mathbf{R}_5\mathbf{L}_5\dot{\mathbf{u}}_5 \tag{5.32a}$$

$$\mathbf{h}_2 = \dot{q}_1\mathbf{g}_1 + \dot{q}_3\mathbf{g}_2 + \mathbf{G}_3\dot{\mathbf{u}}_1 + \mathbf{G}_4\dot{\mathbf{u}}_3 + \mathbf{G}_5\dot{\mathbf{u}}_4 - \mathbf{R}_6\mathbf{L}_6\dot{\mathbf{u}}_6 \tag{5.32b}$$

Table 5.2: Physical parameters of the planar parallel manipulator

Link	Dimension (m)	Mass (Kg)	Stiffness $EI(\mathrm{Nm}^2)$
$1(O_1O_4)$, $2(O_2O_5)$ and $3(O_3O_6)$	0.8	0.1108	7.815
$4(O_4O_7)$, $5(O_5O_8)$ and $6(O_6O_9)$	1.2	0.1652	7.815
$7(O_7O_8O_9)$	0.8	0.384	Rigid

Having obtained the values of $\dot{\theta}_4$, $\dot{\theta}_5$, $\dot{\theta}_6$ and $\dot{\theta}_7$ from the above equations, one can derive the vector of generalized speeds $\mathbf{v}$ in terms of the independent generalized speeds. Thus, vector $\mathbf{v}$ can be expressed as a linear transformation of the independent generalized speeds, namely,

$$\mathbf{v} = \mathbf{N}\dot{\boldsymbol{\theta}}_I \tag{5.33}$$

where $\mathbf{N}$ is $(21+6n) \times (3+6n)$ NOC and $\mathbf{v}$ is a $(21+6n)$-dimensional vector, i.e.,

$$\mathbf{v} = \begin{bmatrix} \dot{\mathbf{r}}_1^T & \omega_1 & \dot{\mathbf{u}}_1^T & \dot{\mathbf{r}}_2^T & \omega_2 & \dot{\mathbf{u}}_2^T & \dots & \dot{\mathbf{r}}_7^T & \omega_7 \end{bmatrix}^T \tag{5.34}$$

5.3.2 Simulation Results

Now, using the formulation of kinematic constraints obtained in the previous subsection, the entire system can be modelled by assembling all links together via their kinematic constraints, using eq.(3.77).

The physical parameters of the light-weight example are given in Table 5.2. Modal coordinates are used for this example using the first two mode shapes of the flexible links as obtained from the finite element model. The damping coefficient for all the modes of the flexible links are taken equal to 0.01.

A prescribed manoeuvre is chosen for the actuated joints as follows:

$$q_j = q_j(0) + [q_j(t_f) - q_j(0)]\left[\frac{t}{t_f} - \frac{1}{2\pi}\sin\left(\frac{2\pi t}{t_f}\right)\right], \quad \text{for} \quad j = 1,2,3 \qquad (5.35)$$

where $t_f = 1$ s, and

$$q_1(0) = \pi/3 \qquad q_2(0) = 2\pi/3 \qquad q_3(0) = \pi/2$$
$$q_1(t_f) = 2\pi/3 \qquad q_2(t_f) = \pi/3 \qquad q_3(t_f) = 2\pi/3$$

Nominal joint torques are calculated using the inverse dynamics of the rigid-link model for the prescribed joint trajectories, which are plotted in Fig. 5.10. Then, simulating the direct dynamics, joint angles and their time-rates of change are calculated for the given joint torques using a model containing flexible links. There are some remarkable deviations in the case of joint angles due to the structural flexibility, as depicted in Fig. 5.11. It is seen in Fig. 5.12 that greater deviations from the rigid-link model are observed in the time-rates of change of the joint angles. Significant elastic displacements are also observed in the flexible links, as shown for link 1 in Fig. 5.13.

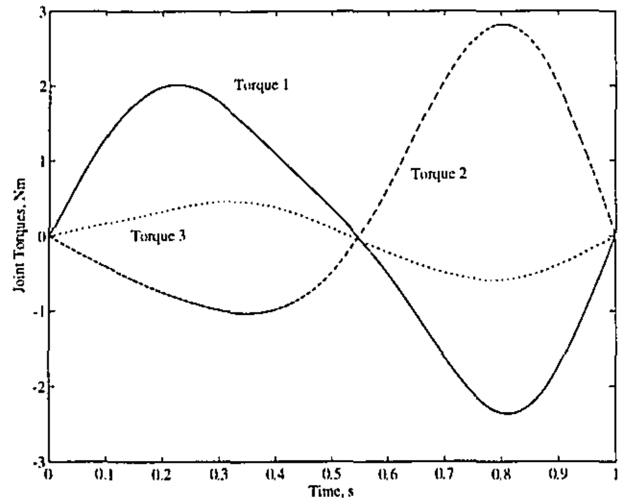

Figure 5.10: Actuated joint torques of the planar parallel manipulator

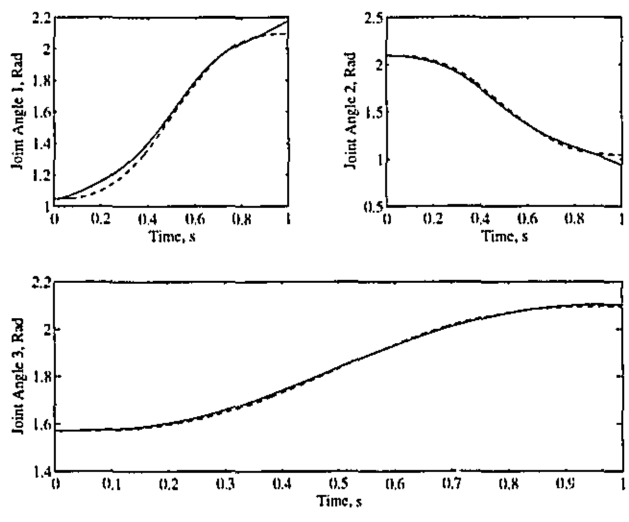

Figure 5.11: Joint angles of the planar parallel manipulator (flexible —, rigid - - -)

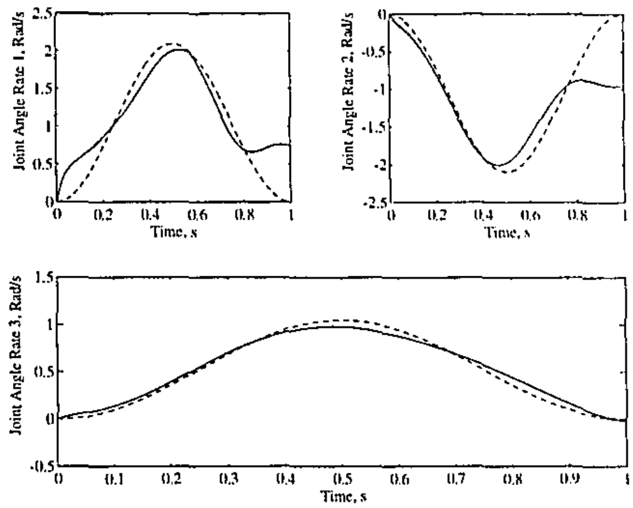

Figure 5.12: Time-rates of change of the joint angles for the planar parallel manipulator (flexible —, rigid - - -)

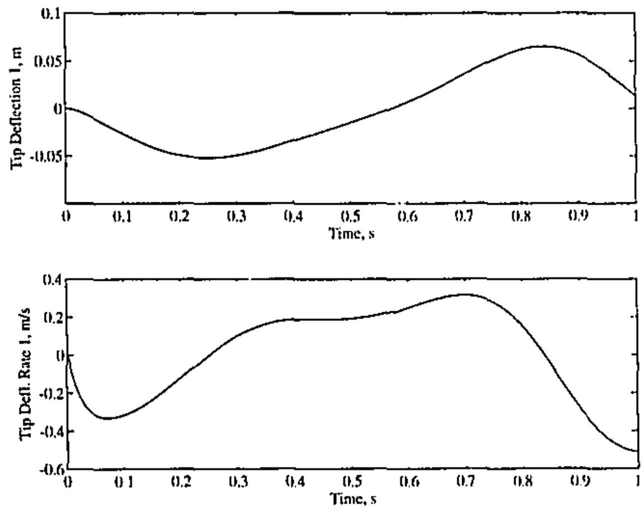

Figure 5.13: Tip deflection and its time-rate of change for link 1 of the planar parallel manipulator

Chapter 6

Kinematics and Dynamics of a Spatial Flexible-Link Parallel Manipulator

6.1 Introduction

Many research works in direct kinematics of parallel manipulators have been reported. Some works (Merlet, 1992; Raghavan, 1993) focus on the direct kinematics of parallel manipulators to find all possible moving platform poses (positions and orientations).

The study of the direct kinematics of parallel manipulators to find the twist of the moving platform, i.e, the velocity of centre of mass of the moving platform and its angular velocity is the subject of other investigations. Mohamed and Duffy (1985), and Sugimoto (1989) used screw theory for solving the direct kinematics of parallel manipulators, while Shi and Fenton (1992, 1994) presented a method for solving the direct kinematics of a general 6-DOF Stewart Platform, which is based on the velocities of three points attached to the moving platform.

Lee and Shah (1988) have also studied the kinematics of a 3-DOF parallel manipulator. Until now, most of the methods for solving the direct kinematics of parallel manipulators are based on rigid legs, while the direct kinematics of parallel manipulators with flexible legs has remained virtually untouched. In some applications, link flexibility cannot be neglected. For example, in space applications, two or more robotic manipulators that usually have long arms, separately mounted on the same base structure and participating in a coordinated activity, give rise to a mechanical system with the aforementioned features.

A method is introduced for solving the direct kinematics of a 3-DOF spatial parallel manipulator with flexible links in Section 6.2. The method is based on the position vectors and velocities of three noncollinear points on the moving platform, that is assumed rigid. Many techniques to obtain the twist of a rigid body, i.e., the velocity of one of its points and the angular velocity, from the given position and velocity vectors of the three noncollinear points, are available. Fenton and Willgoss (1990) reported a comparison of different methods. Here, the method reported in (Angeles, 1986), which is both robust and numerically well conditioned, is used.

As mentioned above, many research works on *kinematics* of parallel manipulators have been reported, but the study of the *dynamics* of parallel manipulators has been the subject of very few investigations (Reboulet and Berthomieu, 1991; Gosselin, 1993). Moreover, most of the works on the dynamics of parallel manipulators are based on rigid links. The modelling and simulation of the manipulator at hand are discussed in Section 6.3.

Shown in Fig. 6.1 is a parallel manipulator composed of three legs $O_iO_{i+3}O_{i+6}$, for $i = 1, 2, 3$, a rigid moving triangular platform $O_7O_8O_9$, henceforth abbreviated as MP, and a fixed platform $O_1O_2O_3$, assumed rigid as well. Each leg contains two flexible links that are coupled by a revolute joint. The legs are connected to

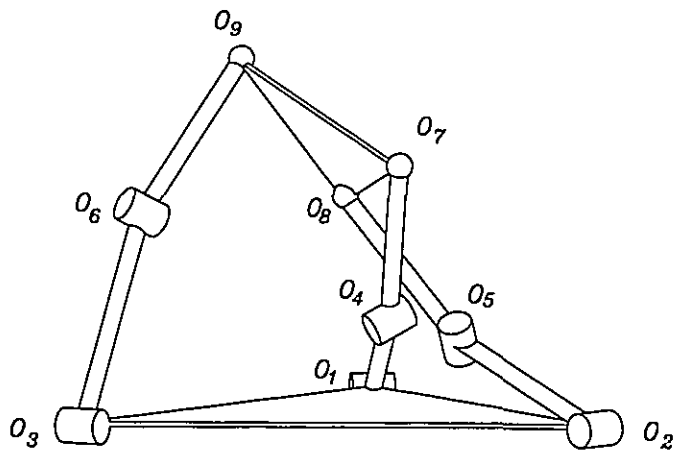

Figure 6.1: A 3-DOF spatial parallel manipulator

the MP by spherical joints and coupled to the base by revolute joints.

The DOF of the manipulator at hand can be obtained by using eq.(2.41) with the following values:

r = number of moving links = 13,

ν = number of joints = 15,

r_f = number of flexible links = 6,

n_i = number of nodal coordinates of link i associated with link flexibility = n

where the generalized coordinates associated with flexibility for all flexible links are assumed to have the same dimension, i.e., all flexible links have the same number n of nodal coordinates. Here, note that each spherical joint may be replaced by 3 revolute joints and 2 intermediate links with negligible length. Therefore, the DOF of the manipulator is

$$q = 3 + \sum_{i=1}^{6} n_i = 3 + 6n \tag{6.1}$$

This manipulator has three rigid DOF and three motors, located on the fixed platform, that drive the actuated joints.

6.2 Direct Kinematics Solution

6.2.1 Modelling of Flexible Legs

Figure 6.2 shows the manipulator of Fig. 6.1 with its leg links in their deformed configuration, leg i carrying the flexible links i and $i+3$. The flexible link i is now modelled as follows: The position vector of point O_{i+3} on link i, in frame $X_iY_iZ_i(\mathcal{F}_i)$, which is attached to link i, as shown in Fig. 6.3, expressed in the inertial frame $\mathcal{F}_0$, can be written as

$$\mathbf{a}_i = \mathbf{R}_i[\mathbf{a}_i]_i \tag{6.2}$$

where $\mathbf{R}_i$ is the rotation matrix of the frame $\mathcal{F}_i$ with respect to the inertial frame, while $[\mathbf{a}_i]_i$ is the position vector of point O_{i+3} in frame $\mathcal{F}_i$. Moreover, from Fig. 6.3,

$$[\mathbf{a}_i]_i = [\mathbf{a}_{0i}]_i + [\mathbf{a}_{ei}]_i \tag{6.3}$$

where $[\mathbf{a}_{0i}]_i$ is the position vector of point O_{i+3} in the undeformed configuration of link i, i.e., point $O_{0i,i+3}$ and $[\mathbf{a}_{ei}]_i$ is the elastic displacement of point O_{i+3} in the deformed configuration of link i, both in frame $\mathcal{F}_i$.

Using eq.(2.31), $\mathbf{a}_i$ can be expressed as

$$\mathbf{a}_i = \mathbf{R}_i[\mathbf{a}_i]_i = \mathbf{R}_i\{[\mathbf{a}_{0i}]_i + \mathbf{L}_i(O_{0i,i+3})\mathbf{u}_i(t)\} \tag{6.4}$$

where $\mathbf{L}_i(O_{0i,i+3})$ is the $3 \times n$ dimensional shape-function matrix evaluated at point $O_{0i,i+3}$ in the undeformed configuration of link i, as defined in eq.(2.31), and $\mathbf{u}_i(t)$ is the n-dimensional vector of generalized coordinates associated with link flexibility. The time derivative of $\mathbf{a}_i$ can be derived as

$$\dot{\mathbf{a}}_i = \dot{\mathbf{R}}_i[\mathbf{a}_i]_i + \mathbf{R}_i\mathbf{L}_i(O_{0i,i+3})\dot{\mathbf{u}}_i(t) \tag{6.5}$$

Here, $\dot{\mathbf{R}}_i[\mathbf{a}_i]_i$ can be written as

$$\dot{\mathbf{R}}_i[\mathbf{a}_i]_i = \boldsymbol{\omega}_i \times \mathbf{a}_i \tag{6.6}$$

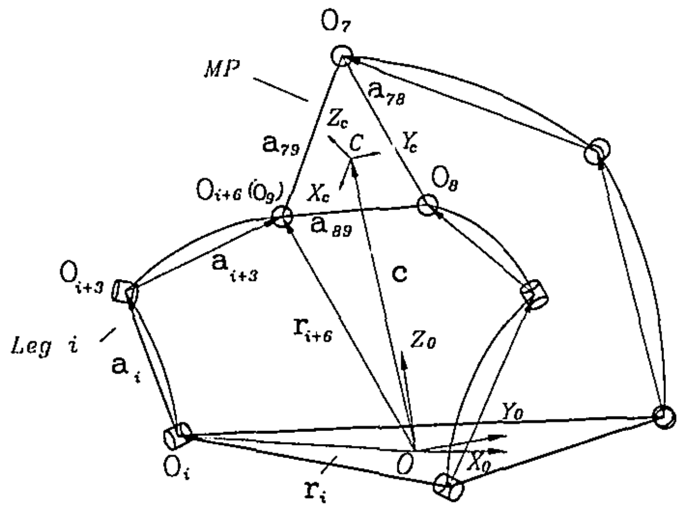

Figure 6.2: Geometric properties of leg i and MP of the spatial parallel manipulator

where $\boldsymbol{\omega}_i$ is the angular velocity of the frame $\mathcal{F}_i$ with respect to $\mathcal{F}_0$. Thus,

$$\dot{\mathbf{a}}_i = \boldsymbol{\omega}_i \times \mathbf{a}_i + \mathbf{R}_i \mathbf{L}_i(O_{0i,i+3})\dot{\mathbf{u}}_i(t) \tag{6.7}$$

6.2.2 Direct Position Kinematics

The direct position kinematics is defined as follows: Given the vector of independent generalized coordinates $\boldsymbol{\theta}_I$, which is composed of actuated joint angles and generalized coordinates associated with link flexibility, determine the pose of the MP in Cartesian space, i.e., the position and orientation of the MP. The vector of independent generalized coordinates $\boldsymbol{\theta}_I$ can be written as

$$\boldsymbol{\theta}_I = \begin{bmatrix} \theta_1 & \theta_2 & \theta_3 & \mathbf{u}_1^T(t) & \mathbf{u}_2^T(t) & \mathbf{u}_3^T(t) & \mathbf{u}_4^T(t) & \mathbf{u}_5^T(t) & \mathbf{u}_6^T(t) \end{bmatrix}^T \tag{6.8}$$

where θ_1, θ_2 and θ_3 are the actuated joint angles measured in radians, as shown in Fig. 6.4 and $\mathbf{u}_i(t)$ is as defined after eq.(6.4).

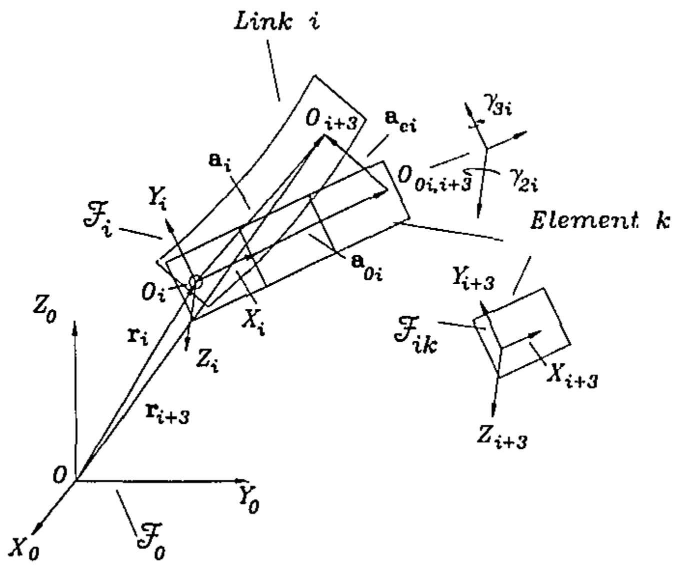

Figure 6.3: Modelling of spatial flexible links

The configuration of the MP is obtained from the position vectors of the three noncollinear points on the MP, i.e., O_7, O_8 and O_9. The position vector of point O_{i+6}, depicted in Fig. 6.2, can be written as

$$\mathbf{r}_{i+6} = \mathbf{r}_i + \mathbf{a}_i + \mathbf{a}_{i+3}, \quad \text{for} \quad i = 1, 2, 3 \tag{6.9}$$

where $\mathbf{r}_i$ is the position vector of the origin O_i. Upon substitution of $\mathbf{a}_i$ from eq.(6.4) into eq.(6.9), one obtains

$$\mathbf{r}_{i+6} = \mathbf{r}_i + \mathbf{R}_i[\mathbf{a}_i]_i + \mathbf{R}_{i+3}[\mathbf{a}_{i+3}]_{i+3} \quad \text{for} \quad i = 1, 2, 3 \tag{6.10}$$

with

$$\mathbf{R}_i = \mathbf{R}_{0i}\mathbf{Q}_i \tag{6.11a}$$

$$\mathbf{R}_{i+3} = \mathbf{R}_i\mathbf{A}_i\mathbf{F}_i\mathbf{Q}_{i+3} \tag{6.11b}$$

Here,

$$\mathbf{Q}_j = \begin{bmatrix} \cos\theta_j & -\sin\theta_j & 0 \\ \sin\theta_j & \cos\theta_j & 0 \\ 0 & 0 & 1 \end{bmatrix} \quad \text{for} \quad j = 1, \cdots, 6 \tag{6.12}$$

where θ_j is the angle of rotation of the j^{th} joint. $\mathbf{R}_{0i}$ is the rotation matrix of frame $X_{0i}Y_{0i}Z_{0i}$, attached to frame $\mathcal{F}_i(X_iY_iZ_i)$ at the home configuration $\theta_i = 0$, as shown in Fig. 6.4. This matrix is constant, while $\mathbf{A}_i$ takes on the form

$$\mathbf{A}_i = \begin{bmatrix} 1 & 0 & 0 \\ 0 & \cos\alpha_i & -\sin\alpha_i \\ 0 & \sin\alpha_i & \cos\alpha_i \end{bmatrix} \tag{6.13}$$

where α_i is the angle between joint axes Z_i and Z_{i+3}, depicted in Fig. 6.4. Moreover, $\mathbf{F}_i$ is the rotation matrix associated with the flexibility of link i, which, under the assumption of small displacements, can be written as

$$\mathbf{F}_i = \begin{bmatrix} 1 & -\gamma_{2i} & \gamma_{3i} \\ \gamma_{2i} & 1 & 0 \\ -\gamma_{3i} & 0 & 1 \end{bmatrix} \tag{6.14a}$$

with

$$\gamma_{ki} = \tan^{-1}\left(\frac{([\mathbf{a}_{ei}]_i)_k}{\|\mathbf{a}_{0i}\|}\right) \quad \text{for} \quad k = 2, 3 \tag{6.14b}$$

where γ_{2i} and γ_{3i} are the components of the rotation of the tip of the link i associated with the link flexibility, depicted in Fig. 6.3, and $[\mathbf{a}_{ei}]_i$ and $[\mathbf{a}_{0i}]_i$ are defined in eq.(6.4). Moreover, $(\cdot)_k$ is the k^{th} component of vector $(\cdot)$, and $\|\cdot\|$ is the Euclidean norm of the same.

Substituting $\mathbf{R}_i$ and $\mathbf{R}_{i+3}$ from eqs.(6.11) into eq.(6.10) and expanding the equation thus resulting, one obtains $\mathbf{r}_{i+6}$ in terms of the independent generalized coordinates and three dependent joint angles, θ_4, θ_5 and θ_6. These dependent joint angles can be expressed in terms of independent generalized coordinates by using three constraint equations, which can be obtained by writing the expression for the Euclidean norm of the three sides of the MP as

$$\|\mathbf{a}_{78}\|^2 = \mathbf{a}_{78}^T\mathbf{a}_{78} \tag{6.15a}$$

$$\|\mathbf{a}_{79}\|^2 = \mathbf{a}_{79}^T\mathbf{a}_{79} \tag{6.15b}$$

$$\|\mathbf{a}_{89}\|^2 = \mathbf{a}_{89}^T\mathbf{a}_{89} \tag{6.15c}$$

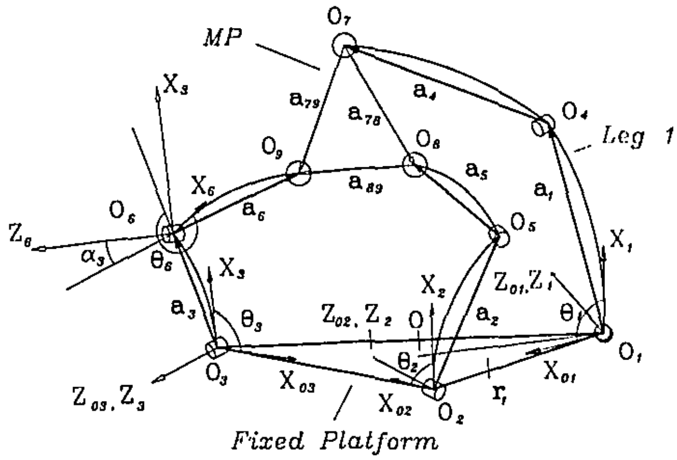

Figure 6.4: Geometric configuration of the spatial parallel manipulator

Here, $\mathbf{a}_{78}$, $\mathbf{a}_{79}$ and $\mathbf{a}_{89}$ are derived by writing three loop equations, as shown in Fig. 6.4, namely,

$$\mathbf{r}_1 + \mathbf{a}_1 + \mathbf{a}_4 + \mathbf{a}_{78} - \mathbf{a}_5 - \mathbf{a}_2 - \mathbf{r}_2 = \mathbf{0}_3 \tag{6.16a}$$

$$\mathbf{r}_1 + \mathbf{a}_1 + \mathbf{a}_4 + \mathbf{a}_{79} - \mathbf{a}_6 - \mathbf{a}_3 - \mathbf{r}_3 = \mathbf{0}_3 \tag{6.16b}$$

$$\mathbf{r}_2 + \mathbf{a}_2 + \mathbf{a}_5 + \mathbf{a}_{89} - \mathbf{a}_6 - \mathbf{a}_3 - \mathbf{r}_3 = \mathbf{0}_3 \tag{6.16c}$$

where $\mathbf{0}_3$ is the 3-dimensional zero vector. Moreover, vectors $\mathbf{a}_{78}$, $\mathbf{a}_{79}$ and $\mathbf{a}_{89}$ are obtained by substituting $\mathbf{a}_i$ from eq.(6.4) into the above equations and expanding them, with the aid of eqs.(6.11) for $\mathbf{R}_i$. Then, these vectors can be substituted into eqs.(6.15) to derive three nonlinear equations that should be solved numerically to obtain the three dependent joint angles in terms of known quantities. Therefore, one can express the position vectors of points O_7, O_8 and O_9 in terms of the independent generalized coordinates.

The position vector of point C, centre of mass of the MP, depicted in Fig. 6.2, can be readily written as

$$\mathbf{c} = \frac{1}{3}(\mathbf{r}_7 + \mathbf{r}_8 + \mathbf{r}_9) \tag{6.17}$$

Finally, to determine the orientation of the MP with respect to the inertial frame, one assigns frame $\mathcal{F}_C$ to point C of the MP, with unit vectors $\mathbf{e}_x$, $\mathbf{e}_y$ and $\mathbf{e}_z$ along X_C, Y_C and Z_C, respectively. Here, X_C is parallel to the side O_7O_9 of the MP and Z_C is perpendicular to the plane of points O_7, O_8 and O_9. The rotation matrix $\mathbf{R}_C$ of frame $\mathcal{F}_C$ with respect to inertial frame can then be written as

$$\mathbf{R}_C = \begin{bmatrix} \mathbf{e}_x & \mathbf{e}_y & \mathbf{e}_z \end{bmatrix} \tag{6.18}$$

with $\mathbf{e}_x$, $\mathbf{e}_y$ and $\mathbf{e}_z$ expressed in the inertial frame. These unit vectors are, in turn, calculated as

$$\mathbf{e}_x = \frac{\mathbf{r}_9 - \mathbf{r}_7}{\|\mathbf{r}_9 - \mathbf{r}_7\|} \tag{6.19a}$$

$$\mathbf{e}_z = \frac{\mathbf{e}_x \times \mathbf{e}_{78}}{\|\mathbf{e}_x \times \mathbf{e}_{78}\|} \tag{6.19b}$$

$$\mathbf{e}_y = \mathbf{e}_z \times \mathbf{e}_x \tag{6.19c}$$

where $\mathbf{e}_{78}$ is the unit vector along the side O_7O_8 of the MP.

6.2.3 Direct Velocity Kinematics

The direct velocity kinematics is defined as follows: Given the vector of independent generalized speeds $\dot{\boldsymbol{\theta}}_I$, with $\boldsymbol{\theta}_I$ defined as in eq.(6.8), and the geometric configuration of the manipulator, determine the twist of the MP, i.e., the velocity of the centre of mass of the MP and its angular velocity. This can be done by using the velocity of three noncollinear points on the MP, i.e., O_7, O_8 and O_9. The velocities of these three points can be obtained by differentiating both sides of eq.(6.9) with respect to time, thus obtaining

$$\dot{\mathbf{r}}_{i+6} = \dot{\mathbf{a}}_i + \dot{\mathbf{a}}_{i+3}, \quad \text{for} \quad i = 1, 2, 3 \tag{6.20}$$

where it is recalled that $\mathbf{r}_i$, for $i = 1, 2, 3$, in eq.(6.9) is constant. Substituting $\dot{\mathbf{a}}_i$ from eq.(6.7) into eq.(6.20) yields

$$\dot{\mathbf{r}}_{i+6} = \boldsymbol{\omega}_i \times \mathbf{a}_i + \mathbf{R}_i\mathbf{L}_i\dot{\mathbf{u}}_i(t) + \boldsymbol{\omega}_{i+3} \times \mathbf{a}_{i+3} + \mathbf{R}_{i+3}\mathbf{L}_{i+3}\dot{\mathbf{u}}_{i+3}(t) \tag{6.21}$$

where $\mathbf{L}_j \equiv \mathbf{L}_j(O_{0j,j+3})$ is as defined in eq.(6.4) and

$$\boldsymbol{\omega}_i = \dot{\theta}_i \mathbf{z}_i \tag{6.22a}$$

$$\boldsymbol{\omega}_{i+3} = \boldsymbol{\omega}_i + \dot{\theta}_{i+3}\mathbf{z}_{i+3} + \mathbf{w}_{i,i+3} \tag{6.22b}$$

where $i = 1, 2, 3$ and $\mathbf{z}_j$ is the unit vector parallel to joint axis Z_j, depicted in Fig. 6.4. Moreover, $\mathbf{w}_{i,i+3}$ is the angular velocity of $\mathcal{F}_{i+3}$ with respect to $\mathcal{F}_i$, resulting from the elastic displacement of link i, that can be written for small displacements as

$$\mathbf{w}_{i,i+3} = \frac{1}{\|\mathbf{a}_{0i}\|}\begin{bmatrix} 0 & -(\mathbf{L}_i\dot{\mathbf{u}}_i)_3 & (\mathbf{L}_i\dot{\mathbf{u}}_i)_2 \end{bmatrix} \tag{6.23}$$

with $[\mathbf{a}_{0i}]_i$ defined in eq.(6.4) and $(\cdot)_j$ is the j^{th} component of vector $(\cdot)$. Here, $\mathbf{u}_i$ and $\mathbf{L}_i$ are as defined in eq.(6.4) as well.

Upon substitution of eqs.(6.22) into eq.(6.21) and expansion of the equation thus obtained, one derives three equations for the velocity of the three non-collinear points, that are expressed in terms of the independent generalized speeds and the three dependent joint rates $\dot{\theta}_4$, $\dot{\theta}_5$ and $\dot{\theta}_6$. Three constraint equations are required to eliminate the dependent joint rates from these equations. They are obtained by differentiating both sides of eqs.(6.15) with respect to time, namely,

$$\mathbf{a}_{78}^T\dot{\mathbf{a}}_{78} = 0 \tag{6.24a}$$

$$\mathbf{a}_{79}^T\dot{\mathbf{a}}_{79} = 0 \tag{6.24b}$$

$$\mathbf{a}_{89}^T\dot{\mathbf{a}}_{89} = 0 \tag{6.24c}$$

where $\mathbf{a}_{78}$, $\mathbf{a}_{79}$ and $\mathbf{a}_{89}$ can be obtained from eqs.(6.16), while their time derivatives are derived from differentiation of the both sides of the eqs.(6.16) with respect to time. Upon expansion and simplification of eqs.(6.24), one derives three linear equations involving the dependent joint rates. By solving these three linear equations for $\dot{\theta}_4$, $\dot{\theta}_5$ and $\dot{\theta}_6$, and substituting the results into eq.(6.21), one obtains the velocity of three noncollinear points that are now expressed in terms of vector of the independent generalized speeds.

The method presented in (Angeles 1986, 1988) is used to obtain the twist of the MP from given velocities of three noncollinear points. The velocity of point C of the MP is calculated as

$$\dot{\mathbf{c}} = \frac{1}{3}(\dot{\mathbf{r}}_7 + \dot{\mathbf{r}}_8 + \dot{\mathbf{r}}_9) \tag{6.25}$$

Now, the 3×3 matrices $\mathbf{P}$ and $\dot{\mathbf{P}}$ are defined as

$$\mathbf{P} = \begin{bmatrix} \mathbf{r}_7 - \mathbf{c} & \mathbf{r}_8 - \mathbf{c} & \mathbf{r}_9 - \mathbf{c} \end{bmatrix} \tag{6.26a}$$

$$\dot{\mathbf{P}} = \begin{bmatrix} \dot{\mathbf{r}}_7 - \dot{\mathbf{c}} & \dot{\mathbf{r}}_8 - \dot{\mathbf{c}} & \dot{\mathbf{r}}_9 - \dot{\mathbf{c}} \end{bmatrix} \tag{6.26b}$$

where $\mathbf{c}$ and $\dot{\mathbf{c}}$ are defined, in turn, in eqs.(6.17) and (6.25). Moreover,

$$\dot{\mathbf{P}} = \mathbf{\Omega}_C \mathbf{P} \tag{6.27}$$

where $\mathbf{\Omega}_C$ is the cross-product matrix of the angular velocity of MP, $\boldsymbol{\omega}_C$. If one takes the vector of both sides of eq.(6.27), one obtains

$$\mathrm{vect}(\dot{\mathbf{P}}) = \mathrm{vect}(\mathbf{\Omega}_C \mathbf{P}) = \mathbf{T}\boldsymbol{\omega}_C \tag{6.28a}$$

with

$$\mathbf{T} \equiv (1/2)[\mathrm{tr}(\mathbf{P})\mathbf{1}_{33} - \mathbf{P}] \tag{6.28b}$$

with $\mathbf{1}_{33}$ defined as the 3×3 identity matrix (Angeles, 1988). Thus, the angular velocity $\boldsymbol{\omega}_C$ can be obtained as

$$\boldsymbol{\omega}_C = \mathbf{T}^{-1}\mathrm{vect}(\dot{\mathbf{P}}) \tag{6.29}$$

with $\mathbf{T}^{-1}$ derived, under the condition that neither $\mathrm{tr}(\mathbf{P})$ nor $\mathrm{tr}^2(\mathbf{P}) - \mathrm{tr}(\mathbf{P}^2)$ vanish, in the form (Angeles, 1988)

$$\mathbf{T}^{-1} = \frac{2}{\mathrm{tr}(\mathbf{P})}\mathbf{1}_{33} + \frac{4}{\mathrm{tr}(\mathbf{P})[\mathrm{tr}^2(\mathbf{P}) - \mathrm{tr}(\mathbf{P}^2)]}\mathbf{P}^2 \tag{6.30}$$

Table 6.1: Physical parameters of the spatial parallel manipulator

	Dimension (m)	α (deg)	Mass (Kg)	EI_{zz} (Nm^2)	EI_{yy} (Nm^2)
Leg 1 (O_1O_4) and (O_4O_7)	2.109	25	0.292	7.815	31.25
Leg 2 (O_2O_5) and (O_5O_8)	2.470	25	0.342	7.815	31.25
Leg 3 (O_3O_6) and (O_6O_9)	2.700	25	0.373	7.815	31.25
MP ($O_7O_8O_9$)	$2\times 2\times 3$	—	2.748	Rigid	Rigid

6.2.4 Numerical Example

As an example, consider the geometric parameters in Table 6.1 for the manipulator of Fig. 6.1. In this example, beam elements are used to discretize the flexible links and two elements for each flexible link are used, each element thus having eight nodal elastic displacements. Moreover, the generalized coordinates associated with the flexibility of all flexible links are assumed to be grouped in 12-dimensional vectors. At a certain instant, the vector of independent generalized coordinates $\boldsymbol{\theta}_I$ and the vector of independent generalized speeds $\dot{\boldsymbol{\theta}}_I$, are given as

$$\begin{aligned}\boldsymbol{\theta}_I &= [2.570 \quad 2.732 \quad 2.027 \quad \mathbf{u}_1^T \quad \mathbf{u}_2^T \quad \mathbf{u}_3^T \quad \mathbf{u}_4^T \quad \mathbf{u}_5^T \quad \mathbf{u}_6^T]^T \\ \dot{\boldsymbol{\theta}}_I &= [1.047 \quad 0.523 \quad -1.047 \quad \dot{\mathbf{u}}_1^T \quad \dot{\mathbf{u}}_2^T \quad \dot{\mathbf{u}}_3^T \quad \dot{\mathbf{u}}_4^T \quad \dot{\mathbf{u}}_5^T \quad \dot{\mathbf{u}}_6^T]^T\end{aligned} \tag{6.31}$$

with

$$\begin{aligned}\mathbf{u}_i = [&0.00 \quad 0.00 \quad 0.00 \quad 0.00 \quad 0.05 \quad 0.02 \\ &0.06 \quad 0.03 \quad 0.14 \quad 0.07 \quad 0.13 \quad 0.11]^T \\ \dot{\mathbf{u}}_i = [&0.00 \quad 0.00 \quad 0.00 \quad 0.00 \quad 0.65 \quad 0.11 \\ &0.50 \quad 0.13 \quad 1.40 \quad 0.35 \quad 1.25 \quad 0.45]^T\end{aligned}$$

Table 6.2: Configuration of the MP of the spatial parallel manipulator

	Rigid Legs	Flexible Legs
$\mathbf{c}$(m)	$[0.05, 2.35, -1.55]^T$	$[0.03, 2.11, -1.72]^T$
$\mathbf{R}_C$	-0.200, 0.588, -0.784 -0.266, -0.802, -0.533 -0.943, 0.102, 0.317	-0.248, 0.405, -0.880 -0.337, -0.889, -0.313 -0.908, 0.219, 0.356

Table 6.3: Twist of the MP of the spatial parallel manipulator

	Rigid Legs	Flexible Legs
$\dot{\mathbf{c}}$ (m/s)	$[-1.46, -3.05, -0.49]^T$	$[-1.20, -3.92, -1.02]^T$
ω_C (rad/s)	$[-0.76, 1.60, 1.92]^T$	$[-0.37, 1.33, 0.29]^T$

where the values given for $\mathbf{u}_i$ and $\dot{\mathbf{u}}_i$, for $i = 1, \ldots, 6$, are arbitrary. However, these values are obtained from the simulation for a practical application, as will be shown in Section 6.3. In order to highlight the effect of leg flexibility, the above-mentioned example is solved for two cases, one with rigid legs, and one with flexible legs. Upon substitution of the numerical values of $\boldsymbol{\theta}_I$ into the equations given in Subsection 6.2.2, the configuration of the MP is obtained for both cases, as shown in Table 6.2. The twist of the MP is also calculated by substituting the numerical values of $\dot{\mathbf{q}}$ and the geometric configuration of the manipulator, as shown in Table 6.2, into the equations given in Subsection 6.2.3. The velocity of point C of the MP and the angular velocity of the latter for both rigid and flexible cases are shown in Table 6.3. The results show that there is noticeable effect of the flexible legs on the motion of the moving platform, especially for the differential motion.

6.3 Modelling and Simulation

6.3.1 Modelling of the Manipulator

The dynamics model formulated in Chapters 2 and 3 is applied here for the manipulator of Fig. 6.1. The modelling of the dynamics of each flexible link is first carried out as explained in Section 3.2. Then, we rewrite eq.(2.35) as

$$\mathbf{v} = \mathbf{N}\dot{\boldsymbol{\theta}}_I \tag{6.32}$$

where $\mathbf{N}$ is the $m' \times q$ NOC and $\dot{\boldsymbol{\theta}}_I$, for the manipulator at hand, is the time derivative of $\boldsymbol{\theta}_I$ defined in eq.(6.8). Moreover, the $m'(= 42 + 6n)$-dimensional vector of generalized flexible twist $\mathbf{v}$ is defined as

$$\mathbf{v} = \begin{bmatrix} \boldsymbol{\omega}_1^T & \dot{\mathbf{r}}_1^T & \dot{\mathbf{u}}_1^T & \cdots & \boldsymbol{\omega}_6^T & \dot{\mathbf{r}}_6^T & \dot{\mathbf{u}}_6^T & \boldsymbol{\omega}_C^T & \dot{\mathbf{c}}^T \end{bmatrix}^T \tag{6.33}$$

where $\boldsymbol{\omega}_i$, for $i = 1, \ldots, 6$, is defined in eq.(6.22), while $\dot{\mathbf{c}}$ and $\boldsymbol{\omega}_C$ are obtained, respectively, from eqs.(6.25) and (6.29). Furthermore, $\mathbf{r}_i$, for $i = 1, \ldots, 6$, is the position vector of the point O_i, as shown in Fig. 6.3. The NOC $\mathbf{N}$ can be evaluated by using the kinematic constraint equations as well as the loop-constraint equations of the manipulator at hand. This requires the direct kinematic solution of the manipulator, which was derived in Section 6.2. The dependent generalized coordinates can be expressed in terms of the independent ones by considering the loop-constraint equations using the method explained in Subsection 6.2.2.

Upon substitution of $\boldsymbol{\omega}_i$ and $\dot{\mathbf{r}}_i$ from eqs.(6.22) and (2.34b) into eq.(6.33), and expansion of the equation thus obtained, vector $\mathbf{v}$ is obtained in terms of $\dot{\boldsymbol{\theta}}_I$ and three dependent joint rates, $\dot{\theta}_4$, $\dot{\theta}_5$ and $\dot{\theta}_6$. Therefore, upon elimination of the dependent joint rates with the method explained in Subsection 6.2.3, $\mathbf{v}$ can be expressed as a linear transformation of $\dot{\boldsymbol{\theta}}_I$, which leads to $\mathbf{N}$. Finally, using the NOC $\mathbf{N}$, the dynamics model of the manipulator is obtained from eq.(3.77). The model formulated herein has considered the effect of geometric elastic nonlinearities with the same method as suggested for planar beam-shaped links using Subsections 3.2.3 and 5.2.1.

6.3.2 Simulation Results

Some numerical results are obtained using the governing equations of motion of the manipulator at hand for both rigid and flexible-link models. The physical parameters of this example are given in Table 6.1. In this example, two beam elements for each flexible link are used to discretize the flexible links, the first four modes of each flexible link being used for defining the modal coordinates. The damping coefficients for all the modes of the flexible links are taken equal to 0.03. We choose a larger number of modes for each flexible link in the spatial case, as compared with the planar one, because the link has more elastic degrees of freedom in this case.

A prescribed manoeuvre was chosen for the actuated joints as follows:

$$\theta_j = \theta_j(0) + [c_i - \theta_j(0)]\left[t - \frac{t_f}{\pi}\sin(\pi t/t_f)\right]/1.35 \qquad (6.34)$$

where $j = 1,2,3$ and $\theta_1(0) = 1.872$, $\theta_2(0) = 2.340$, $\theta_3(0) = 2.987$, $c_1 = 2.570$, $c_2 = 2.776$ and $c_3 = 1.940$, all in radians and $t_f = 0.15$ s. Nominal joint torques were calculated using inverse dynamics of the rigid-link model for the prescribed joint trajectories, which are plotted in Fig. 6.5. Then, joint angles and their time-rates of change were calculated for the given joint torques using a model containing flexible links by performing the simulation of the model obtained in Subsection 6.3.1. The results show considerable differences between rigid links and flexible links. As an example, Figure 6.6 shows the deviation between rigid and flexible link, in the case of joint angle and its time-rate of change, for link 1. Significant elastic displacements are also observed in the flexible links, as shown for link 4 in Figs. 6.7 and 6.8. It may be pointed out that the tip deflections u_y and u_z are along the Y_i and Z_i axes of Fig. 6.3, respectively.

Although there are noticeable elastic displacements, there are no elastic oscillations in the simulation results due to the smoothness of the trajectory for the actuated joint torques that don't allow any initiation of vibrations.

It was noticed that in this manipulator, flexible links 3 and 6 of leg 3 have larger elastic displacements than those of the other two legs, because they have longer length as well as higher angular velocities, which affect directly the elastic displacements of the flexible links.

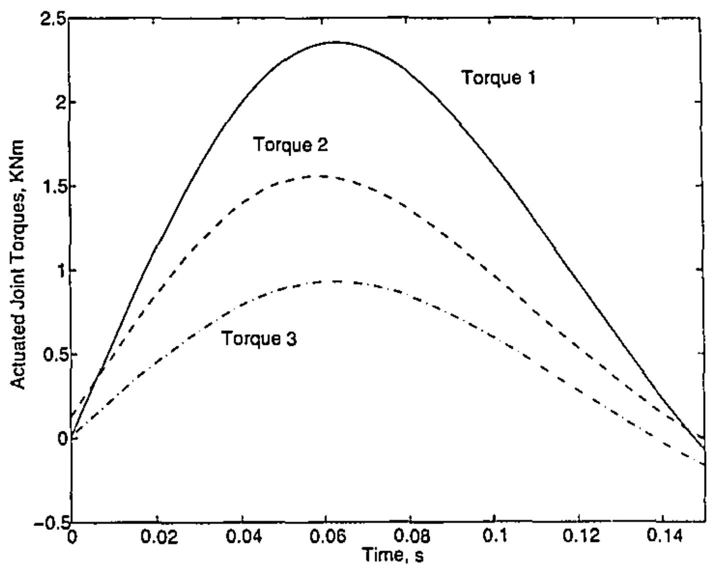

Figure 6.5: Actuated joint torques of the spatial parallel manipulator

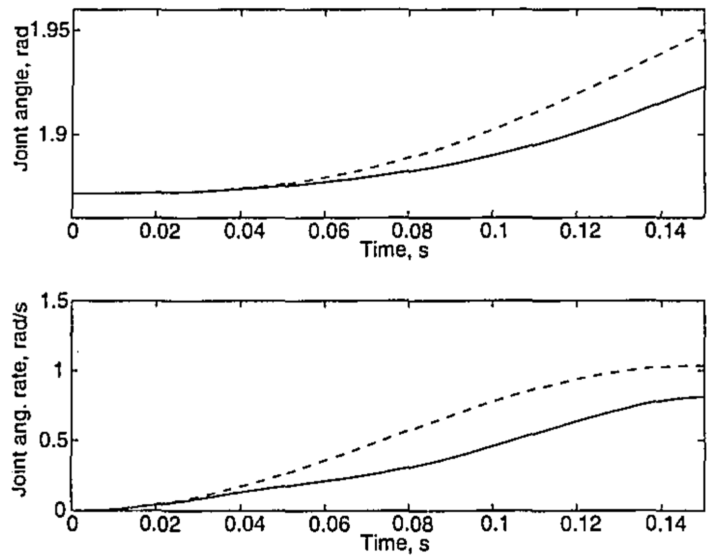

Figure 6.6: Joint angle and its time-rate of change for link 1 of the spatial parallel manipulator (flexible —, rigid - - -)

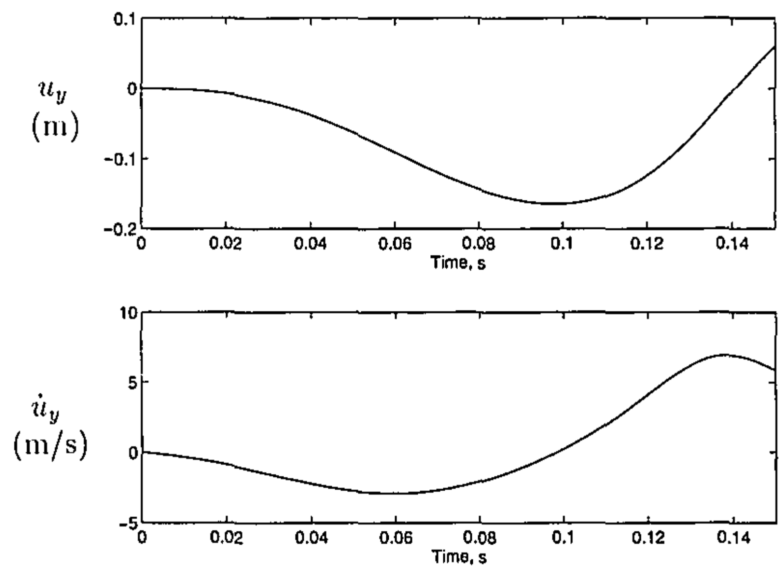

Figure 6.7: Tip deflection and its time-rate of change along the Y axis for link 4 of the spatial parallel manipulator

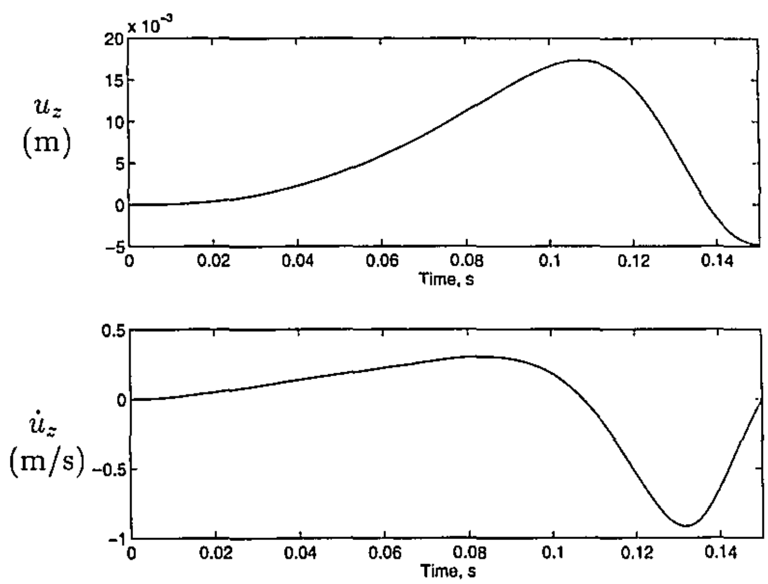

Figure 6.8: Tip deflection and its time-rate of change along the Z axis for link 4 of the spatial parallel manipulator

Chapter 7

Conclusions

In this chapter, conclusions are drawn based on the results of this thesis work. Some suggestions for future research are also put forward.

7.1 Summary of the Work in This Thesis

In this thesis, a general formulation for the modelling and simulation of multibody systems with multiple kinematic loops and flexible links was presented. This thesis links together the subject of the isolated field of flexible manipulators and that of the ones with kinematic loops in a very efficient way.

The kinematics and dynamics modelling were presented in Chapters 2 and 3. The prerequirement for the modelling of a multibody system is the knowledge of the underlying kinematics. To this end, two descriptions of the global position and velocity of a link are defined together: a description using the notion of flexible-pose of a link and a description introducing the flexible-twist. These two sets of variables are linked together via two maps. Thereafter, the finite-element approximation is used to reduce the continuous link to a discrete system with a finite number of elastic degrees of freedom. After defining the velocity of any point of the link in terms of the flexible-twist, the kinetic energy of the link can be written as a quadratic form in the flexible twist. The elastic strain energy is then obtained as a quadratic form in the flexible-pose. Here, the effect of geometric nonlinearities in the elastic displacements, also known as dynamic stiffening and geometric stiffening, which cannot be ignored in high-speed operations, was considered. Moreover, the Lagrange equations of motion for the link are written in terms of the vector of flexible pose and using the mapping relations between the flexible pose and the flexible twist, the dynamics model of the link can be expressed in terms of the flexible twist. The formulation of kinematic constraints allow us to assemble the equations of motion of the system. The natural orthogonal complement (NOC) of the twist-constraint matrix was used to derive the minimum number of equations of motion and to eliminate the nonworking kinematic constraint forces due to the kinematic coupling of the links. The formulation of the problem, which depends on whether the end-effector motion or the manoeuvres of the actuated joints and their time-rates of change are prescribed, was obtained in Cartesian space as well as in joint space.

Chapters 4–6 were devoted to developing a simulation scheme based on the modelling described in the preceding chapters for different types of robotic manipulators with kinematic loops, namely, two cooperating manipulators; planar, and spatial parallel manipulators. To highlight the link flexibility effect, the governing equations of motion were used in the simulation of the aforementioned systems to compare the results obtained with the rigid and the flexible-link models. Several researchers have developed dynamics models of multibody systems but they have often used some simple examples for simulation results. However, results for several realistic systems were presented in this thesis. The simulation results are needed to produce a realistic representation and understanding of the system in the absence of a physical prototype.

The dynamics simulation of two planar cooperating manipulators was presented in Chapter 4. To this end, the modelling of the planar systems was carried out from the beginning to simplify the formulations for the problem at hand. The formulation of the problem in both Cartesian and joint spaces were conducted in order to compare the results and the effort involved in the two formulations. It was observed that the formulation in joint space requires more computational work. Moreover, the results show that the simulation scheme is equally accurate for both formulations.

Structural damping was approximated by a suitable viscous damping coefficient for different modes. It is evident from the results that consideration of structural damping leads to a reduction of the oscillations at the end of the simulation. Structural damping also avoids the growth of oscillations due to numerical roundoff errors.

The overall results presented in Chapters 4–6 show that there are some significant differences in the end-effector motion and the behaviour of joint angles as well as their time-rates of change between robotic manipulators with flexible links and those with rigid links. Significant elastic displacements were also observed in the flexible links. These results indicate the importance of considering link flexibility in modelling the light-weight robotic manipulators with long arms as well as in high-speed operations. We believe that the dynamics of robotic manipulators with flexible links is a subject that is of significant importance in robotics.

7.2 Recommendation for Further Research

The following topics for further research are recommended in order to improve the formulation for the simulation of multibody systems with flexible links and kinematic loops:

- Consideration of nonholonomic as well as acatastatic systems;
- Incorporation of other types of kinematic pairs as well as joint flexibility;
- Investigation of the use of other numerical integration schemes as well as supercomputers to reduce the execution time of the simulation;
- Comparison of the results with experimental data obtained from an actual prototype;
- Singularity analysis of flexible-link manipulators with kinematic loops;
- Solution of the inverse dynamics for flexible-link model in order to increase the accuracy of the results.

References

Amirouche, F. M. L., and Huston, R. L., 1988, "Dynamics of Large Constrained Flexible Structures," *ASME Journal of Dynamic Systems, Measurement, and Control*, Vol. 110, pp. 78–83.

Amirouche, F. M. L., and Jia, T., 1988, "Pseudouptriangular Decomposition Method for Constrained Multibody Systems using Kane's Equations," *Journal of Guidance, Control, and Dynamics*, Vol. 11, No. 1, pp. 39–46.

Amirouche, F. M. L., and Xie, M., 1993, "An Explicit Formulation of the Dynamical Equations for Flexible Multibody Systems: A Recursive Approach," *Computers and Structures*, Vol. 46, No. 2, pp. 311–321.

Angeles, J., 1991, "Die theoretischen Grundlagen zur Behandlung algebraischer Singularitaäten der kinematischen Koordinatetenumkehr in der Robotertechnik," *Mechanism and Machine Theory*, Vol. 26, No. 3, pp. 315–322.

Angeles, J., 1988, *Rational Kinematics*, Springer-Verlag, New York.

Angeles, J., 1986, "Automatic Computation of the Screw Parameters of Rigid Body Motions-Infinitesimally Separated Positions," *ASME Journal of Dynamic Systems, Measurement, and Control*, Vol. 108, No. 1, pp. 39–43.

Angeles, J., and Lee, S, 1988, "The Formulation of Dynamical Equations of Holonomic Mechanical Systems Using Natural Orthogonal Complements," *ASME Journal of Applied Mechanics*, Vol. 55, pp. 243–244.

Badlani, M., and Kleinhenz, W., 1979, "Dynamic Stability of Elastic Mechanisms," *ASME Journal of Mechanical Design*, Vol. 101, No. 1, pp. 149–153.

Badlani, M., and Midha, A., 1982, "Member Initial Curvature Effects on the Elastic Slider-Crank Mechanism Response," *ASME Journal of Mechanical Design*, Vol. 104, No. 1, pp. 159–167.

Bahgat, B., and Willmert, K., 1976, "Finite Element Vibrational Analysis of Planar Mechanisms," *Mechanism and Machine Theory*, Vol. 11, pp. 47–71.

Banerjee, A. K., 1993, "Block-Diagonal Equations for Multibody Elastodynamics with Geometric Stiffness and Constraints," *Journal of Guidance, Control, and Dynamics*, Vol. 16, No. 6, pp. 1092–1100.

Banerjee, A. K., and Dickens, J. M., 1990, "Dynamics of an Arbitrary Flexible Body in Large Rotation and Translation," *Journal of Guidance, Control, and Dynamics*, Vol. 13, No. 2, pp. 221–227.

Banerjee, A. K., and Lemak, M. E., 1991, "Multi-Flexible Body Dynamics Capturing Motion-Induced Stiffness," *ASME Journal of Applied Mechanics* Vol. 58, pp. 766–775.

Book, W. J., 1984, "Recursive Lagrangian Dynamics of Flexible Manipulator Arms," *The International Journal of Robotics Research*, Vol. 3, No. 3, p. 87–101.

Bremer, H., and Pfeiffer, F., 1992, *Elastische Mehrkörpersysteme*, B. G. Teubner, Stuttgart.

Bricout, J. N., Debus, J. C., and Micheau, P., 1990, "A Finite Element Model for the Dynamics of Flexible Manipulators," *Mechanism and Machine Theory*, Vol. 25, No. 1, pp. 119–128.

Carr, R., Wihl, L., Malick, G., and Cyril, X., 1990, "MDSF-A Development and Simulation Facility for Space Robotic Manipulator Systems," *Presented at* *the Simulators for European Space Programmes*", Oct. 90, ESTEC, Noordwijk, Netherlands.

Chang, C. W., and Shabana, A. A., 1990, "Spatial Dynamics of Deformable Multibody Systems with Variable Kinematic Structure: Part 2–Velocity Transformation," *ASME Journal of Mechanical Design*, Vol. 112, pp. 160–167.

Chu, S. C., and Pan, K. C., 1975, "Dynamic Response of a High-Speed Slider-Crank Mechanism with an Elastic Connecting Rod," *ASME Journal of Engineering for Industry*, Vol. 97, No. 2, pp. 542-549.

Cleghorn, W. L., Fenton, R. G., and Tabarrok, B., 1981, "Finite Element Analysis of High-Speed Flexible Mechanisms," *Mechanism and Machine Theory*, Vol. 16, No. 4, pp. 407–424.

Cook, R. D., 1981, *Concepts and Applications of Finite Element Analysis*, John Wiley, New York.

Cyril, X., Angeles, J. and Misra, A. K., 1991, "Dynamics of Flexible Mechanical Systems," *Transactions of Canadian Society of Mechanical Engineering*, Vol. 15, pp. 235–249.

Darcovich, J., Angeles, J., and Misra, A. K., 1992, "Dynamics of Single-Loop Mechanisms with Flexible Links," *Machine Vibration*, Vol. 1, No. 3, pp. 155–163.

D'Eleuterio, G. M. T., 1992, "Dynamics of an Elastic Multibody Chain: Part C–Recursive Dynamics," *Dynamics and Stability of Systems*, Vol. 7, pp. 61–89.

De Luca, A., and Siciliano, B., 1991, "Closed-Form Dynamic Model of Planar Multilink Lightweight Robots," *IEEE Transactions on Systems, Man, and Cybernetics*, Vol. 21, No. 4, pp. 826–839.

Erdman, A. G., 1993, *Modern Kinematics: Developments in the Last Forty Years*, John Wiley, New York, pp. 369–449.

Erdman, A. G., and Sandor, G. N., 1972, "Kineto-Elastodynamic–A Review of the State of the Art and Trends," *Mechanism and Machine Theory*, Vol. 7, No. 1, pp. 19–33.

Erdman, A. G., Sandor, G. N., and Oakberg, R. G., 1972, "A General Method for Kineto- Elastodynamic Analysis and Synthesis of Mechanisms," *ASME Journal of Engineering for Industry*, Vol. 94, No. 4, pp. 1193–1205.

Everett, L. J., 1989, "An Extension of Kane's Method for Deriving Equations of Motion of Flexible Manipulators," *Proceeding of IEEE International Conference on Robotics and Automation*, Vol. 2, pp. 716–721.

Fattah, A., Misra K. A., and Angeles, J., 1995, "Modeling and Simulation of Planar Mechanical Systems with Flexible Links and Kinematic Loops," *To appear in Machine Vibration.*

Fattah, A., Angeles, J., and Misra K. A., 1995-a, "Dynamics of a 3-DOF Spatial Parallel Manipulator with Flexible Legs," *Accepted for presentation at IEEE International Conference on Robotics and Automation*, Nagoya, Japan, May 21–27.

Fattah, A., Angeles, J. and Misra K. A., 1995-b, "Dynamics of Two Cooperating Flexible-link Manipulators," *Accepted for presentation at 15th Canadian Congress of Applied Mechanics CANCAM 95*, Victoria, Canada, May 28–June 2.

Fattah, A., Angeles, J., and Misra K. A., 1994-a, "Direct Kinematics of a 3-DOF Spatial Parallel Manipulator with Flexible Legs," *Proceedings of the 1994 ASME Design Technical Conferences-23rd Biennial Mechanisms Conference*, DE-Vol. 72, pp. 285–291, 1994.

Fattah, A., Misra, K. A., and Angeles, J., 1994, "Dynamics of a Flexible-Link Planar Parallel Manipulator in Cartesian Space," *Proceedings of the 1994 ASME Design Technical Conferences-20th Design Automation Conference*, DE-Vol. 69-2, pp. 483–490, 1994.

Fattah, A., Angeles, J., and Misra K. A., 1994-b, "Direct Kinematics of a Spatial Parallel Manipulator with Flexible Legs," *Presented at the Robotics Mechanical Systems Graduate Students, Forum RMSGS, at the 12th Symposium on Engineering Applications of Mechanics*, Montreal, June 1994.

Fenton, R. G., and Willgoss, R. A., 1990, "Comparison of Methods for Determining Screw Parameters of Infinitesimal Rigid Body Motion From Position and Velocity Data," *ASME Journal of Dynamic Systems, Measurement, and Control*, Vol. 112, pp. 711–716.

Gaultier, P. E., and Cleghorn, W. L., 1989, "Modeling of Flexible Manipulator Dynamics: A Literature Survey," *First National Applied Mechanisms and Robotics Conference*, 89AMR-2C-3, pp. 1–10.

Gear, C. W., 1971, *Numerical Initial Value Problems in Ordinary Differential Equations*, Prentic-Hall, New Jersey.

Gosselin, C., 1993, "Parallel Computational Algorithms for the Kinematics and Dynamics of Parallel Manipulators," *Proceedings of the IEEE International Conference on Robotics and Automation*, Vol. 1, pp. 883–888.

Hanagud, S., and Sarkar, S., 1989, "Problem of the Dynamics of a Cantilever Beam Attached to a Moving Base," *Journal of Guidance, Control, and Dynamics*, Vol. 12, No. 2, pp. 438–441.

Harary, F. 1969, *Graph Theory* Addison-Wesley, Toronto.

Ho, J. Y. L., 1977, "Direct Path Method for Flexible Multibody Spacecraft Dynamics," *Journal of Spacecraft and Rockets*, Vol. 14, pp. 102–110.

Hollerbach, J. M., 1980, "A Recursive Lagrangian Formulation of Manipulator Dynamics and a Comparative Study of Formulation Complexity," *IEEE Journal of Systems, Man and Cybernetics*, Vol. 10, No. 11, pp. 730–736.

Hu., F. L., and Ulsoy, A. G., 1994, "Dynamics Modeling of Constrained Flexible Robot Arms for Controller Design," *ASME Journal of Dynamic Systems, Measurement, and Control*, Vol. 116, pp. 56–65.

Hughes, P. C., 1979, "Dynamics of a Chain of Flexible Bodies," *Journal of the Astronautical Sciences*, Vol. 27, No. 4, pp. 359–380.

Hughes, P. C., 1985, "Multibody Dynamics for Space Station Manipulators: Dynamics of a Chain of Elastic Bodies," *Dynacon Report*, SS-2.

Hughes, P. C., and Sincarsin, G. B., 1989, "Dynamics of an Elastic Multibody Chain: Part B–Global Dynamics," *Dynamics and Stability of Systems*, Vol. 4, Nos. 3&4, pp. 227–244.

Hurty, W. C., 1965, "Dynamic Analysis of Structural Systems Using Component Modes," *AIAA Journal*, Vol. 3, No. 4, pp. 678–685.

Ider, S. K., and Amirouche, F. M. L., 1989-a, "The Influence of Geometric Nonlinearities in the Dynamics of Flexible Tree-Like Structures," *Journal of Guidance, Control, and Dynamics*, Vol. 12, No. 6, pp. 830–837.

Ider, S. K., and Amirouche, F. M. L., 1989-b, "Nonlinear Modelling of Flexible Multibody Systems Dynamics Subjected to Variable Constraints," *ASME Journal of Applied Mechanics* Vol. 56, pp. 444–450.

Ider, S. K., and Amirouche, F. M. L., 1988, "Coordinate Reduction in the Dynamics of Constrained Multibody Systems–A New Approach," *ASME Journal of Applied Mechanics*, Vol. 55, pp. 899-904.

Imam, I., and Sandor, N. G., 1973, "A General Method of Kineto-Elastodynamic Design of High-Speed Mechanisms," *Mechanism and Machine Theory*, Vol. 8, pp. 497–516.

Imam, I., Sandor, N. G., and Kramer, N. S., 1973, "Deflection and Stress Analysis in High-Speed Planar Mechanisms with Elastic Links," *ASME Journal of Engineering for Industry*, Vol. 95, No. 2, pp. 541–548.

Jasinski, P. W., Lee, H. C., and Sandor, G. N., 1971, "Vibrations of Elastic Connecting Rod of a High-Speed Slider-Crank Mechanism," *ASME Journal of Engineering for Industry*, Vol. 93, No. 2, pp. 636–644.

Jerkovsky, W., 1978, "The Structure of Multibody Dynamics Equations," *Journal of Guidance and Control*, Vol. 1, No. 3, pp. 173-182.

Kamman, J., W., and Huston, R. L., 1984, "Constrained Multibody System Dynamics–An Automated Approach," *Computers and Structures*, Vol. 18, No. 6, pp. 999-1003.

Kane, T. R., Ryan, R. R., and Banerjee, A. K., 1987, "Dynamics of a Cantilever Beam Attached to a Moving Base," *Journal of Guidance, Control, and Dynamics*, Vol. 10, No. 2, pp. 139–151.

Kane, T. R., and Levinson, D. A., 1985, *Dynamics: Theory and Applications*, McGraw-Hill, New York.

Kane, T. R., and Levinson, D. A., 1983, "Use of Kane's Dynamical Equations in Robotics," *The International Journal of Robotics Research*, Vol. 2, No. 3, pp. 3–20.

Kelly, F. A., and Huston, R. L., 1981, "Modeling of Flexibility Effects in Robot Arms," *Proceedings of Joint Automatic Control Conference: American Automatic Control Council*, Paper WP-2C.

Kim. S. S., and Vanderploeg, M. J., 1986, "A General and Efficient Method for Dynamic Analysis of Mechanical Systems Using Velocity Transformations," *ASME Journal of Mechanisms, Transmissions, and Automation in Design*, Vol. 108, No. 2, pp. 176-182.

Lebert, G., Liu, K., and Lewis, F. L., 1993, "Dynamic Analysis and Control of a Stewart Platform Manipulator," *Journal of Robotic Systems*, Vol. 10, No. 5, pp. 629–635.

Lee, K. M., and Shah, K., 1988, "Kinematic Analysis of a Three-Degrees-of-Freedom In-Parallel Actuated Manipulator," *IEEE Journal of Robotics and Automation*, Vol. 4, No. 3, pp. 354–360.

Lieh, J., 1991, "An Alternative Method to Formulate Closed-Form Dynamics for Elastic Manipulators Using Symbolic Process," *Proceedings of IEEE International Conference on Robotics and Automation*, Vol. 3, pp. 2369–2374.

Lilly K. W., and Orin, D. E., 1994, "Efficient Dynamic Simulation of Multiple Chain Robotic Mechanisms," *ASME Journal of Dynamic Systems, Measurement, and Control*, Vol. 116, pp. 223–231.

Likins, P. W., 1974, "Geometric Stiffness Characteristics of a Rotating Elastic Appendage," *International Journal of Solids and Structures*, Vol. 10, No. 2, pp. 161–167.

Likins, P. W., Barbera, F. J., and Baddeley, V., 1973, "Mathematical Modeling of Spinning Elastic Bodies for Modal Analysis," *AIAA Journal*, Vol. 11, pp. 1251–1258.

Lowen, G. G., and Chassapis, C., 1986, "The Elastic Behavior of Linkages: An Update," *Mechanism and Machine Theory*, Vol. 21, No. 1, pp. 33–42.

Lowen, G. G., and Jandrasits, W. G., 1972, "Survey of Investigations into the Dynamic Behavior of Mechanisms Containing Links with Distributed Mass and Elasticity," *Mechanism and Machine Theory*, Vol. 7, No. 1, pp. 3–17.

Ma, O., 1991, *Mechanical Analysis of Parallel Manipulators with Simulation, Design and Control Applications*, Ph.D Thesis, Department of Mechanical Engineering, McGill University.

Ma, O., and Angeles, J., 1989, "Direct Kinematics and Dynamics of a Planar Parallel Manipulator," *Proceedings of The ASME Design Automation Conference*, DE-Vol. 3, pp. 313–320.

Mani, N. K., 1984, *Use of Singular Value Decomposition for Analysis and Optimization of Mechanical Systems Dynamics*, Ph.D. Thesis, The University of Iowa.

McMillan, S., Sadayappan, P., and Orin, D. E., 1992, "Efficient Dynamic Simulation of Multiple Manipulator systems with Singularities," *Proceedings of IEEE International Conference on Robotics and Automation*, Vol. 1, pp. 299–304.

Meirovitch, L., 1991, "Hybrid State Equations of Motion for Flexible Bodies in Terms of Quasi-Coordinates," *Journal of Guidance, Control, and Dynamics*, Vol. 14, No. 5, pp. 1008–1013.

Merlet, J. P., 1992, "Direct Kinematics and Assembly Model of Parallel Manipulators," *International Journal of Robotics Research*, Vol. 11, pp. 150–162.

Midha, A., Erdman, A., and Frohrib, D., 1979, "A Closed-Form Numerical Algorithm for the Periodic Response of High-Speed Elastic Linkages," *ASME Journal of Mechanical Design*, Vol. 101, No. 1, pp. 154–162.

Modi, V. J., and Ibrahim, A. M., 1988, "On the Dynamics of Flexible Orbiting Structures," *Large Space Structures: Dynamics and Control, edited by S. N. Atluri and A. K. Amos*, Springer Verlag, New York, pp. 93–114.

Mohamed, M. G., and Duffy, J., 1985, "A Direct Determination of the Instantaneous Kinematics of Fully Parallel Robot Manipulators," *ASME Journal of Mechanisms, Transmissions, and Automation in Design*, Vol. 107, pp. 226–229.

Naganathan, G., and Soni, A. H., 1988, "Nonlinear Modelling of Kinematic and Flexibility Effects in Manipulator Design," *ASME Journal of Mechanisms, Transmissions, and Automation in Design*, Vol. 110, pp. 243–254.

Nagarajan, S., and Turcic, D. A., 1990-a, "Lagrangian Formulation of the Equations of Motion for Elastic Mechanisms With Mutual Dependence Between Rigid Body and Elastic Motions. Part I: Element Level Equations," *ASME Journal of Dynamic Systems, Measurement, and Control*, Vol. 112, No. 2, pp. 203–214.

Nagarajan, S., and Turcic, D. A., 1990-b, "Lagrangian Formulation of the Equations of Motion for Elastic Mechanisms With Mutual Dependence Between Rigid Body and Elastic Motions. Part II: Systems Equations," *ASME Journal of Dynamic Systems, Measurement, and Control*, Vol. 112, No. 2, pp. 215–224.

Nikravesh, P. E., and Gim, G., 1993, "Systematic Construction of the Equations of Motion for Multibody Systems Containing Closed Kinematic Loops," *ASME Journal of Mechanical Design*, Vol. 115, pp. 143–149.

Nikravesh, P. E., Wehage, R. A., and Kwon, O. K., 1985-a, "Euler Parameters in Computational Kinematics and Dynamics: Part 1," *ASME Journal of Mechanisms, Transmissions and Automation in Design*, Vol. 107, pp. 358–365.

Nikravesh, P. E., Wehage, R. A., and Kwon, O. K., 1985-b, "Euler Parameters in Computational Kinematics and Dynamics: Part 2," *ASME Journal of Mechanisms, Transmissions and Automation in Design*, Vol. 107, pp. 366–369.

Novozhilov, V. V., 1961, *Theory of Elasticity*, Pergamon Press, New York.

Przemieniecki, J. S., 1967, *Theory of Matrix Structural Analysis*, McGraw Hill, New York.

Raghavan, M., 1993, "The Stewart Platform of General Geometry Has 40 Configurations," *ASME Journal of Mechanical Design*, Vol. 115, No. 1, pp. 277–282.

Reboulet C. and Berthomieu T., 1991, "Dynamic Models of a Six-degree-of-freedom Parallel Manipulator," *Proceedings of the Fifth International Conference on Advanced Robotics*, Vol. 2, pp. 1153–1157.

Sadigh, M. J., Misra, A. K., 1993, "More on the So-Called Dynamic Stiffening Effect," *Proceedings of the AAS/AIAA Astrodynamics Specialist Conference*, Paper No. AAS 93-677.

Saha, S. K., 1993, *Dynamics and Design of Nonholonomic Robotic Mechanical Systems*, , Ph.D Thesis, Department of Mechanical Engineering, McGill University.

Saha, S. K., and Angeles, J., 1991, "Dynamics of Nonholonomic Mechanical Systems Using a Natural Orthogonal Complement," *ASME Journal of Applied Mechanics*, Vol. 58, PP. 238–243.

Serna, M. A., and Bayo, E., 1989, "A Simple and Efficient Computational Approach for the Forward Dynamics of Elastic Robots," *Journal of Robotic Systems*, Vol. 6, No. 4, pp. 362–382.

Shabana, A. A., 1991, "Constrained Motion of Deformable Bodies," *International Journal for Numerical Methods in Engineering*, Vol. 32, pp. 1813–1831.

Shabana, A. A., and Wehage, R., 1984, "Spatial Transient Analysis of Inertia-Variant Flexible Mechanical Systems," *ASME Journal of Mechanisms, Transmissions and Automation in Design*, Vol. 106, pp. 172–178.

Shabana, A. A., and Wehage, R., 1983, "Variable Degree-of-Freedom Component Mode Analysis of Inertia Variant Flexible Mechanical Systems," *ASME Journal of Mechanisms, Transmissions and Automation in Design*, Vol. 105, pp. 371–378.

Sharf, I., and D'Eleuterio, G. M. T., 1992, "Parallel Simulation Dynamics for Elastic Multibody Chains," *IEEE Transactions on Robotics and Automation*, Vol. 8, No. 5, pp. 597–606.

Sharf, I., and D'Eleuterio, G. M. T., 1988, "Computer Simulation of Elastic Chains Using a Recursive Formulation," *Proceedings of IEEE International Conference on Robotics and Automation*, Vol. 3, pp. 1539-1545.

Shi, X., and Fenton, R. G., 1994, "A Complete and General Solution to the Forward Kinematics Problem of the Platform-Type Robotic Manipulators," *Proceedings of the IEEE International Conference on Robotics and Automation*, Vol. 4, pp. 3055–3062.

Shi, X., and Fenton, R. G., 1992, "Solution to the Forward Instantaneous Kinematics for a General 6-DOF Stewart Platform," *Mechanism and Machine Theory*, Vol. 27, No. 3, pp. 251–259.

Sincarsin, G. B., and Hughes, P. C., 1989, "Dynamics of an Elastic Multibody Chain: Part A–Body Motion Equations," *Dynamics and Stability of Systems*, Vol. 4, Nos. 3&4, pp. 209–226.

Singh, R. P., Van der Voort, R. J., and Likins, P. W., 1985, "Dynamics of Flexible Bodies in Tree Topology–A Computer Oriented Approach," *Journal of Guidance, Control, and Dynamics*, Vol. 8, No. 5, pp. 584–590.

Singh, R. P., and Likins, P. W., 1985, "Singular Value Decomposition for Constrained Dynamical Systems," *ASME Journal of Applied Mechanics*, Vol. 52, pp. 943–948.

Song, J. O., and Haug, E. J., 1980, "Dynamic Analysis of Planar Flexible Mechanisms," *Computer Methods in Applied Mechanics and Engineering*, Vol. 24, pp. 359–381.

Sugimoto, K., 1989, "Computational Scheme for Dynamic Analysis of Parallel Manipulators," *ASME Journal of Mechanisms, Transmissions, and Automation in Design*, Vol. 111, pp. 29–33.

Sun, Q., Nahon, M., and Sharf, I., 1994, "Force Optimization in Multi-Armed Manipulators with Flexible links," in Jamshidi, M., Yuh, J., Nguyen, C. C. and Lumia, R. (editors) *Intelligent Automation and Soft Computing*, TSI press, Vol. 2, pp. 183–187.

Sunada, W., and Dubowsky, S., 1983, "On the Dynamic Analysis and Behavior of Industrial Robotic Manipulators with Elastic Members," *ASME Journal of Mechanisms, Transmissions, and Automation in Design*, Vol. 105, pp. 42–51.

Sunada, W., and Dubowsky, S., 1981, "The Applications of Finite Element Methods to the Dynamic Analysis of Flexible Spatial and Co-Planar Linkage Systems," *ASME Journal of Mechanical Design*, Vol. 103, pp. 643–651.

Tadjbakhsh, I. G., 1982, "Stability of Motion of Elastic Planar Linkages with Application to Slider Crank Mechanism," *ASME Journal of Mechanical Design*, Vol. 104, No. 4, pp. 698–703.

Tadjbakhsh, I. G., and Younis, C. J., 1986, "Dynamic Stability of the Flexible Connecting Rod of a Slider Crank Mechanism," *ASME Journal of Mechanisms, Transmissions, and Automation in Design*, Vol. 108, No. 4, pp. 487–496.

Turcic, D. A., and Midha, A., 1984-a, "Generalized Equations of Motion for the Dynamic Analysis of Elastic Mechanism Systems," *ASME Journal of Dynamic Systems, Measurement, and Control*, Vol. 106, pp. 243–248.

Turcic, D. A., and Midha, A., 1984-b, "Dynamics Analysis of Elastic Mechanism Systems–Part I: Applications," *ASME Journal of Dynamic Systems, Measurement, and Control*, Vol. 106, pp. 249–254.

Usoro, P. B., Nadira, R., and Mahil, S. S., 1986, "A Finite Element/Lagrange Approach to Modelling Lightweight Flexible Manipulators," *ASME Journal of Dynamic Systems, Measurement, and Control*, Vol. 108, pp. 198–205.

Yoo, W. S., and Haug, E. J., 1986, "Dynamics of Flexible Mechanical Systems Using Vibration and Static Correction Modes," *ASME Journal of Mechanisms, Transmissions, and Automation in Design*, Vol. 108, pp. 315–322.

Winfrey, R. C., 1972, "Dynamic Analysis of Elastic Link Mechanisms by Reduction of Coordinates," *ASME Journal of Engineering for Industry*, Vol. 94, No. 2, pp. 577–582.

Zheng Y. F., and Luh J. Y. S., 1989 "Optimal Load Distribution for two Industrial Robots Handling a Simple Object," *ASME Journal of Dynamic Systems, Measurement, and Control*, Vol. 111, No. 2, pp. 232–237.

Zienkiewicz, O. C., 1979, *The Finite Element Method in Engineering Science*, McGraw-Hill Book Co., New York.

Appendix A

Euler Parameters

The Euler parameters of the orientation of a frame $\mathcal{F}_i$, as defined in eq.(2.1), with respect to an inertial frame $\mathcal{F}_0$, are defined as

$$\hat{\mathbf{q}}_i = \begin{bmatrix} \mathbf{r}_i \\ r_i^0 \end{bmatrix} \tag{A.1a}$$

where

$$\mathbf{r}_i = \mathbf{e}_i \sin(\phi_i/2), \quad r_i^0 = \cos(\phi_i/2) \tag{A.1b}$$

Here, $\mathbf{e}_i$ is the unit vector along the axis of rotation, and ϕ_i is the angle of rotation about that axis. The algebraic constraint among the Euler parameters is expressed as

$$\hat{\mathbf{q}}_i^T \hat{\mathbf{q}}_i = 1 \tag{A.2}$$

The rotation matrix $\mathbf{R}_i$ of frame $\mathcal{F}_i$ with respect to the inertial frame $\mathcal{F}_0$ can be related to the Euler parameters (Angeles, 1988) as

$$\mathbf{R}_i = \left[(2r_i^0)^2 - 1\right] \mathbf{1}_{33} + 2\mathbf{r}_i\mathbf{r}_i^T + 2r_i^0\tilde{\mathbf{R}}_i = \mathbf{G}_i\mathbf{L}_i^T \tag{A.3a}$$

where $\tilde{\mathbf{R}}_i$ is the cross product matrix of $\mathbf{r}_i$, namely,

$$\tilde{\mathbf{R}}_i \equiv \frac{\partial(\mathbf{r}_i \times \mathbf{v})}{\partial \mathbf{v}} \quad \forall \ \mathbf{v} \tag{A.3b}$$

Moreover, $\mathbf{G}_i$ and $\mathbf{L}_i$ are 3×4 matrices that have the forms (Nikravesh et. al., 1985-a; 1985-b):

$$\mathbf{G}_i = \begin{bmatrix} \tilde{\mathbf{R}}_i + r_i^0 \mathbf{1}_{33} & -\mathbf{r}_i \end{bmatrix} \tag{A.4a}$$

$$\mathbf{L}_i = \begin{bmatrix} -\tilde{\mathbf{R}}_i + r^0 \mathbf{1}_{33} & -\mathbf{r}_i \end{bmatrix} \tag{A.4b}$$

where $\mathbf{1}_{33}$ is the 3×3 identity matrix. The Euler parameters can be expressed in terms of $\mathbf{R}_i$ (Angeles, 1991) as follows:

$$\mathbf{r}_i = \mathsf{vect}(\sqrt{\mathbf{R}_i}), \quad r_0 = \frac{\mathrm{tr}(\sqrt{\mathbf{R}_i}) - 1}{2} \tag{A.5}$$

where $\sqrt{\mathbf{R}_i}$ is the proper orthogonal square root of $\mathbf{R}_i$.

The angular velocity $\boldsymbol{\omega}_i$ of $\mathcal{F}_i$ with respect to $\mathcal{F}_0$ can be related to $\dot{\mathbf{q}}_i$ as

$$\boldsymbol{\omega}_i = 2\mathbf{G}_i \dot{\mathbf{q}}_i \tag{A.6a}$$

or

$$\dot{\mathbf{q}}_i = \frac{1}{2}\mathbf{G}_i^T \boldsymbol{\omega}_i \tag{A.6b}$$

The flexible twist of link i, $\mathbf{v}_i$, and the time-rate change of its flexible pose, $\dot{\mathbf{q}}_i$, are related by

$$\mathbf{v}_i = \boldsymbol{\Gamma}_i \dot{\mathbf{q}}_i \tag{A.7a}$$

or

$$\dot{\mathbf{q}}_i = \boldsymbol{\Lambda}_i \mathbf{v}_i \tag{A.7b}$$

where $\boldsymbol{\Gamma}_i$ and $\boldsymbol{\Lambda}_i$ are $m_i' \times n_i'$ and $n_i' \times m_i'$ matrices, respectively, that are defined as

$$\boldsymbol{\Gamma}_i = \begin{bmatrix} 2\mathbf{G}_i & \mathbf{O}_{33} & \mathbf{O}_{3n_i} \\ \mathbf{O}_{34} & \mathbf{1}_{33} & \mathbf{O}_{3n_i} \\ \mathbf{O}_{n_i4} & \mathbf{O}_{n_i3} & \mathbf{1}_{n_in_i} \end{bmatrix} \tag{A.8a}$$

$$\boldsymbol{\Lambda}_i = \begin{bmatrix} \frac{1}{2}\mathbf{G}_i^T & \mathbf{O}_{43} & \mathbf{O}_{4n_i} \\ \mathbf{O}_{33} & \mathbf{1}_{33} & \mathbf{O}_{3n_i} \\ \mathbf{O}_{n_i3} & \mathbf{O}_{n_i3} & \mathbf{1}_{n_in_i} \end{bmatrix} \tag{A.8b}$$

where $\mathbf{O}_{jk}$ and $\mathbf{1}_{mm}$ are the $j \times k$ zero and the $m \times m$ identity matrices, respectively. Moreover, n_i is as defined in eq.(2.1)

Using eq.(A.4a) for $\mathbf{G}_i$, it can be readily shown that

$$\mathbf{G}_i \mathbf{G}_i^T = \mathbf{1}_{33} \tag{A.9}$$

where $\mathbf{1}_{33}$ is the 3×3 identity matrix. Moreover, using the above equation, it may be shown that $\mathbf{\Gamma}_i$ and $\mathbf{\Lambda}_i$ are related by

$$\mathbf{\Lambda}_i^T \mathbf{\Gamma}_i^T = \mathbf{1}_{m_i' m_i'} \tag{A.10}$$

where $\mathbf{1}_{m_i' m_i'}$ is the $m_i' \times m_i'$ identity matrix.

Appendix B

Derivation of $\frac{\partial}{\partial \hat{\mathbf{q}}_i}(\mathbf{v}_i^T \mathbf{M}_i \mathbf{v}_i)$

Upon substitution of $\mathbf{M}_i^{rr}$, $\mathbf{M}_i^{rd}$, $\mathbf{M}_i^{re}$ and $\mathbf{M}_i^{de}$ from eqs.(3.7), (3.14), (3.16a) and (3.16b) into eq.(3.63a), one obtains

$$\frac{\partial}{\partial \hat{\mathbf{q}}_i}(\mathbf{v}_i^T \mathbf{M}_i \mathbf{v}_i) = 2\frac{\partial}{\partial \hat{\mathbf{q}}_i}(\boldsymbol{\omega}_i^T \mathbf{R}_i \mathbf{V}_i^{rd} \mathbf{R}_i^T \dot{\mathbf{r}}) + 2\frac{\partial}{\partial \hat{\mathbf{q}}_i}(\dot{\mathbf{r}}_i^T \mathbf{R}_i \mathbf{V}_i^{de} \dot{\mathbf{u}}_i) + 2\frac{\partial}{\partial \hat{\mathbf{q}}_i}(\boldsymbol{\omega}_i^T \mathbf{R}_i \mathbf{V}_i^{re} \dot{\mathbf{u}}_i) + \frac{\partial}{\partial \hat{\mathbf{q}}_i}(\boldsymbol{\omega}_i^T \mathbf{R}_i \mathbf{V}_i^{rr} \mathbf{R}_i^T \boldsymbol{\omega}_i) \qquad \text{(B.1)}$$

It may be noted that $\mathbf{R}_i$ is the only term which is a function of $\hat{\mathbf{q}}_i$ inside the parentheses with the assumption made just after eq.(3.60).

The derivation of the above equation leads to the computation of partial derivatives of $\mathbf{a}_i^T \mathbf{R}_i \mathbf{b}_i$ and $\mathbf{a}_i^T \mathbf{R}_i \mathbf{H}_i \mathbf{R}_i^T \mathbf{b}_i$ with respect to $\hat{\mathbf{q}}_i$. Here, $\mathbf{a}_i$ and $\mathbf{b}_i$ are 3-dimensional vectors and $\mathbf{H}_i$ is a 3×3 matrix. For simplicity, subscript i is henceforth deleted.

B.1 Partial Derivatives of $\mathbf{a}^T\mathbf{R}\mathbf{b}$

The derivative of the expression of interest with respect to $\hat{\mathbf{q}}$ can be represented as

$$\frac{\partial}{\partial \hat{\mathbf{q}}}(\mathbf{a}^T\mathbf{R}\mathbf{b}) = \begin{bmatrix} \partial(\mathbf{a}^T\mathbf{R}\mathbf{b})/\partial\mathbf{r} \\ \\ \partial(\mathbf{a}^T\mathbf{R}\mathbf{b})/\partial r^0 \end{bmatrix} \tag{B.2}$$

By differentiating $\mathbf{a}^T\mathbf{R}\mathbf{b}$ with respect to $\mathbf{r}$ and r^0, respectively, we obtain

$$\frac{\partial}{\partial \mathbf{r}}(\mathbf{a}^T\mathbf{R}\mathbf{b}) = \frac{\partial \mathbf{a}^T}{\partial \mathbf{r}} + \frac{\partial(\mathbf{b}^T\mathbf{R}^T)}{\partial \mathbf{r}}\mathbf{a} = \left[\frac{\partial(\mathbf{R}\mathbf{b})}{\partial \mathbf{r}}\right]^T \mathbf{a} \tag{B.3a}$$

$$\frac{\partial}{\partial r^0}(\mathbf{a}^T\mathbf{R}\mathbf{b}) = \frac{\partial \mathbf{a}^T}{\partial r^0} + \frac{\partial(\mathbf{b}^T\mathbf{R}^T)}{\partial r^0}\mathbf{a} = \left[\frac{\partial(\mathbf{R}\mathbf{b})}{\partial r^0}\right]^T \mathbf{a} \tag{B.3b}$$

where $\mathbf{a}$ is not function of $\mathbf{r}$, and hence, $\partial\mathbf{a}^T/\partial\mathbf{r}$ and $\partial\mathbf{a}^T/\partial r^0$ vanish. Upon substitution of $\mathbf{R}$ from Appendix A into $\mathbf{R}\mathbf{b}$, one obtains

$$\mathbf{R}\mathbf{b} = (2(r^0)^2 - 1)\mathbf{b} + 2(\mathbf{b}^T\mathbf{r})\mathbf{r} + 2r^0(\mathbf{r} \times \mathbf{b}) \tag{B.4}$$

Differentiating the above equation with respect to $\mathbf{r}$ and r^0, respectively, one has

$$\frac{\partial(\mathbf{R}\mathbf{b})}{\partial \mathbf{r}} = 2\frac{\partial[(\mathbf{b}^T\mathbf{r})\mathbf{r}]}{\partial \mathbf{r}} + 2r^0\mathbf{B} \tag{B.5a}$$

$$\frac{\partial(\mathbf{R}\mathbf{b})}{\partial r^0} = 4r^0\mathbf{b} + 2(\mathbf{r} \times \mathbf{b}) \tag{B.5b}$$

where $\mathbf{B}$ is the cross-product matrix of $\mathbf{b}$. Recalling that $\partial\mathbf{v}^T/\partial\mathbf{v} = \mathbf{1}$, $\forall \quad \mathbf{v}$, and expanding eq.(B.5a), one obtains

$$\frac{\partial(\mathbf{R}\mathbf{b})}{\partial \mathbf{r}} = 2\mathbf{r}\mathbf{b}^T + 2(\mathbf{b}^T\mathbf{r})\mathbf{1}_{33} + 2r^0\mathbf{B} \tag{B.6}$$

where $\mathbf{1}_{33}$ is the 3×3 identity matrix. Finally, substituting eqs.(B.5b) and (B.6) into eqs.(B.3), $\partial(\mathbf{a}^T\mathbf{R}\mathbf{b})/\partial\hat{\mathbf{q}}$ becomes

$$\frac{\partial}{\partial \hat{\mathbf{q}}}(\mathbf{a}^T\mathbf{R}\mathbf{b}) = \begin{bmatrix} 2\mathbf{b}\mathbf{r}^T\mathbf{a} + 2(\mathbf{b}^T\mathbf{r})\mathbf{a} - 2r^0\mathbf{B}\mathbf{a} \\ \\ 4r^0(\mathbf{b}^T\mathbf{a}) + 2(\mathbf{r} \times \mathbf{b} \cdot \mathbf{a}) \end{bmatrix} \tag{B.7}$$

B.2 Partial Derivative of $\mathbf{a}^T\mathbf{RHR}^T\mathbf{b}$

The derivative of the expression of interest with respect to $\hat{\mathbf{q}}$ can be represented as

$$\frac{\partial}{\partial \hat{\mathbf{q}}}(\mathbf{a}^T\mathbf{RHR}^T\mathbf{b}) \equiv \frac{\partial}{\partial \hat{\mathbf{q}}}(\mathbf{a}^T\mathbf{Re}) = \begin{bmatrix} \partial(\mathbf{a}^T\mathbf{Re})/\partial \mathbf{r} \\ \\ \partial(\mathbf{a}^T\mathbf{Re})/\partial r^0 \end{bmatrix} \tag{B.8}$$

where $\mathbf{e} \equiv \mathbf{HR}^T\mathbf{b}$. Differentiating $\mathbf{a}^T\mathbf{Re}$ with respect to $\mathbf{r}$ and r^0, we obtain

$$\frac{\partial}{\partial \mathbf{r}}(\mathbf{a}^T\mathbf{Re}) = \frac{\partial}{\partial \mathbf{r}}(\mathbf{e}^T\mathbf{R}^T\mathbf{a}) = \frac{\partial \mathbf{e}^T}{\partial \mathbf{r}}\mathbf{R}^T\mathbf{a} + \frac{\partial(\mathbf{a}^T\mathbf{R})}{\partial \mathbf{r}}\mathbf{e} \tag{B.9a}$$

$$\frac{\partial}{\partial r^0}(\mathbf{a}^T\mathbf{Re}) = \frac{\partial}{\partial r^0}(\mathbf{e}^T\mathbf{R}^T\mathbf{a}) = \frac{\partial \mathbf{e}^T}{\partial r^0}\mathbf{R}^T\mathbf{a} + \frac{\partial(\mathbf{a}^T\mathbf{R})}{\partial r^0}\mathbf{e} \tag{B.9b}$$

Upon differentiation of $\mathbf{e}$ with respect to $\mathbf{r}$ and r^0, and using the value of $\mathbf{R}$ from Appendix A, one obtains

$$\frac{\partial \mathbf{e}}{\partial \mathbf{r}} = \mathbf{H}\frac{\partial(\mathbf{R}^T\mathbf{b})}{\partial \mathbf{r}} = \mathbf{H}\frac{\partial}{\partial \mathbf{r}}[(2(r^0)^2 - 1)\mathbf{b} + 2(\mathbf{b}^T\mathbf{r})\mathbf{r} - 2r^0(\mathbf{r} \times \mathbf{b})] \tag{B.10a}$$

$$\frac{\partial \mathbf{e}}{\partial r^0} = \mathbf{H}\frac{\partial(\mathbf{R}^T\mathbf{b})}{\partial r^0} = \mathbf{H}\frac{\partial}{\partial r^0}[(2(r^0)^2 - 1)\mathbf{b} + 2(\mathbf{b}^T\mathbf{r})\mathbf{r} - 2r^0(\mathbf{r} \times \mathbf{b})] \tag{B.10b}$$

Expanding the above expressions and performing the corresponding differentiations gives

$$\frac{\partial \mathbf{e}}{\partial \mathbf{r}} = 2(\mathbf{b}^T\mathbf{r})\mathbf{H} + 2\mathbf{Hrb}^T - 2r^0\mathbf{HB} \tag{B.11a}$$

$$\frac{\partial \mathbf{e}}{\partial r^0} = 4r^0\mathbf{Hb} - 2\mathbf{H}(\mathbf{r} \times \mathbf{b}) \tag{B.11b}$$

Finally, by substituting the above equations into the eqs.(B.9) and applying eq.(B.7) for $\partial(\mathbf{a}^T\mathbf{R})\mathbf{e}/\partial \mathbf{r}$ and $\partial(\mathbf{a}^T\mathbf{R})\mathbf{e}/\partial r^0$ and substituting the result into eqs.(B.9), one derives

$$\frac{\partial}{\partial \hat{\mathbf{q}}}(\mathbf{a}^T\mathbf{RHR}^T\mathbf{b}) = \begin{bmatrix} \mathbf{u} \\ l \end{bmatrix} \tag{B.12}$$

where

$$\mathbf{u} \equiv 2(\mathbf{b}^T\mathbf{r})\mathbf{f} + 2(\mathbf{r}^T\mathbf{f})\mathbf{b} + 2r^0\mathbf{B}\mathbf{f} + 2\mathbf{e}\mathbf{r}^T\mathbf{a} + 2(\mathbf{e}^T\mathbf{r})\mathbf{a} - 2r^0\mathbf{E}\mathbf{a} \tag{B.13}$$

$$l \equiv 4r^0\mathbf{b}^T\mathbf{f} - 2(\mathbf{r} \times \mathbf{b})^T\mathbf{f} + 4r^0(\mathbf{e}^T\mathbf{a}) + 2(\mathbf{r} \times \mathbf{e} \cdot \mathbf{a}) \tag{B.14}$$

and $\mathbf{E}$ is the cross-product matrix of $\mathbf{e}$ and $\mathbf{f} \equiv \mathbf{H}^T\mathbf{R}^T\mathbf{a}$.

Appendix C

Derivation of $\frac{\partial}{\partial \mathbf{u}_i}(\mathbf{v}_i^T \mathbf{M}_i \mathbf{v}_i)$

Upon substitution of $\mathbf{M}_i^{rr}$, $\mathbf{M}_i^{rd}$ and $\mathbf{M}_i^{re}$ from eqs.(3.7), (3.14) and (3.16a) into eq.(3.63c), one obtains

$$\frac{\partial}{\partial \mathbf{u}_i}(\mathbf{v}_i^T \mathbf{M}_i \mathbf{v}_i) = 2\frac{\partial}{\partial \mathbf{u}_i}(\mathbf{b}_i^T \mathbf{V}_i^{rd} \mathbf{s}_i) + 2\frac{\partial}{\partial \mathbf{u}_i}(\mathbf{b}_i^T \mathbf{V}_i^{re} \dot{\mathbf{u}}_i) + \frac{\partial}{\partial \mathbf{u}_i}(\mathbf{b}_i^T \mathbf{V}_i^{rr} \mathbf{b}_i) \tag{C.1a}$$

where $\mathbf{s}_i$ and $\mathbf{b}_i$ are 3-dimensional vectors defined as

$$\mathbf{b}_i \equiv \mathbf{R}_i^T \boldsymbol{\omega}_i \tag{C.1b}$$

$$\mathbf{s}_i \equiv \mathbf{R}_i^T \dot{\mathbf{r}}_i \tag{C.1c}$$

Note that $\mathbf{b}_i$ and $\mathbf{s}_i$ are not function of $\mathbf{u}_i$.

The three terms of the right-hand side of eq.(C.1a) are derived below.

C.1 Derivation of $\frac{\partial}{\partial \mathbf{u}_i}(\mathbf{b}_i^T \mathbf{V}_i^{rd} \mathbf{s}_i)$

The derivative of the expression of interest with respect to $\mathbf{u}_i$ can be rewritten as

$$\frac{\partial}{\partial \mathbf{u}_i}(\mathbf{b}_i^T \mathbf{V}_i^{rd} \mathbf{s}_i) = \frac{\partial}{\partial \mathbf{u}_i}(\mathbf{b}_i^T \mathbf{c}_i) \tag{C.2a}$$

where

$$\mathbf{c}_i \equiv \mathbf{V}_i^{rd} \mathbf{s}_i \tag{C.2b}$$

Upon differentiation of the eq.(C.2a) with respect to $\mathbf{u}_i$ and noting that $\mathbf{b}_i$ is not function of $\mathbf{u}_i$, one obtains

$$\frac{\partial}{\partial \mathbf{u}_i}(\mathbf{b}_i^T \mathbf{c}_i) = \frac{\partial \mathbf{c}_i^T}{\partial \mathbf{u}_i} \mathbf{b}_i = \frac{\partial (\mathbf{V}_i^{rd} \mathbf{s}_i)^T}{\partial \mathbf{u}_i} \mathbf{b}_i \tag{C.3}$$

Hence, we note the relation

$$\mathbf{V}_i^{rd} \mathbf{s}_i = -\mathbf{S}_i \mathbf{v}_i^{rd} \tag{C.4}$$

where $\mathbf{v}_i^{rd}$ is the vector of the skew-symmetric matrix $\mathbf{V}_i^{rd}$ and $\mathbf{S}_i$ is the cross-product matrix of vector $\mathbf{s}_i$; it is then possible to write

$$\frac{\partial (\mathbf{V}_i^{rd} \mathbf{s}_i)^T}{\partial \mathbf{u}_i} \mathbf{b}_i = \frac{\partial (-\mathbf{S}_i \mathbf{v}_i^{rd})^T}{\partial \mathbf{u}_i} \mathbf{b}_i \tag{C.5}$$

Differentiating $-\mathbf{S}_i \mathbf{v}_i^{rd}$ with respect to $\mathbf{u}_i$ and, in light of eq.(3.14b), one obtains

$$\frac{\partial (-\mathbf{S}_i \mathbf{v}_i^{rd})^T}{\partial \mathbf{u}_i} \mathbf{b}_i = \left(-\mathbf{S}_i \mathbf{C}_i^{i1}\right)^T \mathbf{b}_i = -(\mathbf{C}_i^{i1})^T (\mathbf{S}_i)^T \mathbf{b}_i \tag{C.6}$$

Thus, inserting the above equation into eq.(C.2a), one obtains

$$\frac{\partial}{\partial \mathbf{u}_i}(\mathbf{b}_i^T \mathbf{V}_i^{rd} \mathbf{s}_i) = -(\mathbf{C}_i^{i1})^T (\mathbf{S}_i)^T \mathbf{b}_i \tag{C.7}$$

where $\mathbf{s}_i$ and $\mathbf{b}_i$ are defined in eqs.(C.1c) and (C.1b), respectively.

C.2 Derivation of $\frac{\partial}{\partial \mathbf{u}_i}(\mathbf{b}_i^T \mathbf{V}_i^{rr} \mathbf{b}_i)$

Upon differentiation of the expression of interest with respect to $\mathbf{u}_i$, one obtains

$$\frac{\partial}{\partial \mathbf{u}_i}(\mathbf{b}_i^T \mathbf{V}_i^{rr} \mathbf{b}_i) = \frac{\partial (\mathbf{V}_i^{rr} \mathbf{b}_i)^T}{\partial \mathbf{u}_i} \mathbf{b}_i \tag{C.8}$$

The 3-dimensional vector $(\mathbf{V}_i^{rr} \mathbf{b}_i)$ can be written as

$$(\mathbf{V}_i^{rr} \mathbf{b}_i) = \begin{bmatrix} \mathbf{v}_1^T \mathbf{b} & \mathbf{v}_2^T \mathbf{b} & \mathbf{v}_3^T \mathbf{b} \end{bmatrix}_i^T \tag{C.9}$$

where $(\mathbf{v}_j)_i^T$ is the j^{th} row of the matrix $\mathbf{V}_i^{rr}$. Substituting eq.(C.9) into eq.(C.8) and differentiating the result thus obtained with respect to $\mathbf{u}_i$, one obtains

$$\begin{aligned}\frac{\partial}{\partial \mathbf{u}_i}(\mathbf{b}_i^T \mathbf{V}_i^{rr} \mathbf{b}_i) &= \frac{\partial (\mathbf{V}_i^{rr} \mathbf{b}_i)^T}{\partial \mathbf{u}_i} \mathbf{b}_i \\ &= \begin{bmatrix} (\partial \mathbf{v}_1^T / \partial \mathbf{u})\mathbf{b} & (\partial \mathbf{v}_2^T / \partial \mathbf{u})\mathbf{b} & (\partial \mathbf{v}_3^T / \partial \mathbf{u})\mathbf{b} \end{bmatrix}_i \mathbf{b}_i \quad \text{(C.10)}\end{aligned}$$

Here,

$$\left[\frac{\partial \mathbf{v}_j^T}{\partial \mathbf{u}}\right]_i = \begin{bmatrix} \partial v_{j1}/\partial \mathbf{u} & \partial v_{j2}/\partial \mathbf{u} & \partial v_{j3}/\partial \mathbf{u} \end{bmatrix}_i \tag{C.11}$$

where $j = 1, 2, 3$, and the components of the 3×3 matrix $\left[\partial \mathbf{v}_j^T / \partial \mathbf{u}\right]_i$ are obtained using eqs.(3.12) as

$$\left(\frac{\partial v_{11}}{\partial \mathbf{u}}\right)_i = 2\left(\mathbf{C}_{22}^{i3} + \mathbf{C}_{33}^{i3}\right) \mathbf{u}_i(t) + 2\left(\mathbf{C}_{22}^{i5} + \mathbf{C}_{33}^{i5}\right) \mathbf{u}_i^o \tag{C.12}$$

$$\left(\frac{\partial v_{12}}{\partial \mathbf{u}}\right)_i = -2\mathbf{C}_{12}^{i3} \mathbf{u}_i(t) - \left(\mathbf{C}_{12}^{i5} + \mathbf{C}_{21}^{i5}\right) \mathbf{u}_i^o \tag{C.13}$$

$$\left(\frac{\partial v_{13}}{\partial \mathbf{u}}\right)_i = -2\mathbf{C}_{13}^{i3} \mathbf{u}_i(t) - \left(\mathbf{C}_{13}^{i5} + \mathbf{C}_{31}^{i5}\right) \mathbf{u}_i^o \tag{C.14}$$

The other components are obtained by suitable permutations. Here, $\mathbf{b}_i$ is defined in eq.(C.1b) and matrices $\mathbf{C}_{kl}^{ij}$ were defined in eqs.(3.11). Moreover, $\mathbf{u}_i(t)$ and $\mathbf{u}_i^o$ are defined in eqs.(2.1) and (2.12).

C.3 Derivation of $\frac{\partial}{\partial \mathbf{u}_i}(\mathbf{b}_i^T \mathbf{V}_i^{re} \dot{\mathbf{u}}_i)$

Differentiating the expression of interest with respect to $\mathbf{u}_i$ leads to

$$\frac{\partial}{\partial \mathbf{u}_i}(\mathbf{b}_i^T \mathbf{V}_i^{re} \dot{\mathbf{u}}_i) = \frac{\partial (\mathbf{V}_i^{re} \dot{\mathbf{u}}_i)^T}{\partial \mathbf{u}_i} \mathbf{b}_i \tag{C.15}$$

Using the same approach as in Sections C.1 and C.2, one thus obtains

$$\frac{\partial}{\partial \mathbf{u}_i}(\mathbf{b}_i^T \mathbf{V}_i^{re} \dot{\mathbf{u}}_i) = \mathbf{I}_i^{re} \mathbf{b}_i \tag{C.16}$$

where $\mathbf{I}_i^{rc}$ is the $n_i \times 3$ matrix defined as

$$\mathbf{I}_i^{rc} = \left[\begin{array}{ccc} (\mathbf{C}_{32}^{i3} - \mathbf{C}_{23}^{i3})\dot{\mathbf{u}}_i & (\mathbf{C}_{31}^{i3} - \mathbf{C}_{13}^{i3})\dot{\mathbf{u}}_i & (\mathbf{C}_{21}^{i3} - \mathbf{C}_{12}^{i3})\dot{\mathbf{u}}_i \end{array} \right] \tag{C.17}$$

where $\mathbf{b}_i$ is defined in eq.(C.1b) and matrices $\mathbf{C}_{kl}^{ij}$ are defined in eqs.(3.11). Moreover, $\mathbf{u}_i(t)$ and $\mathbf{u}_i^o$ are defined in eqs.(2.1) and (2.12).